การวิเคราะห์ข้อมูลไวร์ไลน์ฟอร์เมชั่นเทสเตอร์สำหรับหาประเภทของของไหลในแหล่งกักเก็บที่มีค่าความซึมผ่านได้ของหินต่ำ

นายอรรถวิทย์ ชูเดช

วิทยานิพนธ์นี้เป็นส่วนหนึ่งของการศึกษาตามหลักสูตรปริญญาวิศวกรรมศาสตรมหาบัณฑิต
สาขาวิชาวิศวกรรมปิโตรเลียม ภาควิชาวิศวกรรมเหมืองแร่และปิโตรเลียม
คณะวิศวกรรมศาสตร์ จุฬาลงกรณ์มหาวิทยาลัย
ปีการศึกษา 2554

ลิขสิทธิ์ของจุฬาลงกรณ์มหาวิทยาลัย

บทคัดย่อและแฟ้มข้อมูลฉบับเต็มของวิทยานิพนธ์ตั้งแต่ปีการศึกษา 2554 ที่ให้บริการในคลังปัญญาจุฬาฯ (CUIR)
เป็นแฟ้มข้อมูลของนิสิตเจ้าของวิทยานิพนธ์ที่ส่งผ่านทางบัณฑิตวิทยาลัย
The abstract and full text of theses from the academic year 2011 in Chulalongkorn University Intellectual Repository(CUIR)
are the thesis authors' files submitted through the Graduate School.

ANALYSIS OF WIRELINE FORMATION TESTER DATA FOR DETERMINATION OF FLUID TYPE IN LOW PERMEABILITIES RESERVOIRS

Mr. Attawit Choodesh

A Thesis Submitted in Partial Fulfillment of the Requirements
for the Degree of Master of Engineering Program in Petroleum Engineering
Department of Mining and Petroleum Engineering
Faculty of Engineering
Chulalongkorn University
Academic Year 2011

Copyright of Chulalongkorn University

5 1 7 1 6 1 8 0 2 1

Thesis Title	ANALYSIS OF WIRELINE FORMATION TESTER DATA FOR DETERMINATION OF FLUID TYPE IN LOW PERMEABILITIES RESERVOIRS
By	Mr. Attawit Choodesh
Field of Study	Petroleum Engineering
Thesis Advisor	Assistant Professor Jirawat Chewaroungroaj, Ph.D.
Thesis Co-advisor	Yothin Tongpenyai, Ph.D.

Accepted by the Faculty of Engineering, Chulalongkorn University in Partial Fulfillment of the Requirements for the Master's Degree

..... Dean of the Faculty of Engineering
(Associate Professor Boonsom Lerdhirunwong, Dr. Ing.)

THESIS COMMITTEE

..... Chairman
(Associate Professor Sarithdej Pathanasethpong)

..... Thesis Advisor
(Assistant Professor Jirawat Chewaroungroaj, Ph.D.)

..... Thesis Co-advisor
(Yothin Tongpenyai, Ph.D.)

..... Examiner
(Assistant Professor Suwat Athichanagorn, Ph.D.)

..... External Examiner
(Saifon (Daungkaew) Sirimongkolkitti, Ph.D.)

อรรถวิทย์ ชูเดช : การวิเคราะห์ข้อมูลไวร์ไลน์ฟอร์เมชั่นเทสเตอร์สำหรับหาประเภทของของไหลในแหล่งกักเก็บที่มีค่าความซึมผ่านได้ของหินต่ำ. (ANALYSIS OF WIRELINE FORMATION TESTER DATA FOR DETERMINATION OF FLUID TYPE IN LOW PERMEABILITIES RESERVOIRS) อ.ที่ปรึกษาวิทยานิพนธ์หลัก: ผศ.ดร.จิรวัฒน์ ชีวรุ่งโรจน์, อ.ที่ปรึกษาวิทยานิพนธ์ร่วม: ดร.โยธิน ทองเป็นใหญ่, 118 หน้า

การทดสอบแหล่งกักเก็บที่มีค่าความซึมผ่านได้ต่ำนั้นนำมาซึ่งปัญหามากมาย อาทิเช่น ใช้เวลานานในการรวบรวมแรงดัน , การมีแรงดันสะสมมากเกินไป และการเสียความสามารถในการปิดผนึก เวลาในการรวบรวมแรงดันที่นานเกินไปไม่เป็นที่ต้องการเพราะว่าความน่าจะเป็นในการติดแน่นในหลุมของอุปกรณ์หยั่งธรณีจะมีมากขึ้นและเสียเวลาในการทำงานของแท่นขุดเจาะ

วิทยานิพนธ์ฉบับนี้ศึกษาเกี่ยวกับการตอบสนองของแรงดันจากไวน์ไลน์ฟอร์เมชั่นเทสเตอร์ในแหล่งกักเก็บที่มีความซึมผ่านได้ต่ำ เฉพาะเจาะจงลงไปที่พฤติกรรมของแรงดันและวิธีที่จะจำแนกชนิดของของไหลในแหล่งกักเก็บ การศึกษานี้ตั้งใจที่จะศึกษาเรื่องการตอบสนองของแรงดันในแหล่งกักเก็บที่มีความซึมผ่านได้ต่ำโดยได้สร้างแบบจำลองที่ในเงื่อนไขที่ค่าความซึมผ่านได้ต่ำถึง 0.1มิลิดาร์ซี่ และเปลี่ยนแปลงชนิดของของไหลในแหล่งกักเก็บ แนวความคิดเกี่ยวกับการมีพื้นที่ที่มีการไหลจำกัดรวมไปถึงการมีแผ่นหินดินดานได้ถูกนำมากล่าวถึงในแหล่งกักเก็บและอาจจะเป็นผลที่ทำให้การไหลของของไหลเข้าสู่ตัวตรวจสอบค่าความดันทำได้ยากขึ้นเมื่อตัวตรวจสอบถูกแทงเข้าไปในบริเวณชั้นหินดินดานในแหล่งกักเก็บ

ผลจากการศึกษาครั้งนี้ทำให้ทราบว่าบริเวณที่มีพื้นที่ที่มีการไหลจำกัดจะปฏิบัติตัวเหมือนกับโช๊คที่ทำหน้าที่ลดการไหลของแล่งกักเก็บเข้าไปสู่ตัวตรวจสอบค่าความดันและห้องกักเก็บ ดังนั้นจึงทำให้การตอบสนองของแรงดันช้าลง สมสมมติฐานนี้ทำให้เราได้จำลองปรากฏการณ์ที่เมื่อมีการแทงตัวตรวจสอบค่าความดันเข้าไปในบริเวณที่มีชั้นหินดินดานแทรกอยู่ในแหล่งกักเก็บที่มีค่าความซึมผ่านได้ปานกลางและต่ำ เมื่อไม่มีบริเวณที่มีพื้นที่ที่มีการไหลจำกัดในแหล่งกักเก็บที่มีค่าความซึมผ่านได้ต่ำ (0.1mD) เวลาที่ใช้ในรวบรวมแรงดันแค่ห้านาทีก็เพียงพอแล้วสำหรับที่จะใช้ในการจำแนกชนิดของของไหล สำหรับกรณีที่มีบริเวณที่มีพื้นที่ที่มีการไหลจำกัดรอบๆตัวตรวจสอบค่าความดันเวลาที่ใช้ในรวบรวมแรงดันสามารถยาวนานได้ถึง 35 วัน การใช้การตอบสนองของแรงดันที่สั้นจนเกินไปสามารถทำให้เราได้ผลสรุปที่ผิดพลาดเนื่องจากการสภาวะผันผวนเนื่องจากผลของเวลบอร์สโตร์เรจ (ห้องกักเก็บ) และช่วงเวลาของการส่งข้ามขอบเขต

ภาควิชา วิศวกรรมเหมืองแร่และปิโตรเลียม....ลายมือชื่อนิสิต.....

สาขาวิชา วิศวกรรมปิโตรเลียม..... ลายมือชื่อ อ.ที่ปรึกษาวิทยานิพนธ์หลัก.....

ปีการศึกษา 2554.....ลายมือชื่อ อ.ที่ปรึกษาวิทยานิพนธ์ร่วม.....

5171618021: MAJOR PETROLEUM ENGINEERING
KEYWORDS: LOW PERMEABILITY / WIRELINE FORMATION TEST

ATTAWIT CHOODESH: ANALYSIS OF WIRELINE FORMATION TESTER DATA FOR DETERMINATION OF FLUID TYPE IN LOW PERMEABILITIES RESERVOIRS. ADVISOR: ASST. PROF. JIRAWAT CHEWAROUNGROAJ, Ph.D., THESIS CO ADVISOR: YOTHIN TONGPENYAI, Ph.D., 118 pp.

Formation tests in low-permeability reservoir have been impeded by several problems, such as excessively long buildup time, supercharging, and loss of packer seals. A long pressure buildup time is not desirable because the possibility of the tools getting stuck would increase and waste of rig time.

This thesis studies the pressure response data from wireline formation tester in low permeability reservoirs, focusing on pressure behavior and method to identify fluid type in reservoir. The study is conducted by simulating the pressure response in the low permeability reservoir condition with reservoir permeability as low as 0.1 mD, and with various fluid types in the reservoir. The concept of restricted zone is introduced to take into account shale in a reservoir that may cause difficulty in fluid flow into a probe when the probe is inserted into the shale region in the reservoir.

According to this study, the restricted zone acts as a choke to reduce flow from the reservoir into the probe and chamber, hence slowing down the pressure response. This assumption allows us to simulate the phenomena when the probe is inserted into a shale region in a low to moderate permeability reservoir. When there is no restricted zone existing in low permeability reservoir (0.1 mD), the 5-minute buildup time is enough to identify the reservoir pressure and also identify pressure gradient or fluid type. For the case with restricted zone around the probe, the buildup time can be as long as 35 days. The pressure gradient or fluid type determination using pressure from too short period of time can lead to wrong conclusion due to unstable conditions caused by wellbore (chamber) storage effect and/or transition regime.

Department: Mining and Petroleum Engineering..... Student's Signature.....
Field of Study: Petroleum Engineering..... Advisor's Signature.....
Academic Year: 2011.....Co-advisor's Signature.....

ACKNOWLEDGEMENTS

First of all, I would like to thank you Dr. Jirawat Chewaroungroaj and Dr. Yothin Tongpenyai for being my thesis adviser and co-adviser and always give me very helpful and invaluable advices.

Also, I would like thank all lecturers who are advocated in teaching students both in classes and out of classes. I would like to give my special thank to all my classmates in petroleum engineering program, especially Ms. Wiriya Kiatpadungkul, for invaluable discussions, encouragement, and friendship.

I wish to thank the thesis committee members for their comments and recommendations.

I would like to express my deep appreciation to my family and my friends who give me their support, encouragement endless love.

CONTENTS

Page

Abstract (Thai) iv

Abstract (English) v

Acknowledgements vi

Contents vii

List of Tables x

List of Figures xii

List of Abbreviations xviii

Nomenclature xix

Greek Letters xx

CHAPTER

I. Introduction 1

1.1 Methodology 2

1.2 Thesis Outline 3

II. Literature Review 4

2.1 Repeat Formation Tester (RFT) in Low Permeability Reservoir. 4

2.2 Tight Gas Sand Analysis. 6

III. Theories And Concepts 10

3.1 Repeat Formation Tester 10

3.2 Repeat Formation Test Concept 10

3.3 Flow Regime 12

3.4 Low Permeability Reservoir 15

3.5 Tight Gas Sand Analysis and Tool Storage Effect 17

3.6 Reservoir Model for Wireline Formation Tester 22

CHAPTER Page

3.7 Mathematical Modeling 22

3.8 Pressure Gradient Analysis 23

3.9 Curve Fitting..... 25

IV.Reservoir Model..... 28

4.1 Reservoir Model 28

4.2 Restricted Flow Model 31

4.3 RFT Parameter and Fluid Properties 32

V.Simulation Studies, Results and Analysis..... 39

5.1 Pressure Response in Low Permeability Oil Reservoir..... 39

5.2 Effect of the restricted zone severity in oil reservoir with restricted zone permeability. 42

5.3 Curve Fitting for Oil Reservoir 54

5.4 Effect of the Restricted Zone Severity in Oil Reservoir with Low Restricted Zone Permeability. 56

5.5 Pressure Response in Low Permeability Oil Reservoir..... 71

5.6 Effect of the restricted zone severity in oil reservoir with restricted zone permeability. 72

5.7 Pressure response in low permeability gas reservoir..... 82

5.8 Effect of the restricted zone severity in gas reservoir with restricted zone permeability. 84

VI.Conclusion And Recommendation 98

6.1 Conclusions..... 98

6.2 Recommendations..... 99

References. 100

Appendices 106

APPENDIX A: Sample ECLIPSE data file:..... 107
APPENDIX B: Sample curve fitting data:..... 111
Vitae…….114

LIST OF TABLES

Page

Table 3.1: Typical fluid gradients 24

Table 4.1: Model properties. 29

Table 4.2: Reservoir parameter 33

Table 4.3: RFT parameter 34

Table 4.4: Grid position for probe plugging 35

Table 4.5: Grid position for restricted zone effect 35

Table 4.6: Oil formation volume factor and oil viscosity 36

Table 4.7: Gas formation volume factor and gas viscosity 37

Table 5.1: Summary data with the different reservoir permeability 41

Table 5.2: Summarized data with different restricted zone permeability in 30 minute testing time 45

Table 5.3: Final reading pressure in 30-minute 51

Table 5.4: Extrapolation pressure in 30-minute 51

Table 5.5: Summary of fluid gradient interpretation from the final reading pressure and extrapolated pressure in 30-minute 52

Table 5.6: Summary data of input value and coefficient of different restricted zone permeability for oil reservoir 54

Table 5.7: The buildup time result for each restricted zone permeability 56

Table 5.8: Estimate total time to reach initial reservoir pressure for restricted zone effect 57

Table 5.9: Summary of time readings from log-log plot 65

Table 5.10: First reading pressure after passing transition period. 68

Table 5.11: Extrapolation pressure after extended time. 68

Page

Table 5.12: Summary of fluid gradient interpretation from the first reading pressure and extrapolated pressure after extended testing time. 69

Table 5.13: Summary data with the different reservoir permeability 72

Table 5.14: Summary of data with the different restricted zone permeability in 30 minute testing time..... 74

Table 5.15: Final reading pressure in 30-minute 79

Table 5.16: Extrapolation pressure in 30-minute..... 79

Table 5.17: Summary of fluid gradient interpretation from the final reading pressure and extrapolated pressure in 30-minute 80

Table 5.18: Summary data of input value and coefficient of different restricted zone permeability for gas reservoir 82

Table 5.19 The buildup time result for each restricted zone permeability 84

Table 5.20: Estimate total time to reach initial reservoir pressure for restricted zone effect 84

Table 5.21: Summary of time readings from log-log plot 91

Table 5.22: First reading pressure after passing transition period. 94

Table 5.23: Extrapolation pressure after extended time. 94

Table 5.24: Summary of fluid gradient interpretation from the final reading pressure and extrapolated pressure after extended time 95

Table B-1: Summary data of input value and coefficient of tight reservoir 115

Table B-2: Summary data from Exponential model and real data..... 118

LIST OF FIGURES

Page

Figure 3.1: RFT tool configuration 11
Figure 3.2: Pressure response from pretest sequence 12
Figure 3.3: Spherical flow regime in reservoir 13
Figure 3.4: Relationship between grain sorting and porosity 16
Figure 3.5: Relationship between grain size and permeability 16
Figure 3.6: Resource triangle for oil and natural gas 17
Figure 3.7a: Repeat Formation Tester flow sequence 19
Figure 3.7b: Flow rate for RFT flow sequence 20
Figure 3.7c: Pressure response for RFT flow sequence 21
Figure 3.8: Flow pattern during the test 22
Figure 3.9: Pressure gradient plot example 24
Figure 3.10: Exponential model plot 27
Figure 4.1a: Schematic reservoir description in top view 30
Figure 4.1b: Schematic reservoir description in 3D 30
Figure 4.2: Flow geometry of the restricted zone model 31
Figure 4.3: Reservoir grid model for the restricted zone assumption in 3D 32
Figure 4.4: Cross sectional view for the restricted zone assumption 32
Figure 4.5: Schematic for RFT probe location for a base case and modification model 34
Figure 4.6: Oil and water relative permeability 38
Figure 4.7: Gas and water relative permeability 38
Figure 5.1: Schematic reservoir description for the base case oil reservoir 39
Figure 5.2: Schematic sampling points for base case oil reservoir. 40
Figure 5.3: Pressure response for the base case oil reservoir 40
Figure 5.4: Pressure response with the different reservoir permeability in oil reservoir 41
Figure 5.5: Tool mechanical when probe is inserted into formation. 43

Page

Figure 5.6: Schematic reservoir description for the restricted zone assumption in oil reservoir 44

Figure 5.7a: Pressure response for the restricted zone permeability 10^{-1} mD to 10^{-3} mD at depth 6,567.5 ft 44

Figure 5.7b: Pressure response for the restricted zone permeability 10^{-4} mD to 10^{-7} mD at depth 6,567.5 ft 45

Figure 5.8: Log-log plot of dP vs dt and unit slope line and spherical pressure buildup plot for the restricted zone 10^{-4} mD at depth 6,567.5 ft with 30-minute testing time 46

Figure 5.9: Log-log plot of dP vs dt and unit slope line and spherical pressure buildup plot for the restricted zone 10^{-5} mD at depth 6,567.5 ft with 30-minute testing time 47

Figure 5.10: Log-log plot of dP vs dt and unit slope line and spherical pressure buildup plot for the restricted zone 10^{-6} mD at depth 6,567.5 ft with 30-minute testing time 47

Figure 5.11: Log-log plot of dP vs dt and unit slope line and spherical pressure buildup plot for the restricted zone 10^{-7} mD at depth 6,567.5 ft with 30-minute testing time 47

Figure 5.12: Pressure gradient plot from final reading pressure, extrapolation pressure and initial pressure for the restricted zone 10^{-4} mD 48

Figure 5.13: Pressure gradient plot from final reading pressure, extrapolation pressure and initial pressure for the restricted zone 10^{-5} mD 49

Figure 5.14: Pressure gradient plot from final reading pressure, extrapolation pressure and initial pressure for the restricted zone 10^{-6} mD 49

Figure 5.15: Pressure gradient plot from final reading pressure, extrapolation pressure and initial pressure for the restricted zone 10^{-7} m 50

Figure 5.16: Final pressure error from final reading pressure and extrapolation pressure in 30-minute 52

Figure 5.17: Fluid gradient error for final reading pressure and extrapolation pressure in 30-minute 53

Figure 5.18: The differentiation value plot for a base case 55

Page

Figure 5.19: Pressure buildup profile from reservoir simulation and exponential model for the restricted zone permeability 10^{-2} mD 55

Figure 5.20: Schematic reservoir description for the restricted zone permeability of 10^{-4} mD to 10^{-7} mD for oil reservoir..... 57

Figure 5.21: Schematic reservoir description for testing point for the restricted zone permeability of 10^{-4} mD to 10^{-7} mD for oil reservoir..... 57

Figure 5.22: Pressure response for the restricted zone permeability 10^{-4} mD with 120 minutes 58

Figure 5.23: Pressure response for the restricted zone permeability 10^{-5} mD with 12 hours 59

Figure 5.24: Pressure response for the restricted zone permeability 10^{-6} mD with 5 days..... 59

Figure 5.25: Pressure response for the restricted zone permeability 10^{-7} mD with 35 days..... 60

Figure 5.26: Log-log plot of dP vs dt , unit slope line and spherical pressure buildup plot for the restricted zone 10^{-4} mD with 120 minutes a) depth 6,571.25ft b) depth 6,567.50 ft c) 6,563.75 ft..... 61

Figure 5.27: Log-log plot of dP vs dt , unit slope line and spherical pressure buildup plot for the restricted zone 10^{-5} mD with 12 hours a) depth 6,571.25ft b) depth 6,567.50 ft c) 6,563.75 ft..... 62

Figure 5.28: Log-log plot of dP vs dt , unit slope line and spherical pressure buildup plot for the restricted zone 10^{-6} mD with 5 days a) depth 6,571.25ft b) depth 6,567.50 ft c) 6,563.75 ft..... 63

Figure 5.29: Log-log plot of dP vs dt , unit slope line and spherical pressure buildup plot for the restricted zone 10^{-7} mD with 35 days a) depth 6,571.25ft b) depth 6,567.50 ft c) 6,563.75 ft..... 64

Figure 5.30: Pressure gradient result from the first reading pressure, extrapolation pressure and initial pressure for the restricted zone 10^{-4} mD..... 65

Figure 5.31: Pressure gradient result from the first reading pressure, extrapolation pressure and initial pressure for the restricted zone 10^{-5} mD..... 66

Page

Figure 5.32: Pressure gradient result from the first reading pressure, extrapolation pressure and initial pressure for the restricted zone 10^{-6} mD..... 66

Figure 5.33: Pressure gradient result from the first reading pressure, extrapolation pressure and initial pressure for the restricted zone 10^{-7} mD..... 67

Figure 5.34: Final pressure error for the first reading pressure and extrapolation pressure after extended time 69

Figure 5.35: Fluid gradient error for the first reading pressure and extrapolation pressure after extended time 70

Figure 5.36: Pressure response for a base case gas reservoir 71

Figure 5.37: Pressure response with the different reservoir permeability in gas reservoir..... 72

Figure 5.38a: Pressure response for the restricted zone permeability 10^{-2} mD to 10^{-3} mD at depth 6,567.5 ft..... 73

Figure 5.38b: Pressure response for the restricted zone permeability 10^{-4} mD to 10^{-7} mD at depth 6,567.5 ft..... 74

Figure 5.39: Log-log plot of d*m(P)* vs dt ,unit slope line and spherical pressure buildup plot for the restricted zone 10^{-4} mD at depth 6,567.5 ft with 30-minute testing time 75

Figure 5.40: Log-log plot of d*m(P)* vs dt ,unit slope line and spherical pressure buildup plot for the restricted zone 10^{-5} mD at depth 6,567.5 ft with 30-minute testing time 75

Figure 5.41: Log-log plot of d*m(P)* vs dt ,unit slope line and spherical pressure buildup plot for the restricted zone 10^{-6} mD at depth 6,567.5 ft with 30-minute testing time 76

Figure 5.42: Log-log plot of d*m(P)* vs dt ,unit slope line and spherical pressure buildup plot for the restricted zone 10^{-7} mD at depth 6,567.5 ft with 30-minute testing time 76

Figure 5.43: Pressure gradient plot from final reading pressure, extrapolation pressure and initial pressure for the restricted zone 10^{-4} mD..... 77

Figure 5.44: Pressure gradient plot from final reading pressure, extrapolation pressure and initial pressure for the restricted zone 10^{-5} mD..... 77

Page

Figure 5.45: Pressure gradient plot from final reading pressure, extrapolation pressure and initial pressure for the restricted zone 10^{-6} mD..... 78

Figure 5.46: Pressure gradient plot from final reading pressure, extrapolation pressure and initial pressure for the restricted zone 10^{-7} mD..... 78

Figure 5.47: Pressure error from final reading pressure and extrapolation pressure in 30-minute..... 80

Figure 5.48: Fluid gradient error for final reading pressure and extrapolation pressure in 30-minute..... 81

Figure 5.49: The differentiation value plot for a base case..... 83

Figure 5.50: Pressure buildup profile from reservoir simulation and exponential model for the restricted zone permeability 10-4 mD 83

Figure 5.51: Pressure response for the restricted zone permeability 10^{-4} mD with 60 minutes..... 85

Figure 5.52: Pressure response for the restricted zone permeability 10^{-5} mD with 8 hours 85

Figure 5.53: Pressure response for the restricted zone permeability 10^{-6} mD with 5 days..... 86

Figure 5.54: Pressure response for the restricted zone permeability 10^{-7} mD with 30 days..... 86

Figure 5.55: Log-log plot of d*m(P)* vs dt , unit slope line and spherical pressure buildup plot for the restricted zone permeability 10^{-4} mD with 60 minutes a) depth 6,571.25ft b) depth 6,567.50 ft c) 6,563.75 ft..... 87

Figure 5.56: Log-log plot of d*m(P)* vs dt , unit slope line and spherical pressure buildup plot for the restricted zone permeability 10^{-5} mD with 8 hours a) depth 6,571.25ft b) depth 6,567.50 ft c) 6,563.75 ft..... 88

Figure 5.57: Log-log plot of d*m(P)* vs dt , unit slope line and spherical pressure buildup plot for the restricted zone permeability 10^{-6} mD with 5 days a) depth 6,571.25ft b) depth 6,567.50 ft c) 6,563.75 ft 89

Figure 5.58: Log-log plot of dm(P) vs dt , unit slope line and spherical pressure buildup plot for the restricted zone permeability 10-7 mD with 30 days a) depth 6,571.25ft b) depth 6,567.50 ft c) 6,563.75 ft 90

Page

Figure 5.59: Pressure gradient result from the first reading pressure, extrapolation pressure and initial pressure for the restricted zone 10^{-4} mD..... 91

Figure 5.60: Pressure gradient result from the first reading pressure, extrapolation pressure and initial pressure for the restricted zone 10^{-5} mD..... 92

Figure 5.61: Pressure gradient result from the first reading pressure, extrapolation pressure and initial pressure for the restricted zone 10-6 mD 92

Figure 5.62: Pressure gradient result from the first reading pressure, extrapolation pressure and initial pressure for the restricted zone 10-7 mD 93

Figure 5.63: Final pressure error for the first reading pressure and extrapolation pressure after extended time 95

Figure 5.64: Fluid gradient error for the first reading pressure and extrapolation pressure after extended time 96

Figure B-1: Pressure buildup from simulation and exponential model plot versus buildup time 114

Figure B-2: R^2 value from simulation and exponential model 114

Figure B-3: The differentiation value plot for tight reservoir..... 116

Figure B-4: Pressure buildup profile from real data and exponential model for the mobility 1.83 mD/cp 116

Figure B-5: Pressure buildup profile from real data and exponential model for the mobility 2.61 mD/cp 117

Figure B-6: Pressure buildup profile from real data and exponential model for the mobility 0.41 mD/cp 118

LIST OF ABBREVIATIONS

CQG	Crystal Quartz Gauge
FVF	Formation Volume Factor
GOR	Gas / Oil Ratio
GWC	Gas / Water contact
IFAS	Infinite acting flow regime
MDT	Modular Dynamic Formation Tester
OWC	Oil / Water contact
PVT	Pressure-Volume-Temperature
RFT	Repeat Formation Tester
WFT	Wireline Formation Tester

NOMENCLATURE

A	cross-section area
B	formation volume factor
c_{sys}	total compressibility
C_1	constant for pressure on exponential model
C_2	constant for restricted zone
h	reservoir thickness
k	formation permeability
k_{rg}	gas relative permeability
k_{ro}	oil relative permeability
k_{rw}	water relative permeability
k_s	spherical permeability
p	pressure
P_b	Bubble Point Pressure
p_{dd}	final producing pressure
p_{est}	estimate reservoir pressure
p_i	initial reservoir pressure
p_t	pressure at time t
p^*	extrapolation pressure
q	Flow rate
Rs	Solution Gas / Oil Ratio
r_e	reservoir radius
r_s	probe radius
r_w	wellbore radius
s_o	oil saturation
s_w	water saturation
s_g	gas saturation
t	producing time
Δt	shut-in time

GREEK LETTERS

μ	fluid viscosity
φ	porosity
Δ	difference operator
θ	theta
α	alpha

CHAPTER I

INTRODUCTION

Today, wireline formation tester is one of methods which offer valuable information from a reservoir. Conventional wireline formation tester is known as Repeat Formation Tester (RFT), by Schlumberger, Formation Multi-Tester (FMT) by Baker Atlas, Selective Formation Tester (SFT) and Sequential Formation Tester (SFTT) by Halliburton. Conventional wireline formation testers have a fixed-volume pretest chamber from 5-cc to 30-cc. Generally, applications of pressure profile analysis include identification of fluid type, estimation of fluid properties, estimation of fluid contacts and hydrocarbon column heights, quantification of depletion and overpressure, etc. In this study the wireline formation tester is called Repeat Formation Tester (RFT).

Formation tests in low-permeability reservoir have been impeded by general problem, such as excessively long buildup time, supercharging, and loss of packer seals. A long pressure buildup time is not desirable because the possibility of the tools getting stuck would increase and waste of rig time. This problem results in abandonment of tests or incorrect reservoir pressures that also give false fluid gradients.

1.1 Methodology

This thesis studies the pressure response data from Repeat Formation Tester in low permeability reservoirs, focusing on pressure behavior and method to identify fluid type in a reservoir. The study is conducted by simulating the pressure response in a low permeability reservoir condition. A simple reservoir model was used to study the pressure response on the low permeability reservoir as follows:

1. Gather necessary information and construct a base reservoir model.
2. Design grid block to be used as a base case that characterizes reservoir properties, such as wellbore radius, reservoir boundary, reservoir thickness, porosity, permeability, reservoir pressure, and other information
3. Build the simulation model with the conventional probe with the smallest grid cell size equal to single probe's flow area for observe the pressure response in low permeability reservoir. The reservoir permeability is set as low as 0.1 mD with varying fluid types in the reservoir.
4. Run simulation software, ECLIPSE, to simulate pressure response in low permeability reservoir. Analyze pressure response in the low permeability reservoir.
5. Introducing the probe plugging due to partially or fully inserting into shale region (in the reservoir) and restricted zone assumption into the models. Various degree of restricted zone severity is created. The restricted zone assumption is brought into this study. The modification model is done by generating lower permeability grid block or shale region around the probe in 3-dimension.
6. Analyze the pressure response from simulation result to identify fluid type using pressure data.
7. Introducing the curve fitting method to estimate total testing time. Analyze the pressure response from simulation result to identify fluid type using pressure data at various buildup times.
8. Conclude the result obtained from simulation runs to justify if the result provides satisfying information.

1.2 Thesis Outline

This thesis consists of six chapters.

Chapter I is an introduction chapter for the study.

Chapter II is a reviewed chapter for the previous works on Repeat Formation Tester (RFT) in low permeability reservoir.

Chapter III is a theory and concept chapter that related to this study such as RFT concept, tight gas analysis, reservoir model for RFT, pressure gradient analysis, etc.

Chapter IV is a reservoir model chapter. The reservoir parameter and reservoir grid models of low permeability reservoir, fluid properties and SCAL data are presented.

Chapter V is simulation studies, results and analysis for oil and gas reservoir. The simulation data, pressure response analysis, result of the oil reservoir with several restricted zone permeability and also the method to identify fluid type in reservoir are presented.

Chapter VI is a conclusions and recommendations chapter that helped for further study based on this study point of view.

CHAPTER II

LITERATURE REVIEW

This chapter discusses and reviews previous works and developing on Repeat Formation Tester (RFT) in low permeability reservoir.

2.1 Repeat Formation Tester (RFT) in Low Permeability Reservoir.

Moran and Finklea [1] studied the pressure buildup analysis to determining permeability from wireline formation tester data and also studied the flow parameter such as rate of flow and flow geometry by assuming a single phase flow, homogeneous medium, and finite thickness. The result shows that in the early stage of pressure build up, the movement tends towards a spherical flow. Finally, spherical flow equation is used to estimate the reservoir pressure and permeability during the buildup period by plotting, $p_{(t_0+\Delta t)}\ vs.\ \frac{1}{\sqrt{\Delta t}} - \frac{1}{\sqrt{t+\Delta t}}$, the initial reservoir pressure and reservoir permeability can be determined.

Culham [2] studied the spherical flow regime by conducting a pressure buildup test in a well which did not completely penetrate the formation thickness. That is, the well only took up a small portion of the total thickness. Then, he derived the equations for determining static reservoir pressure, formation permeability, and skin factor. He verified the equations under a theoretical condition. By deriving and employing the continuous point source solution in spherical coordinates for an infinite reservoir with superposition principle, a plot of wellbore pressure during shut-in period versus $\frac{1}{\sqrt{\Delta t}} - \frac{1}{\sqrt{t+\Delta t}}$ should result in straight line with slope, m, where m = $A\sqrt{B}q\mu\beta_0/4\pi^{3/2}k\sqrt{n}$ and pressure interception, p*

Abbott *et al.* [12] studied the practical application of spherical flow transient

analysis and reviewed the theory for transient spherical flow by assuming homogeneous reservoir and neglecting skin factor. The analysis for spherical and hemi-spherical is the same though they differ in the probe position. If the probe locates in the middle of the thickness, the spherical flow is assumed. However, if the probe locates near the boundary, the hemispherical flow is assumed. They also provided the field example for analyzing spherical flow regime using Horner plot and Spherical flow plot to determine the formation pressure, and spherical permeability.

Smolen and Litsey [3] studied formation evaluation using the pressure data from wireline formation tester during the pretest stage. Pressure profile was collected from Webber sandstone reservoir. They found that reservoir pressure varied greatly and can be distributed erratically both vertically and horizontally. During the drawdown phase of the pretest, the pressure behavior showed that the minimum local permeability at that depth was based on a steady state spherical flow model.

Stewart and Wittman [5] studied the analytical theory of pressure buildup response associated with pretest stage. Both infinite and finite systems, as well as a layered reservoir, are considered. The spherical flow analysis method for the infinite acting case yielded an equivalent spherical permeability which was influenced by formation anisotropy. By knowing the buildup curve we can thus interpret the reservoir pressure.

Joseph and Koederitz [19] studied the unsteady state spherical flow and taking into account storage and skin by assuming homogeneous and isotropic reservoir while considering the effects of wellbore storage and damage skin. They derived and created type curve for the unsteady state spherical flow. By using the type curve, the permeability and skin were easy to determine. Then, replacing them back into the spherical solution, it will yield the formation pressure.

Raghavan et al. [28] analyzed the pressure build up of a short flow period. A method for converting build up data was discussed. This method can be used to combine buildup and drawdown data to obtain a longer band of data for type curve matching. This method can be used for constant rate production, constant pressure production and for the

case where both pressure and rate vary during production.

Kuchuk [20] studied a new method for interpretating the short producing time, compared to the Horner method. This new method deals with a unstable flow rate and an unidentified flow regime. This new method works well in the low permeability reservoir because frequently they do not sustain the flow rate long enough so the conventional interpretation method can be used. The build-up time to reach the reservoir pressure is reasonable for moderate and high permeability reservoir. However, for low permeability reservoir, the build-up time could be extremely long. It is important to determine the extrapolation reservoir pressure accurately. Therefore, he developed and modified the equation for the short producing time and also proved that a normal Cartesian plot of P_{ws} and $(1/\Delta t)^{1.5}$ will yield a straight line and extrapolated reservoir pressure is the same as that of the Horner method.

Soliman *et al.* [23] reviewed application of short term transient pressure testing of wells. The method called "FastTest" is developed, especially for analyzing build up tests with the short producing periods. Instead of using the principle of superposition to derive the solution for buildup test, the change in flow rate into boundary condition is included and directly solved the drawdown-buildup problem. The modified spherical flow equation needs only the total producing fluid in the equation, one does not need to know the flow rate of individual fluid. Furthermore, the time term in this equation represents the total testing time, i.e. from the start of flow through the buildup period. The generalized form for "FastTest" equation is given by $p_i - p_w = c\left(t_p + \Delta t\right).^{-1.5}$ The initial reservoir pressure can be solved by this equation.

2.2 Tight Gas Sand Analysis.

Lee [22] outlines the test design for pressure transient test for the tight gas formations. He tried to generate the testing procedure for tight gas formations. Base on field experience, in the low permeability reservoir, a well will rarely build up completely to discover the initial pressure following a production period. A common problem in low

permeability reservoir test is too short, not only too short in shut-in period but also too short in flow period that wellbore unloading is incomplete. This results in uninterpretable data. The test design procedure is that consists of wellbore unloading, afterflow, and estimated permeability equations. However, the buildup test design is not exact solution. The equation in test design is approximated by the end of wellbore storage distortion or afterflow. In terms of equivalent shut-in times, Δt_e, the duration of afterflow is given by $\Delta t_{e,wbs} = (200{,}000 + 12{,}000 s_a) C / k_g \frac{h}{\mu}$

Branagan and Cotner [25] studied the competent and practical approach to well testing and analysis in tight gas reservoirs. Well testing in low permeability gas reservoirs generally requires the quantitative information of reservoir parameters such as initial reservoir pressure, reservoir permeability, skin damage, and reservoir boundaries. Some of the compounding effects lead to wrong interpretation. First involved water base fluid invasion (overbalanced) and the second assumed that unmeasured quantity of gas was lost prior to well testing (underbalanced). Implicit reservoir simulator was used to model the various cases. The permeability input is ranged from 0.1 mD to 0.005 mD. In both cases, the result in extrapolation reservoir pressure yield an initial reservoir pressure but the permeability value is varied from 20% - 40% of the real value.

Yildiz and Langlinals [15] studied the field applications of wireline formation testers in low permeability gas reservoirs. Low permeability reservoirs usually release little or no fluid. In such formations, formation pressure cannot be measured since a full pressure build up cannot be obtained in a reasonable time. To improve the successful of wireline formation tester, the slow flow rate method was introduced. The test results are characterized by the flow rate, chamber size, the duration of drawdown, and the duration of the pressure buildup. The slow flow rate used drawdown portion as well as buildup portion of the pretest. The modified interpretation was introduced in term of sandface pressure term and permeability. More tests were needed to confirm the value of slow flow rate wireline formation tester.

Yildiz and Bassiouni [9] studied the interpretation of wireline formation tester data in the tight gas sand. An interpretation technique is based on type-curve matching. A

wireline formation test consists of three periods: decompression, drawdown, and buildup. In decompression period, pressure decline is due to the decompression of fluid in flowline. In drawdown period, pressure response is a function of the fluid decompression and formation flow. Because of limited flow from the low permeability reservoir, the pressure response is dominated by fluid expansion. When the buildup period started, the pressure in tool was buildup to initial pressure. When the buildup time is short, the interpretation may not be unique. Therefore, it is imperative to design tests so that a stabilized buildup pressure is reached. In this case, the flowline and pretest chamber volumes should be small.

Garcia *et al.* [26] studied a well test of tight gas reservoirs. Conventional well tests conducted in tight gas reservoir give a poor estimation of reservoir pressure and permeability value. So the appropriate test and analysis procedure for tight gas sand is required. The short term tests is considered to obtain reservoir pressure and permeability value. Too short buildup time causes the test interpretation to be non-unique and resulting in reservoir pressure to be significantly wrong. If the buildup time clearly reaches radial flow, analysis and extrapolation of buildup data gives a reservoir pressure that is reliable. When radial flow is not reached, the reservoir pressure estimated by radial flow analysis can be significantly low.

Jahanbani and Aguilera [21] studied well testing of tight gas reservoirs. Because of low permeability, a well will not initially flow at measurable rates and conventional well testing cannot be applied. For the short flow period, a very short radius of investigation is developed and the quality of the data may be poorer than conventional tests. To analyze a buildup test, the testing time should exceed the wellbore storage distortion, unloading or afterflow periods. Most of the methods for analysis of short tests focus on late time data. Pressure data must contain at least some part of the reservoir dominated flow accurate analysis.

Kumar *et al.* [18] studied the use of wireline formation tester for optimization of conventional well test design and interpretation in tight gas sand. An estimation of pressure, fluid properties and permeability obtained from wireline formation tester,

together with simulation software can provide a better result in large scale well testing. In low permeability formations it may not be possible to withdraw fluid from the formation at a sufficient rate. In this study the wireline formation tester was used in the combination of very low permeability and high temperature reservoir. Permeability results in range of 0.0185 mD to 0.02 mD, and the gas flow rate is 0.31 MMscf/d. From these data it is possible to make more information decisions and improving efficiency concerning DST program as well as prioritizing the tested zone.

From the previous study, low permeability reservoirs usually release little or no fluid. Because of limited flow from the low permeability reservoir, the pressure response is dominated by fluid expansion. Some of the compounding effects lead to wrong interpretation. Most of the model is assumed by water base fluid invasion (overbalanced) drilling and supercharge effect. But this study is aimed to study the pressure response in a low permeability reservoir with shale (restricted zone) and determine fluid type in the reservoir. The concept of restricted zone is introduced to take into account shale in a reservoir that may cause difficulty in fluid flow into a probe when the probe is inserted into the shale region in the reservoir. Finally, it hopes that this assumption can assist to describe the low permeability reservoir that experience with long buildup time.

CHAPTER III

THEORIES AND CONCEPTS

3.1 Repeat Formation Tester

Repeat Formation Tester (RFT) is a tool run on an electrical cable. The tool inserts a probe into a formation, allowing production into a small chamber. The tool function is primarily used to obtain formation pressures at targeted locations and permeability estimates may be obtained by pressure analysis. This type of measurement provides formation pressures along the well and gives a measure of pressure with depth. The formation pressure with depth provides an estimation of the fluid gradient, and a change of fluid gradient may indicate a fluid contact.

3.2 Repeat Formation Test Concept

Early RFT were designed primarily to collect fluid samples. Pressures were recorded so that the pressure buildups at the end of sampling could be analyzed to determine permeability and reservoir pressure. The RFT tool introducing the pretest, a short test, turned out to be the representative of reservoir pressure and permeability. As a result, pressure measurements became the main wireline formation tester application. A reservoir pressure is obtained by withdrawing small amount of fluid (10-20 cc) from the reservoir to generate a short transient test. Finally, pretest pressures produced a reservoir pressure versus depth. Plotting the pressure data versus true vertical depth shows the striking linear trends corresponding to gas, oil and water gradients.

To perform a test, the tool is stopped at a specific depth. Then, the packer moves out one side and the backup pistons move on the opposite side. The body of tool is held away from the borehole wall to reduce the chances of differential sticking. Finally the probe is embedded in the reservoir. The pretest chamber is automatically activated every time the tool is set, withdraw 10 cc of fluid. The rate of fluid withdraw is varied by tool

or downhole conditions but it is in the range of 0.5 cc/s to 3 cc/s. These samples are not saved. Figure 3.1 shows the RFT tool configuration.

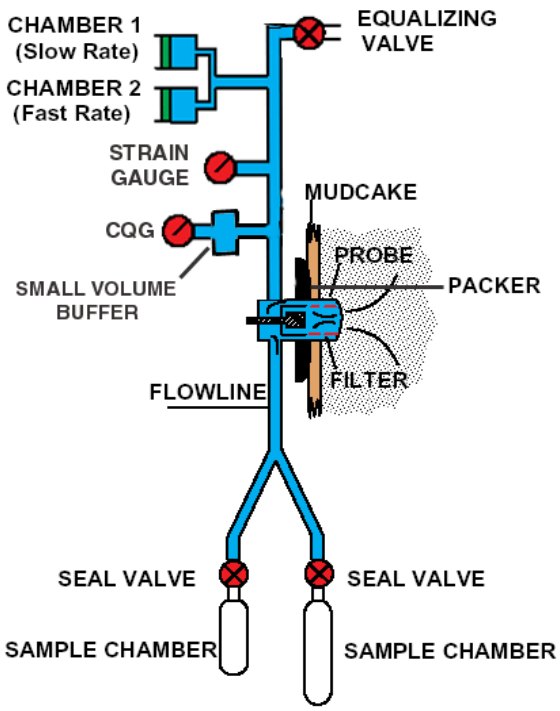

Figure 3.1 : RFT tool configuration[30]

The conventional RFT contains two types of gauge, strain gauge and crystal quartz gauge (CQG), a strain gauge pressure transducer is located in the flowline to monitor the pressure during the test. The CQG (Crystal Quartz Gauge) is a high accuracy, high stability permanent gauge. The CQG design implements pressure and temperature measurements made at the very same location. The pressure continuously recorded at surface both digital and analogue form, given pressure drawdown data and subsequent pressure buildup data whenever the pretest is conducted. A typical pressure data on the record shows initially the mud hydrostatic. When the tool is set, the pressure slightly increase because of the compression of the mudcake by the packer. Then the piston probe retracts and the pressure drops due to the tool flowline storage effect and communication with the reservoir. When the piston stops, the pressure builds up again because the packer

still compress to the mudcake until the tool is fully set. Next the pressure drops as a 10 cc pretest chamber begins moving at a constant rate, this time marked as t_0. When the pretest chamber is full at time t_p , the pressure builds up toward a final pressure, the running time used for pressure analysis, Δt, start to count at t_p. Pressure buildup curve analysis yields the reservoir pressure and permeability. Finally, after the tool is retracted, the mud hydrostatic is measured again as shown in Figure 3.2.

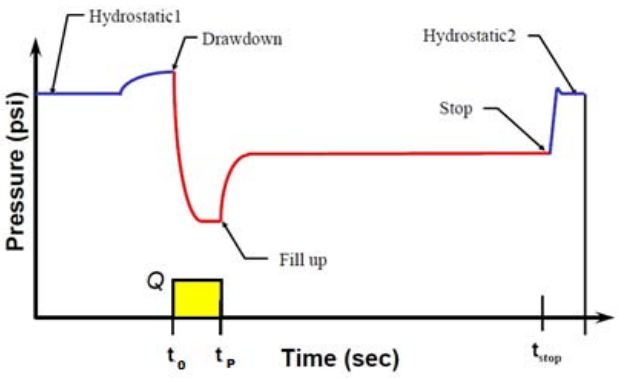

Figure 3.2: Pressure response from pretest sequence[31]

The drawdown period is used to clean up the reservoir. The buildup period provides a first estimate of reservoir pressure such as initial reservoir pressure or mobility. Pressure tests in low-permeability reservoir have been impeded by problems, such as excessively long buildup time. Most of the pressure in the low permeability reservoir cannot build up to its final pressure, build up times can be long and the confidence level of the final pressure is often uncertain. The extrapolation of spherical plot can determine the reservoir pressure.

3.3 Flow Regime

Repeat Formation Tester concept uses the same concept as advance well test analysis, thus basic equation, diffusion equation, was brought to solve the problem. To analyze pressure response in the reservoir the spherical flow is considered.

Spherical flow occurs when a vertical well is partially penetrated or during RFT/MDT/WFT tests. Spherical flow is the occurrence of radial flow in both the horizontal and vertical directions. When a well is partially penetrating or partially completed into the formation, the well is connected to the producing interval (pay thickness) on one fraction of the zone only. As the contact area between the reservoir and the well is reduced, some fluid have to travel further through the formation to get produced through the wellbore.

Spherical flow regime is also occurs when the predominant flow pattern in the reservoir is toward a point sink or source. When fluid in reservoir flow into the probe, which has a smaller diameter than reservoir size, the flow regime is spherical as shown in Figure 3.3.

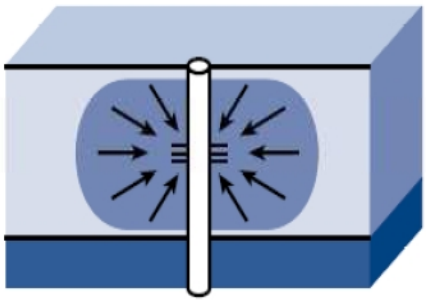

Figure 3.3 : Spherical flow regime in reservoir[32]

Traditional interpretation technique, spherical flow equation is used to estimate the reservoir pressure and permeability during the buildup period. In 1962, Moran and Finklea developed the spherical flow equation.

$$P_{(t)} = P_i - \frac{\mu}{2\pi k}\sqrt{\frac{\alpha}{\pi}}\,\frac{V}{t}\left[\frac{1}{\sqrt{\Delta t}} - \frac{1}{\sqrt{t+\Delta t}}\right] \qquad (3.1)$$

Where

μ = fluid viscosity (poises)

k = formation permeability (cm^2)

α	=	$\mu c\phi$ /k (sec/cm^2)
c	=	compressibility (cm^2/dyne)
V	=	total volume of fluid produced (cm^2)
t	=	total producing time (sec)
Δt	=	shut-in time (sec)
P_i	=	initial reservoir pressure (dynes/cm^2)
$P_{(t)}$	=	pressure at any time t (dynes/cm^2)
A	=	cross-sectional area (cm^2)
h	=	bed thickness of interval tested (cm)

In this study, the spherical flow equation is as follows:

$$P_{(t)} = P^* - 8 \times 10^4 \left(\frac{q\mu}{k_s}\sqrt{\frac{\mu C_{sys}\emptyset}{k_s}}\right)\left(\frac{1}{\sqrt{\Delta t}} - \frac{1}{\sqrt{t+\Delta t}}\right) \qquad (3.2)$$

Where

$P_{(t)}$	=	pressure at time t (psi)
P*	=	extrapolated formation pressure (psi)
q	=	volumetric flow rate (cc/s)
μ	=	fluid viscosity (cp)
k_s	=	spherical permeability (mD)
c_{sys}	=	total compressibility (psi^{-1})
Ø	=	porosity (fraction)

t	=	producing time (sec)
Δt	=	shut-in time (sec)

A plot of observed pressure during the buildup versus spherical time function, yields the straight line function with the slope, m. Extrapolation of this straight line to infinite time, yields the extrapolated reservoir pressure, P*.

3.4 Low Permeability Reservoir

Tight gas is the term commonly used to refer to low-permeability reservoirs that produce mainly dry natural gas. Many of the low permeability reservoirs developed in the past are sandstone, but significant quantities of gas also are produced from low-permeability carbonates, shales, and coal seams.

Weathering, erosion, and deposition, which themselves are controlled by many factors, determine reservoir character from reservoir type and size to grain sizes, porosity and permeability, and type of cement. Grain sizes can be widely variable and related directly to the mineral composition, type of weathering, and ultimate environment deposition. Small, cemented grains usually indicate lower porosity and permeability than large and uncemented grains, which provide greater porosity and permeability. Figure 3.4 shows the grain size distribution and porosity. This means that rocks consisting well-sorted grain are better reservoirs than rocks that contain poor-sorted grains. The clean sandstone, but contain poor-sorted grains will have poor porosity and permeability like mudstone that containing a variety of grains from very coarse to very fine. Figure 3.5 shows the grain size and permeability relation.

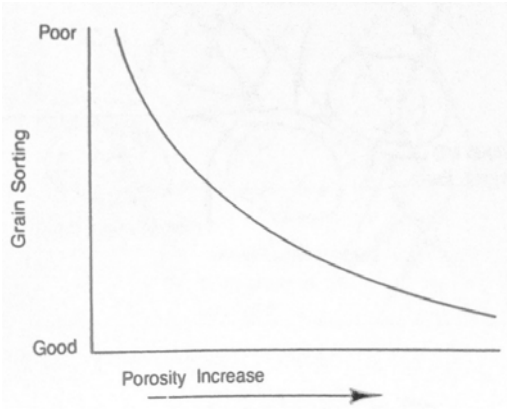

Figure 3.4: Relationship between grain sorting and porosity[29]

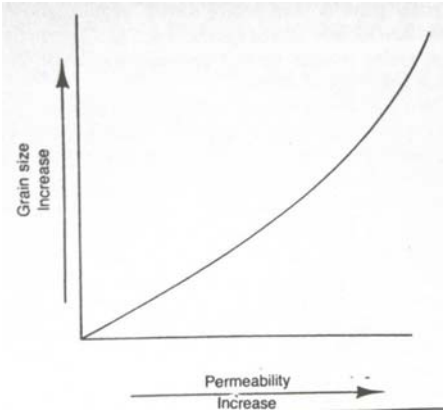

Figure 3.5: Relationship between grain size and permeability[29]

In the 1970s, the U.S. government decided that the definition of a tight gas reservoir is one in which the expected value of permeability to gas flow would be less than 0.1 mD. The permeability cut off of 1mD for oil and 0.1mD for gas are set to define net pay (Law et al., 2001). The best definition of tight gas reservoir is “Reservoirs that cannot be produced at economic flow rates nor recover economic volumes of natural gas unless the well is stimulated by a large hydraulic fracture treatment or produced by use of a horizontal wellbore or multilateral wellbores.” A tight gas reservoir can be deep or shallow, high-pressure or low-pressure, high-temperature or low-temperature, blanket, homogeneous or naturally fractured, and can contain a single layer or multiple layers. Figure 3.6 shows the unconventional resort triangle.

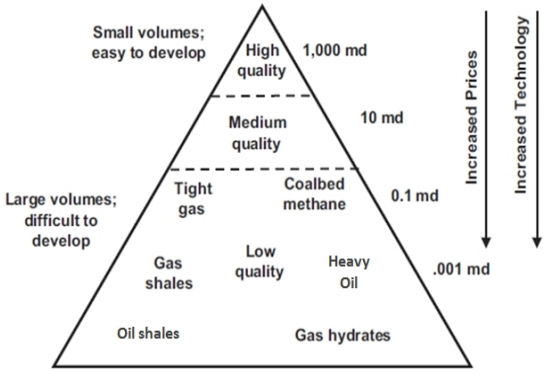

Figure 3.6: Resource triangle for oil and natural gas[27]

The validation for most conventional oil and gas reservoirs, the processes resulting in similar rock properties may not be unique, especially when the rocks have been subject to significant diagenesis. Therefore, three rock types were integrated depositional, petrographic rock type, and hydraulic. Each rock type represents different physical and chemical processes affecting the rock properties during both depositional and paragenetic cycles. The low-permeability structure and the response to overburden stress have a strong impact on the low-permeability structure and the relative permeability relationships. In low-permeability reservoirs there cannot be a broad range of water saturations in which neither gas nor water can flow. In some very low-permeability reservoir, there is virtually no mobile water phase even at very high water saturations. The low permeability of these reservoirs slows down their response to pressure transient testing so it is difficult to obtain dynamic reservoir properties and, therefore, to characterize gas reserves. Moreover, the determination of real composition of fluids trapped in tight reservoirs is very challenging, since recovered fluid often reflects the composition of the ones related to largest pores, interstices and invaded zone.

3.5 Tight Gas Sand Analysis and Tool Storage Effect

Conventional RFT interpretation techniques are primarily based on the spherical flow model, which simplifies the fluid-flow configuration. This model yields acceptable estimates of permeability in medium to high permeability formations. In tight gas sands, however, the model fails to provide a representative estimate of the reservoir

pressure and reservoir permeability.

During the pressure tests in the low permeability reservoir, the pressure recorded by the pressure response of the RFT is affected by the formation fluid flow, the flowline fluid volume, and the flowline fluid compressibility. This phenomenon is called the flowline storage effect. The flowline storage effect was not significant in the high-permeability formation because the drawdown pressure stabilized rapidly. Because the fluid flow from the formation is slow, the flowline storage effect has a significant impact on both the pressure drawdown and buildup phases of the low permeability reservoir test. The drawdown pressure did not reach steady state within the test period. The drawdown permeability could not be determined in the low permeability reservoir because the drawdown pressure remained in the wellbore storage. No straight line exists for either model for low permeability reservoir. Therefore, the pressure-buildup-analysis method based on the slope of a portion of a straight line cannot be applied to determine the reservoir pressure and reservoir permeability. Hence, the flowline storage effect must be considered when interpreting low permeability reservoir

Base on the limited study and laboratory work, it is concluded that the early time of RFT may develop in six phases. The phase and the corresponding pressure profile are shown in Figure 3.7a to 3.7c.

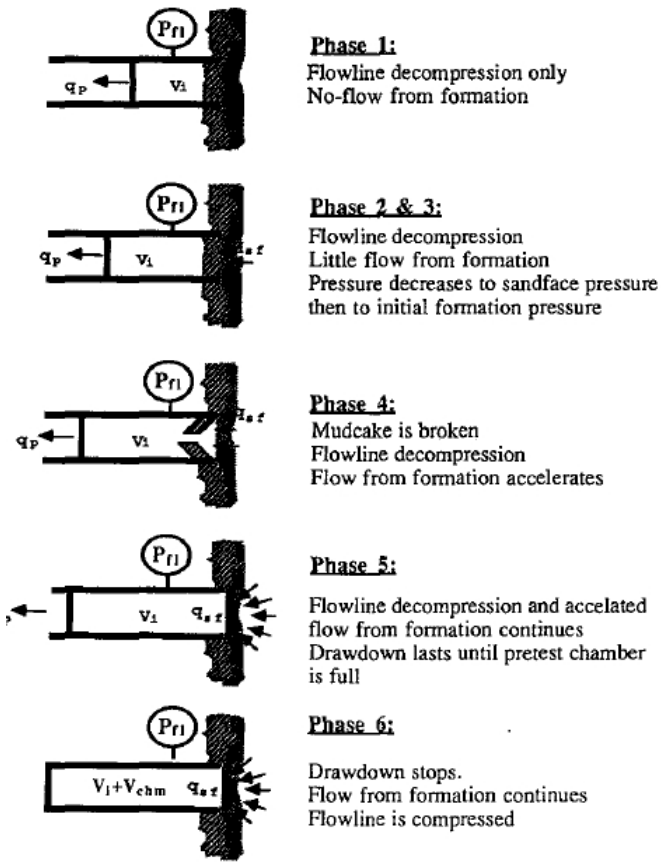

Figure 3.7a: Repeat Formation Tester flow sequence[9]

Phase 1: After the piston is activated, the chamber volume increases and the flowline fluid decompress. Because the pressure in the tool is initially higher than the sandface pressure, there is no flow from the formation. This phase continues until the tool pressure is equal to the sandface formation pressure.

Phase 2: The formation may respond to the test when the pressure in the tool becomes less than the sandface pressure. In this phase, the pressure response is a function of flowline fluid decompression and limited formation flow. However, the pressure response is controlled by tool storage effect. This phase lasts until initial formation pressure is reached.

Phase 3: The contribution of the formation increases after the initial formation

pressure is attained. Decompression of the flowline continues.

Phase 4: When a sufficient differential between the tool and initial formation pressure is established, the mudcake may be broken. A limited number of field and laboratory tests have shown that the mudcake pop-off yields a "bump" on the pressure response curve when the flow rate is low enough, as Figure illustrates.

Phase 5: After the mudcake pop-off, the contribution of the formation is accelerated. Even in this phase of the test, depending on the size of the flowline, tool storage effect may still be a dominant factor. Drawdown continues until the pretest chamber is full.

Phase 6: Once the drawdown period is stopped, the formation-fluid flow toward the tool compresses the formation and flowline fluid back to pretest conditions. Based on limited experimental and field data, it is believed that the pressure in the tool builds up to the initial supercharged sandface pressure provided the test lasts long enough.

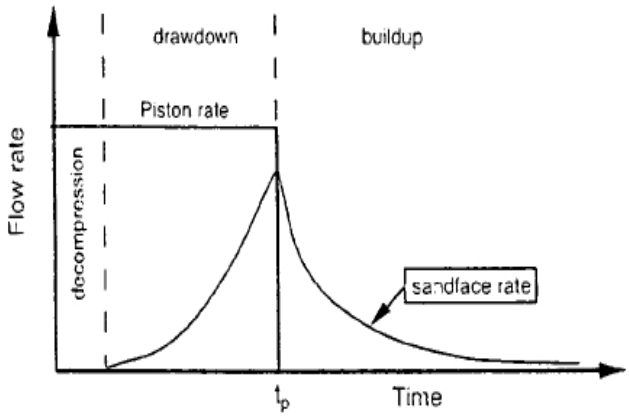

Figure 3.7b: Flow rate for RFT flow sequence[9]

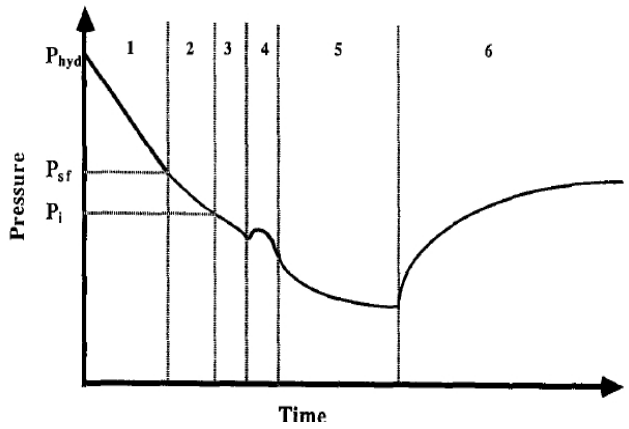

Figure 3.7c: Pressure response for RFT flow sequence[9]

For the decompression period, pressure decline is due to the decompression of fluid in flowline. For the drawdown period, pressure response is a function of the fluid decompression and formation flow. Because of limited flow from the low permeability reservoir, the pressure response is dominated by fluid decompression. When the buildup period started, the pressure in tool was buildup to initial pressure. The factors complicating the modeling and analysis of wireline formation tester are decompression period prior to formation flow, flowline storage effect and supercharging effect.

The flowline storage effect is happened after the fluid decompression. Typically flowline volume ranges from 50 to 500 cc and the pretest chambers volume ranges from 5 to 20 cc. Under these conditions, the decompression of fluid and compression of flowline fluid result in the sandface flow rate. The decompression of fluid and compression of flowline fluid is referred to flowline storage effect. The flowline storage effect is the same concept of wellbore storage effect observed in pressure drawdown and buildup tests.

3.6 Reservoir Model for Wireline Formation Tester

RFT is an openhole logging technique where data are used to determine initial reservoir pressure, vertical pressure distribution, fluid contact and formation permeability. RFT consists of one or two drawdown periods and a build up period. The use of the RFT pressure data for permeability and initial reservoir pressure evaluation was first proposed by Moran and Finklea. The study assumed spherical flow geometry. Now a 3D steady state model in Cartesian coordinates and 3D transient model in radial coordinates are employed.

3.7 Mathematical Modeling

The flow into the RFT probe is a 3D phenomenon, and the flow pattern is convergent. A schematic of the flow pattern during the test is shown in Figure 3.8.

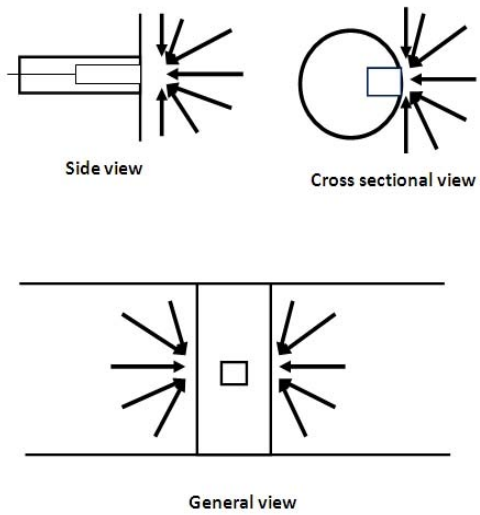

Figure 3.8: Flow pattern during the test

The formulation of the 3D convergent flow into the probe requires the assumption that

1. Darcy's law is valid
2. Single phase flow exists
3. Constant or small fluid compressibility
4. Homogeneous reservoir
5. RFT probe is square
6. No supercharge effect
7. Constant drawdown rates

3.8 Pressure Gradient Analysis

Pressure-depth plots are the most common interpretation tool used for RFT pressure data. Typical applications of pressure profile analysis include (1) identification of fluid type, (2) estimation of fluid properties, (3) estimation of fluid contacts and hydrocarbon column heights, (4) quantification of depletion and overpressure. A plot of formation pressure (either read directly or derived from build-up plots) against depth can give a large amount of valuable information to the reservoir engineer. The extrapolation pressure result from each sampling point will plot on pressure versus depth plot to identify pressure gradient. Figure 3.9 shows the pressure versus depth plot for reservoir fluid identification. Table 3.1 exhibits the typical fluid gradients.

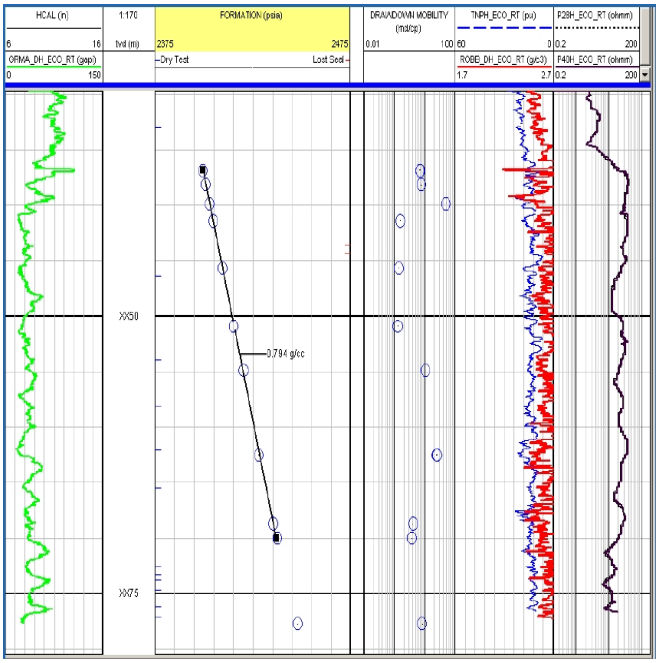

Figure 3.9: Pressure gradient plot example [33]

To calculate the gradient, care should be taken to use true vertical depths rather than logged depths. The pressure gradient can be interpreted in terms of formation fluid density by applying equation.

$$Fluid\ density\ (ppg) = \frac{pressure\ gradeint\ (psi/ft)}{0.052} \qquad (3.3)$$

Table 3.1 : Typical fluid gradients

Fluid	Pressure gradient		
	psi/ft	g/cc	psi/m
Gas	0.04 - 0.09	0.1 - 0.2	0.12 – 0.27
Sour gas (H_2S)	0.08 - 0.26	0.2 - 0.6	0.24 – 0.79
Oil	0.29 - 0.37	0.68 - 0.85	0.88 – 1.12
Water/Filtration	0.41 - 0.45	0.95 - 1.05	1.24 – 1.36
Mud Fluid	0.43 - 0.86	1.00 -2.00	1.30– 2.60

3.9 Curve Fitting

Curve fitting is the process of constructing a curve, or mathematical function, which has the best fit to a series of data points. Curve fitting can involve either interpolation, where an exact fit to the data is required, or smoothing, in which a "smooth" function is constructed that approximately fits the data. Smoothing algorithms are widely used to remove noise from a data set while preserving important patterns. It is usually impossible to describe a phenomenon totally. Therefore one usually strives for a set of equations which describes the physical system approximately and adequately.

A related topic is regression analysis, which focuses more on questions of statistical inference such as how much uncertainty is presented in a curve that is fit to data observed with random errors. Fitted curves can be used as an aid for data visualization, to infer values of a function where no data are available, and to summarize the relationships among two or more variables. Extrapolation refers to the use of a fitted curve beyond the range of the observed data, and is subject to a greater degree of uncertainty since it may reflect the method used to construct the curve as much as it reflects the observed data.

In general, once a set of equations has been indentified, the data generated by the equations are compared with real data collected from the system (by measurement). If the two sets of data "agree" (or are close), then it is confident that the set of equations will lead to a good description of the real-world system.

The purposes of fitting equations are:

1. To arrange data in the form that can be further analyzed,
2. To fit an acceptable correlation to the data.

The basic assumption for build the model

1. The model is used only the pressure buildup section. Time scale is buildup time (Δt, second).

2. The model is valid for the normal pressure gradient profile. The estimation parameter is shown below.
3. The pressure profile in this model is generated by the assumption of restricted zone/near probe concept.

The exponential model in this buildup study has the following equation

$$P_{(t)} = P_{dd} + (C_1) * \left(1 - e^{-\frac{\Delta t}{C_2}}\right) \quad (3.4)$$

Where

$P_{(t)}$ = pressure response at time t, psi

P_{dd} = final pressure drawdown, psi

P_{est} = estimate pressure, (0.433 * TVD), psi

Δt = buildup time, sec

C_1 = constant for pressure, P_{est} - P_{dd}

C_2 = constant for each restricted zone/near probe permeability

From the equation, every parameter can be determined directly from data but constant C_2 is only one unknown left in this equation. So, the objective consists of adjusting the parameters of a model function to best fit a data set. The coefficient of equation is obtained by minimizing the sum of squares of the residuals, the differences between each observed value and its corresponding fitted value. The estimation is solved by iterative refinement, each iterations the system is approximated by a linear one. The iteration process continues until the estimation reaches the minimum value of squares of residual. Figure 3.10 shows the typical exponential model.

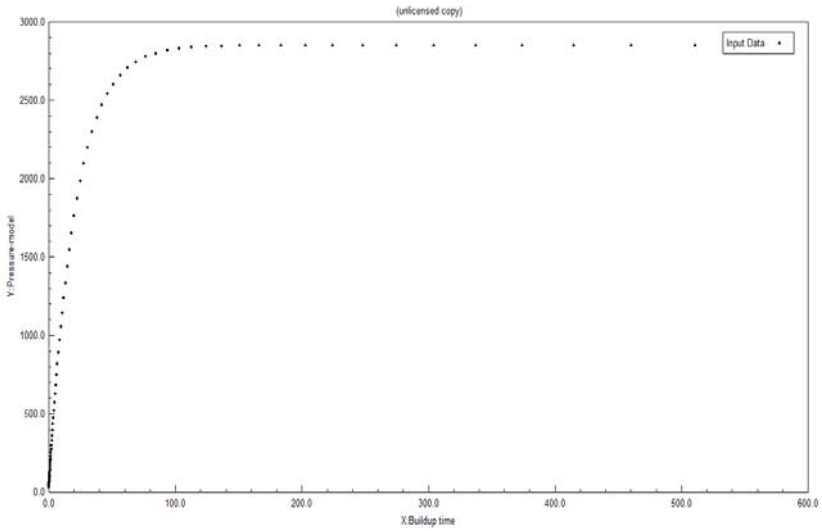

Figure 3.10: Exponential model plot

CHAPTER IV

RESERVOIR MODEL

4.1 Reservoir Model

Classical problem of formation test in low permeability reservoir is excessively long buildup time. To study and analyze the pressure response, some reservoir parameters and fluid properties are used to generate the low permeability condition such as a typical range of permeability, porosity value, reservoir thickness, PVT, and SCAL data. By using ECIPSE black oil simulator, the black-oil simulator used in this thesis is based on a fully-implicit finite-difference solution of the multi-phase fluid flow equation. Initial reservoir conditions and numerical grid specification is also defined based on field data. A single well model with RFT probe is used to simulate pressure response in a low permeability reservoir condition. The base case reservoir permeability is set as low as 1mD for oil reservoir and 0.1mD for gas reservoir. After observing and analyzing the pressure response from low permeability reservoir, probe plugging or restricted zone assumption could be one of the problems that slows the pressure response in the low permeability reservoir. The modification model is brought to the study instead of the base case model. The simulator gives pressure versus time and withdraw rate versus time records.

The base case model is a circular boundary, radial grid model with dimension containing of 50 x 20 x 462 grid blocks in the r, θ (starting in clockwise and counterclockwise direction reference to probe direction), and z directions, respectively. The fluid flows area is calculated from probe's flow area for standard probe. The standard probe cross sectional area is 0.1521 square inches then the initial size of the grid block is calculated base on this area.

Initially, radial and theta absolute porosity and permeability for low permeability reservoir are input as 0.12 and 1 mD, respectively, with isotropic reservoir. Probe plug

and restricted zone effect is simulated by assigning low permeability values (range from 0.1 mD to 10^{-7}mD) to specify grid block representing difference severity for the probe plug and restricted zone effects. The other detailed reservoir parameters and conditions are depicted in Table 4.1 and Figure 4.1a and 4.1b.

Table 4.1 : Model properties.

Radius Direction								Theta direction			
n	Δr	n	Δr	n	Δr	n	Δr	n	ΔΘ	n	ΔΘ
1	0.04589	14	0.39448	27	3.391	40	29.1493	1	7.29644	11	33.4915
2	0.05415	15	0.46548	28	4.00126	41	34.3951	2	9.29115	12	28.5316
3	0.0639	16	0.54925	29	4.72135	42	40.585	3	10.9063	13	24.3062
4	0.07539	17	0.64809	30	5.57103	43	47.8889	4	12.8022	14	20.7066
5	0.08896	18	0.76473	31	6.57362	44	56.5073	5	15.0277	15	17.6401
6	0.10497	19	0.90235	32	7.75664	45	66.6766	6	17.6401	16	15.0277
7	0.12386	20	1.06474	33	9.15257	46	78.6761	7	20.7066	17	12.8022
8	0.14616	21	1.25636	34	10.7997	47	92.835	8	24.3062	18	10.9063
9	0.17246	22	1.48246	35	12.7433	48	109.542	9	28.5316	19	9.29115
10	0.20349	23	1.74925	36	15.0366	49	129.256	10	33.4915	20	7.29644
11	0.24012	24	2.06405	37	17.7427	50	152.517				
12	0.28333	25	2.43551	38	20.9358						
13	0.33432	26	2.87381	39	24.7035						

Δz-direction
0.0325

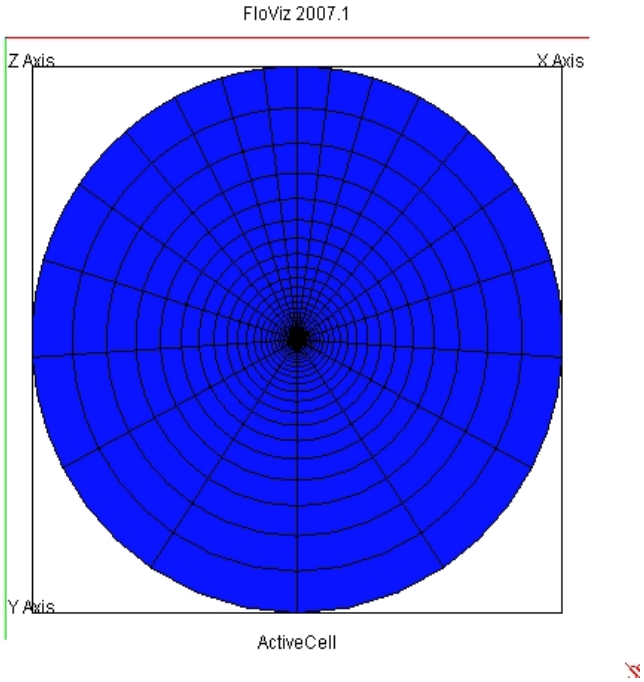

Figure 4.1a: Schematic reservoir description in top view

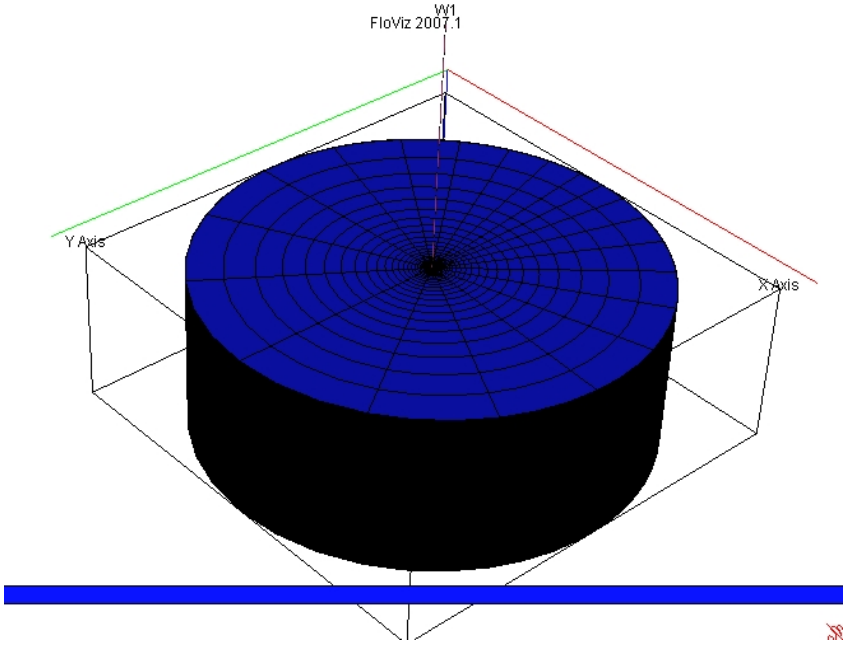

Figure 4.1b: Schematic reservoir description in 3D

4.2 Restricted Flow Model

For the restricted flow assumption as the probe inserted partially or fully into shale region in the reservoir, the modification model is used instead of the base case model.

1. Probe restricted flow occurs in probe grid block. So, the permeability value is modified by reducing from original permeability value.
2. Permeability of the probe block is reduced from the original reservoir permeability by multiplying by 0.1 in all direction. So, the probe block permeability varies from 0.1 to 10^{-7} mD
3. This assumption neglects the probe plugging and the restricted flow permeability in this study is called k_c

Figure 4.2 shows the flow direction into the probe. Figure 4.3 and 4.4 show the reservoir grid model for probe restricted flow assumption.

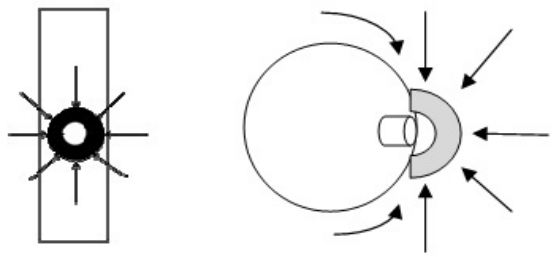

Figure 4.2: Flow geometry of the restricted zone model

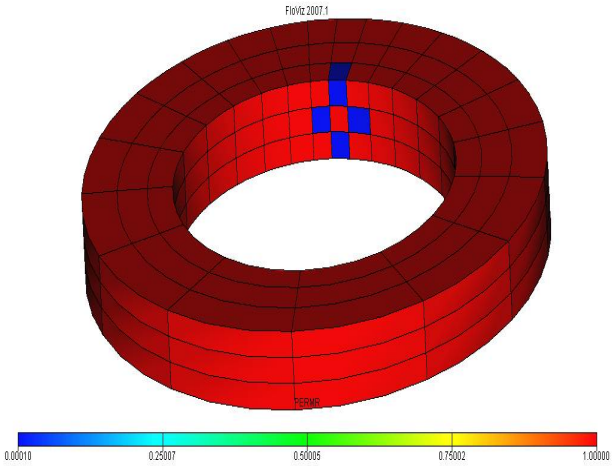

Figure 4.3: Reservoir grid model for the restricted zone assumption in 3D

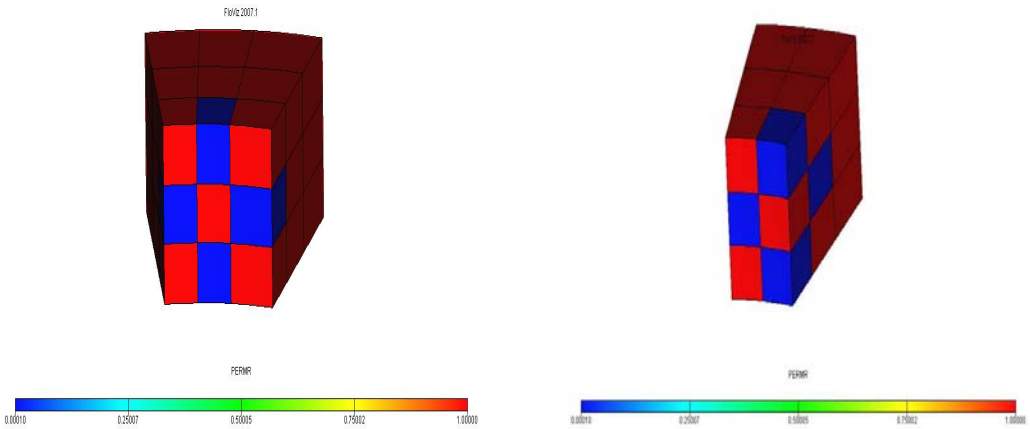

Figure 4.4: Cross sectional view for the restricted zone assumption

4.3 RFT Parameter and Fluid Properties

Table 4.2 and 4.3 show reservoir parameters and RFT parameter that are used in this study. Figure 4.5 shows schematic for RFT probe location for a base case.

Table 4.2: Reservoir parameter

Geometry	radial	-
Boundary	no flow	-
Reservoir radius	1,000	feet
Well bore radius	0.255	feet
Top reservoir depth	6,560	feet
Thickness	15	feet
Permeability	1/0.1	mD
Porosity	12	%
Pressure at datum depth	2850	psia
Reservoir temperature	285	F
Oil SG	0.89	
Gas SG	0.79	
Water SG	1	
Water Salinity	0.1374	%
CO_2	20.66	%
H_2S	0.001362	%
N_2	0.008	%
GOR	400	scf/bbl
Rock compressibility	5.41E-06	psia

Table 4.3: RFT parameter

RFT specification/ Conventional probe	Value	Unit
Probe area/ Probe radius	0.1521/0.22	in^2/in
No. of grids – Radial, Theta and z direction	50 x 20 x 462	-
Vertical-Direction grid size	0.0325	ft
Theta-Direction 1st grid size	7.2964	°
Radius-Direction 1st grid size	0.04589	ft
Probe position 1	6,571.25/346	ft/Grid no.
Probe position 2	6,567.50/231	ft/Grid no.
Probe position 3	6,563.75/115	ft/Grid no.
Pre test volume	10	cc
Pretest rate (single rate, oil/gas)	1/60	cc/sec

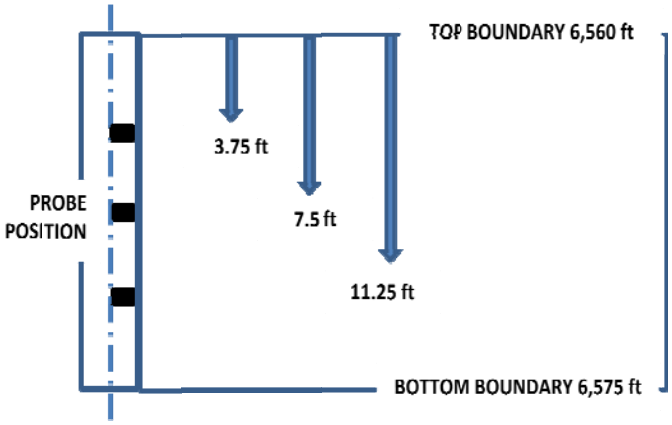

Figure 4.5: Schematic for RFT probe location for a base case and modification model

Table 4.4: Grid position for probe plugging

Depth (ft)	Grid number
6,571.25	346
6,567.50	231
6,563.75	115

Table 4.5: Grid position for restricted zone effect

Depth (ft)	Grid no.	Restricted zone grid no. (r,θ,z)				
6,571.25	346	1,1,345	1,1,347	1,2,346	1,20,346	2,1,346
6,567.50	231	1,1,230	1,1,232	1,2,231	1,20,231	2,1,231
6,563.75	115	1,1,114	1,1,116	1,2,115	1,20,115	2,1,115

Tables 4.7 and 4.8 show reservoir fluid properties which are formation volume factors and viscosity versus depth that were used in this study.

Table 4.6: Oil formation volume factor and oil viscosity

Pressure	B_o	μ_o
1595.52	1.314	0.261
1657.90	1.312	0.263
1736.84	1.309	0.265
1815.79	1.306	0.267
1894.74	1.303	0.269
1973.68	1.301	0.271
2052.63	1.299	0.274
2131.58	1.297	0.276
2289.47	1.293	0.281
2368.42	1.292	0.284
2447.37	1.29	0.287
2526.32	1.289	0.29
2605.26	1.288	0.293
2684.21	1.286	0.296
2763.16	1.285	0.299
2850.00	1.284	0.303

Table 4.7: Gas formation volume factor and gas viscosity

Pressure	B_g	μ_g
54.96	67.77	0.013
95.21	39.00	0.013
135.47	27.34	0.013
296.49	12.35	0.014
336.74	10.84	0.014
457.51	7.92	0.014
658.79	5.43	0.014
819.81	4.32	0.015
1061.34	3.29	0.015
1343.13	2.57	0.016
1785.94	1.89	0.017
1906.71	1.77	0.017
2269.01	1.48	0.018
2389.78	1.40	0.018
2671.57	1.25	0.019
2850.00	1.18	0.019

Figure 4.6 shows the oil and water relative permeability curves at different water saturation that are used in this study. At initial, the initial water saturation is 0.20 and the end point oil relative permeability is 0.500.

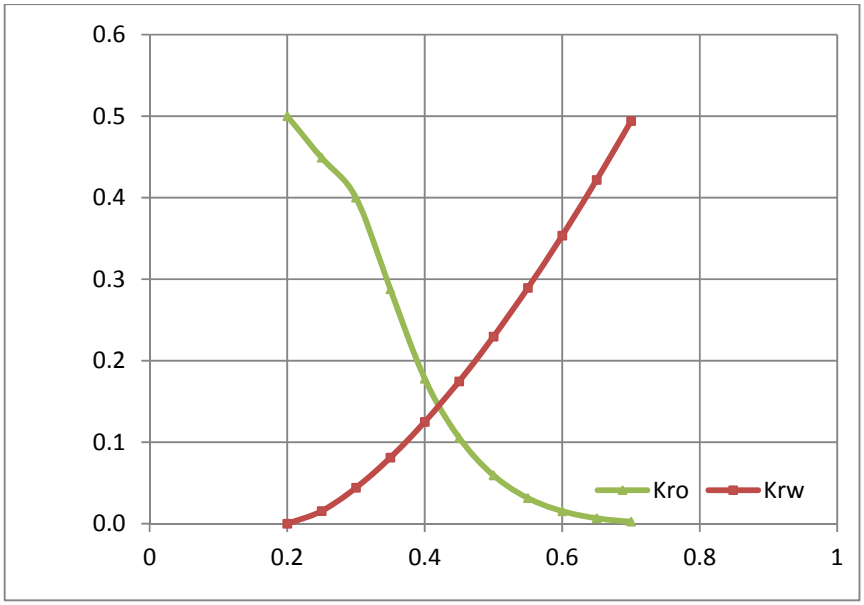

Figure 4.6: Oil and water relative permeability

Figure 4.7 shows the gas and water relative permeability curves at different water saturation that are used in this study. At initial condition, the initial gas saturation is 0.80 and the end point gas relative permeability is 0.800.

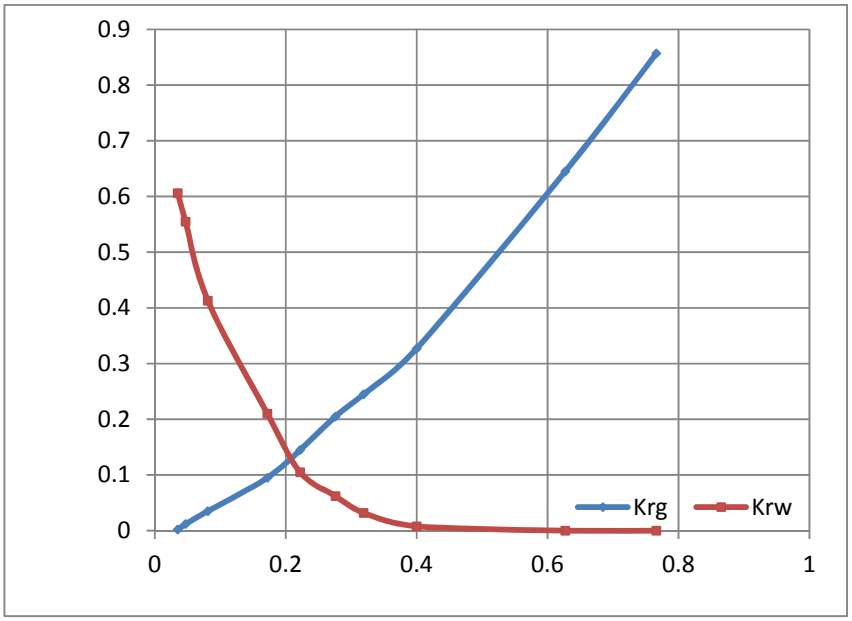

Figure 4.7 : Gas and water relative permeabil

CHAPTER V

SIMULATION STUDIES, RESULTS AND ANALYSIS

5.1 Pressure Response in Low Permeability Oil Reservoir

The base case is used as a reference pressure response from the low permeability reservoir. In this study, the permeability input is isotropic and ranges from 0.1mD to 100mD, pretest chamber is 10cc and the fluid withdraw rate is fixed to 1cc/sec. The buildup period is varied for each case. The long buildup period is allowed to reach stabilized condition and to apply the spherical flow assumption. For the general RFT procedure, the buildup time over a 30- minute is abandoned due to the following two reasons: 1) a long time spent waiting for pressure buildup increases the possibility of the tools stuck downhole and 2) waiting for a pressure buildup under such a situation consumes non-productive rig time. Therefore, total testing time is set to 30-minute in order to observe pressure response. Figure 5.1 shows schematic for base case. There are 3 sampling points at 6,571.25ft, 6567.5 ft, and 6,563.75 ft. Figure 5.2 shows the sampling point for base case

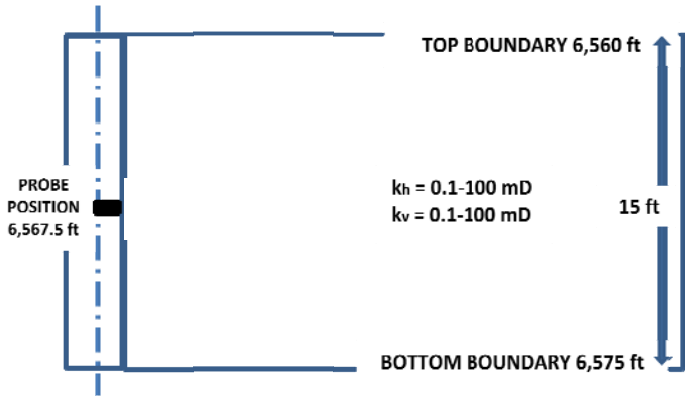

Figure 5.1: Schematic reservoir description for the base case oil reservoir

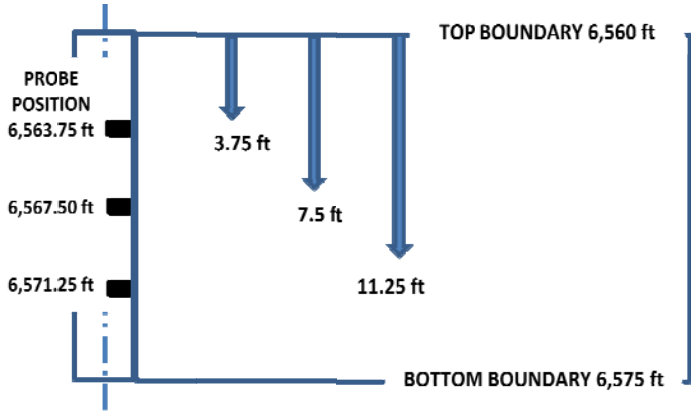

Figure 5.2: Schematic sampling points for base case oil reservoir.

From simulation result, the base case pressure response during producing and buildup time is shown in Figure 5.3. Figure 5.4 and Table 5.1 show other results from the simulation such as initial pressure, final drawdown pressure, fluid volume in pretest chamber and time to reach initial pressure (stabilized time) by different reservoir permeability value.

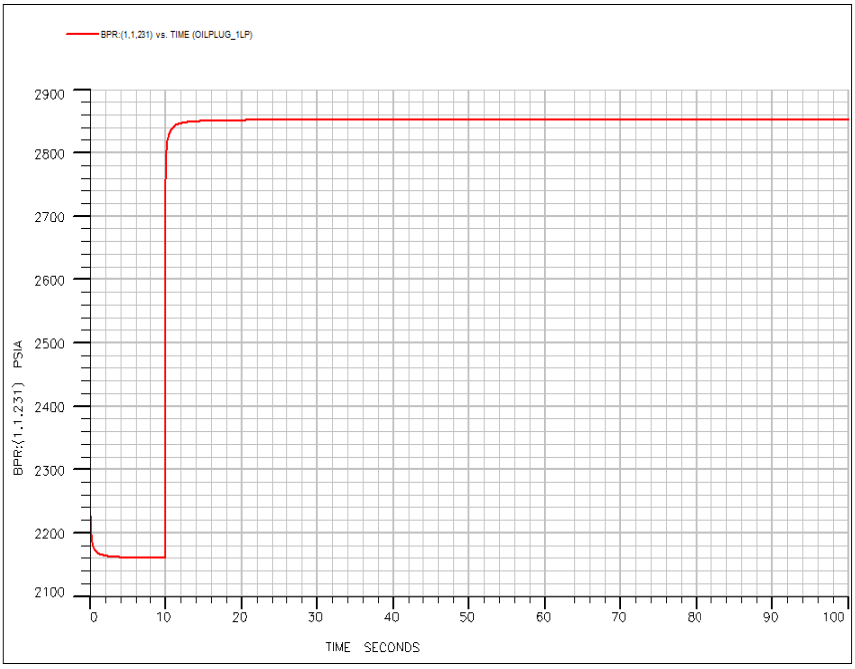

Figure 5.3: Pressure response for the base case oil reservoir

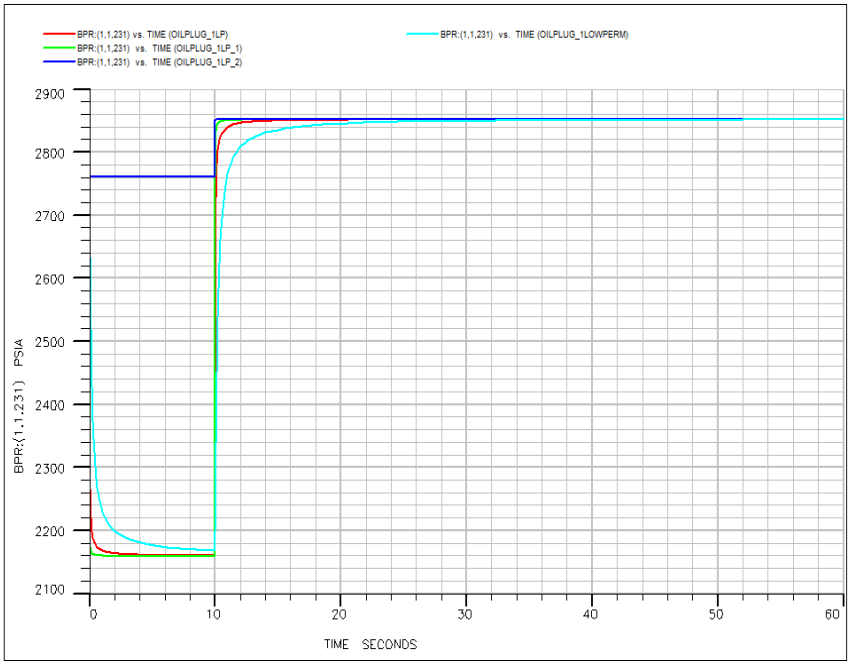

Figure 5.4: Pressure response with the different reservoir permeability in oil reservoir

Table5.1: Summary data with the different reservoir permeability

k, mD	Initial Pressure, psi	Final Drawdown Pressure, psi	Final Buildup Pressure, psi	Fluid Volume, cc	Stabilized time, s
0.1	2,851.991	2,168.279	2,851.991	0.093	193.69
1	2,851.990	2,159.837	2,851.990	0.786	193.62
10	2,851.990	2,158.846	2,851.990	7.712	193.62
100	2,851.990	2,760.159	2,851.990	10.000	30.04

From the simulation result, the total testing time is less than 5-minute for all the permeability value. The reservoir permeability, itself, is not only one factor that affects the pressure response. Back to the tool mechanism, to perform a test, the tool is stopped at the sampling depth. Then, the surface system transmits the power into the tool; the hydraulic pressure drives out packer on one side and the backup pistons move on the opposite side. The body of tool is held away from the borehole wall to reduce the chances of differential sticking. After the tool is properly set, the pressure inside the tool is activated and letting the probe being inserted into the reservoir and starting to withdraw fluid. To insert the probe into the formation, hydraulic power must generate the power to overcome the strength of rock. Then the probe piston starts to withdraw fluid from reservoir.

5.2 Effect of the Restricted Zone Severity in Oil Reservoir

When the probe is inserted into the shale region, the flow from the reservoir into the probe and the chamber may be partially or fully restricted. Based on the probe restricted flow assumption, the RFT probe is inserted on partially or fully into shale regions in the formation then suction piston is moved to allow the reservoir fluid flowing into the pretest chamber as shown in Figure 5.5. Some modification model and assumption are used instead of the base case model.

1. Probe restricted flow occurs in probe grid block. So, the permeability value is modified by reducing from original permeability value.

2. The permeability of probe block is reduced from original reservoir permeability by multiplying 0.1 in all direction. So, the probe block permeability varies from 10^{-1}mD to 10^{-7} mD.

3. This assumption neglects the supercharge effect and the restricted zone permeability in this study is called k_c

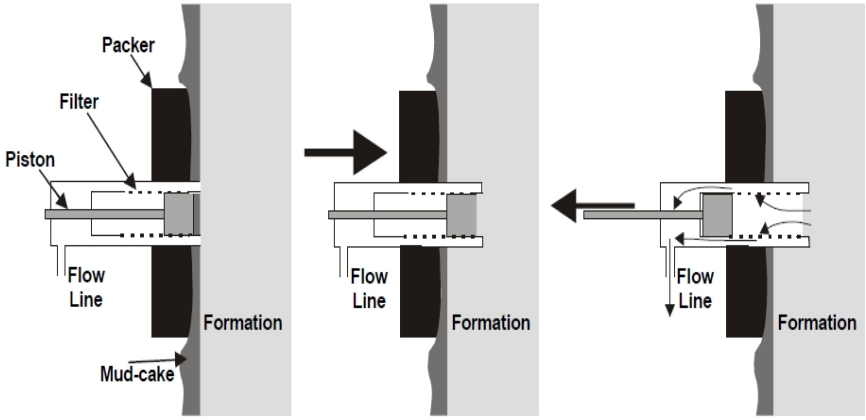

Figure 5.5: Tool mechanical when probe is inserted into formation[31].

To study the effect of probe restricted flow on pressure response and buildup time, the reservoir simulation runs are conducted. The modification model is used with the reservoir permeability value 1 mD in all directions and the probe block permeability is reduced from original reservoir permeability by 10-fold in all directions i.e., the probe block permeability varies from 0.1 mD to 10^{-7} mD. The pretest chamber is fixed to 10 cc and a withdraw rate is 1cc/sec and total testing time is 30-minutes for observe pressure response. The schematic reservoir description for the restricted zone assumption in oil reservoir is shown in Figure 5.6. The pressure response is shown in Figure 5.7a and 5.7b and Table 5.2 summarizes data with the different probe block permeability in 30-minute testing time.

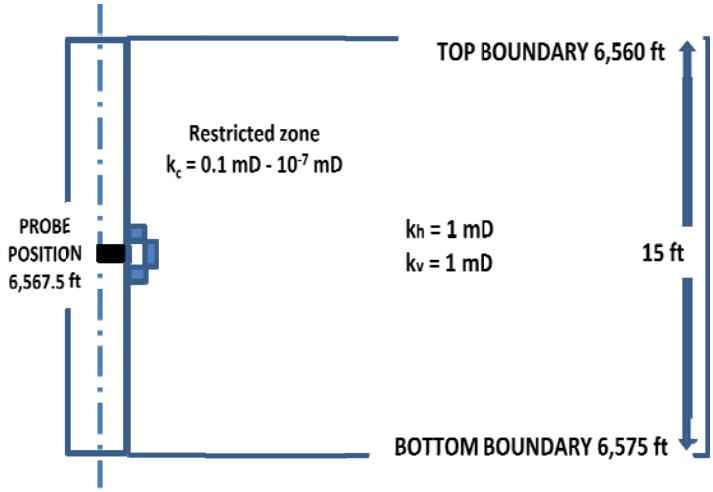

Figure 5.6: Schematic reservoir description for the restricted zone assumption in oil reservoir

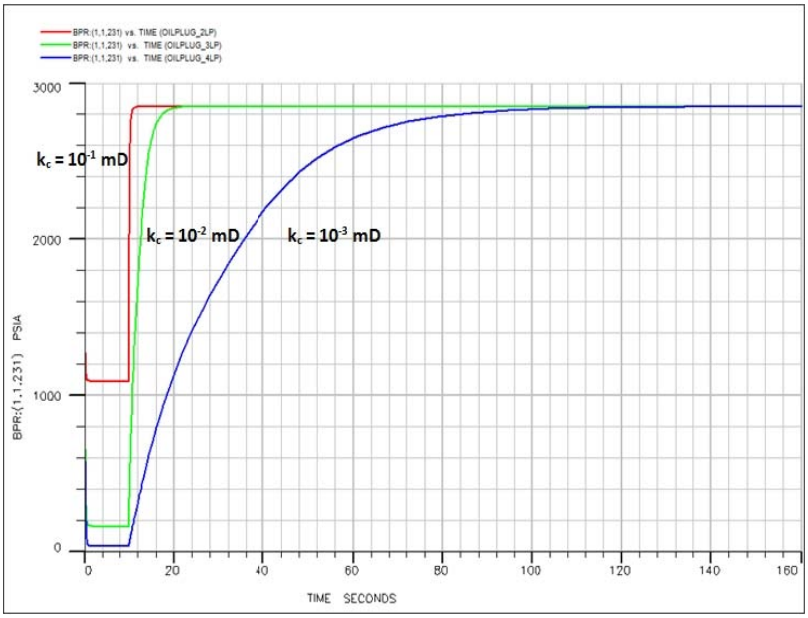

Figure 5.7a: Pressure response for the restricted zone permeability 10^{-1} mD to 10^{-3} mD at depth 6,567.5 ft

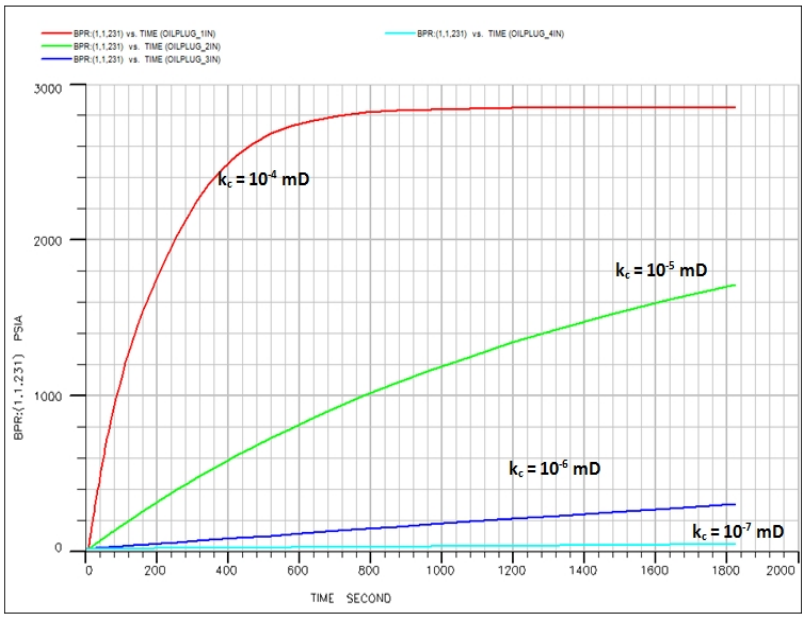

Figure 5.7b: Pressure response for the restricted zone permeability 10^{-4} mD to 10^{-7} mD at depth 6,567.5 ft

Table 5.2: Summarized data with different restricted zone permeability in 30 minute testing time.

k_c, mD	Initial Pressure, psi	Final Drawdown Pressure, psi	Final buildup Pressure, psi	Fluid volume, cc	Stabilized time, sec
Base case	2,851.990	2,159.837	2,851.990	0.786	193.69
0.1	2,851.990	1,088.219	2,851.990	0.434	176.29
0.01	2,851.990	153.733	2,851.990	0.082	86.31
0.001	2,851.991	30.217	2,851.991	0.032	258.27
0.0001	2,851.991	16.399	2,851.827	0.027	> 30 min
0.00001	2,851.944	14.871	1,715.127	0.026	> 30 min
0.000001	2,851.991	14.715	301.596	0.026	> 30 min
0.0000001	2,851.962	14.700	45.382	0.026	> 30 min

From the reservoir simulation result, the probe restricted flow directly effects fluid withdrawal from the reservoir. The reservoir cannot produce the fluid passed to the probe due to permeability reduction at the probe block. From the reservoir simulation result, the high probe restricted flow severity causes no flow from the reservoir into the

probe. This condition is considered to be completely restricted flow test. So, the result of probe restricted flow is considered to impact the fluid flow from reservoir to pre test chamber. It has a direct effect on the drawdown pressure and fluid withdrawn volume. The restricted flow also affects the buildup pressure response and time for pressure build up to initial pressure in oil reservoir. It can be discussed at this point that with the probe permeability less than the 10^{-4} mD, the reservoir pressure cannot be reliably estimated from RFT data.

From the result in Table 5.2, pressure cannot reach to initial pressure in 30-minute from restricted zone permeability ranging from 10^{-4} mD to 10^{-7} mD. Therefore, the restricted zone effect could be one of the phenomena that slows the pressure response from the reservoir. To analyze pressure response, the conventional interpretation technique, the log-log plot is used to determine the flow regime. Then, extrapolation pressure technique is used to determine the reservoir pressure. Figures 5.8 to 5.11 show the log-log plot, extrapolation pressure and pressure gradient plot for 30-minute testing time.

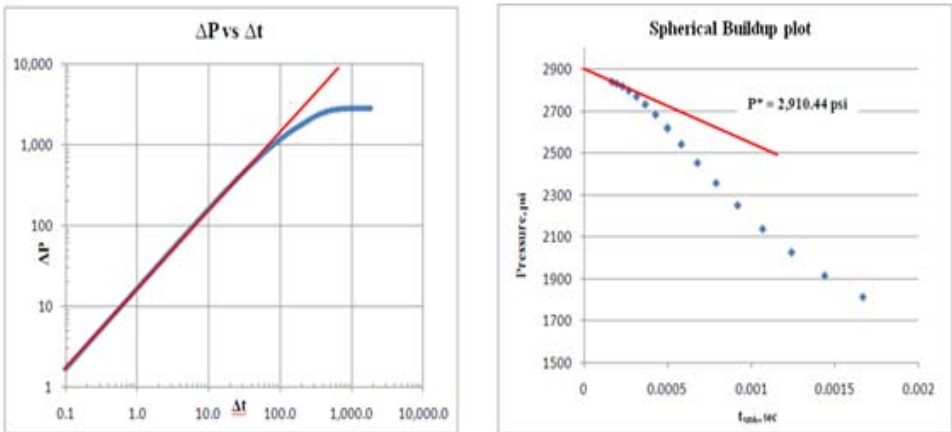

Figure 5.8: Log-log plot of dP vs dt and unit slope line and spherical pressure buildup plot for the restricted zone 10^{-4} mD at depth 6,567.5 ft with 30-minute testing time

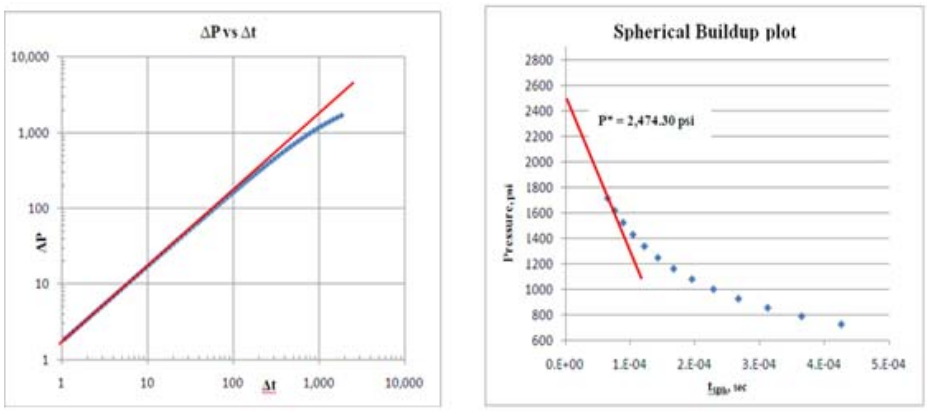

Figure 5.9: Log-log plot of dP vs dt and unit slope line and spherical pressure buildup plot for the restricted zone 10^{-5} mD at depth 6,567.5 ft with 30-minute testing time

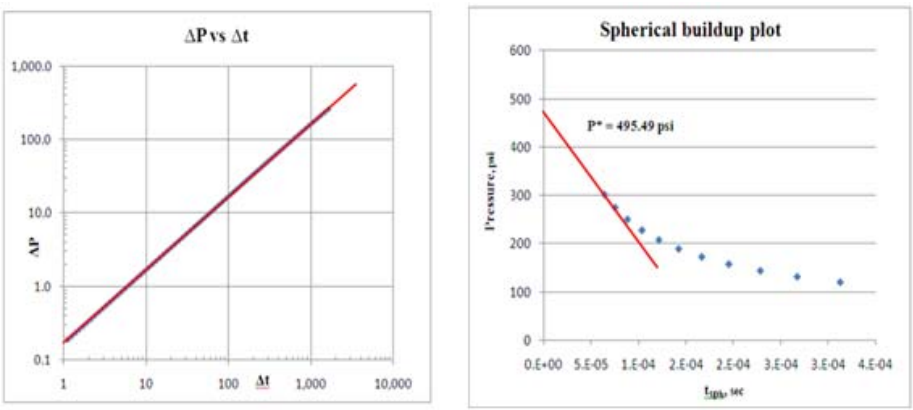

Figure 5.10: Log-log plot of dP vs dt and unit slope line and spherical pressure buildup plot for the restricted zone 10^{-6} mD at depth 6,567.5 ft with 30-minute testing time

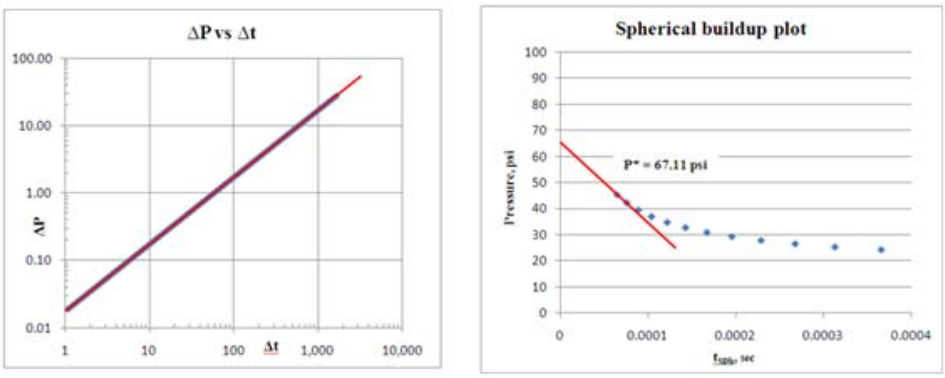

Figure 5.11: Log-log plot of dP vs dt and unit slope line and spherical pressure buildup plot for the restricted zone 10^{-7} mD at depth 6,567.5 ft with 30-minute testing time

Figures 5.12 to 5.15 show the result of pressure gradient plot for 30-minute testing time, the red line represents slope of initial fluid gradient (not on scale), the green line represents slope of extrapolation pressure gradient (not on scale) and blue line represents final reading pressure (plot on scale). Tables 5.3 and 5.4 show the final reading pressure, extrapolated pressure for 30-minute testing time, the error value of pressure is compared to its initial pressure on each point. Table 5.5 shows summary of fluid gradient interpretation from the final reading pressure and extrapolated pressure in 30-minute, the error value of fluid gradient interpretation is compared to its initial fluid gradient.

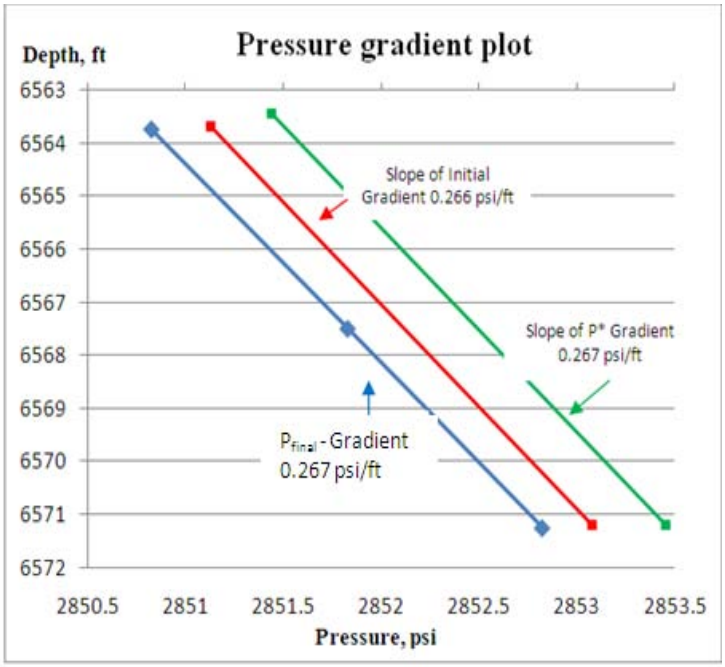

Figure 5.12: Pressure gradient plot from final reading pressure, extrapolation pressure and initial pressure for the restricted zone 10^{-4} mD

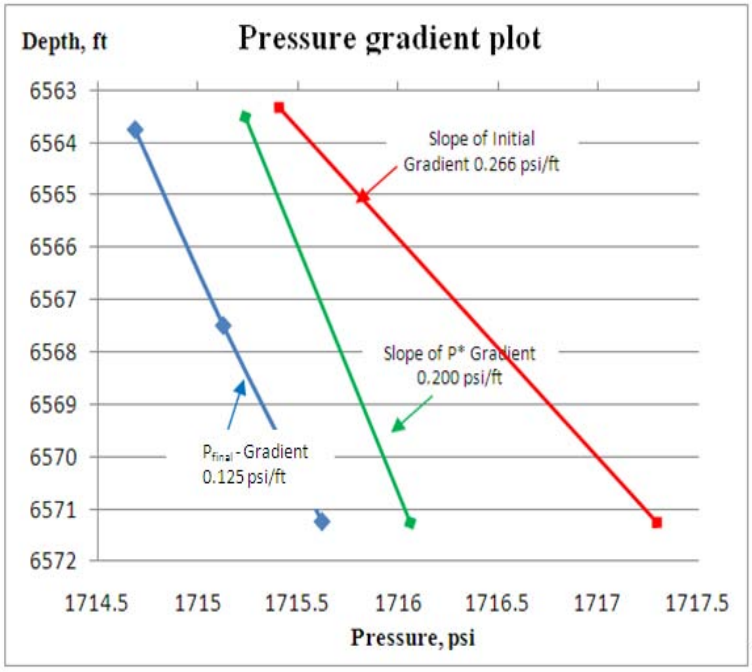

Figure 5.13: Pressure gradient plot from final reading pressure, extrapolation pressure and initial pressure for the restricted zone 10^{-5} mD

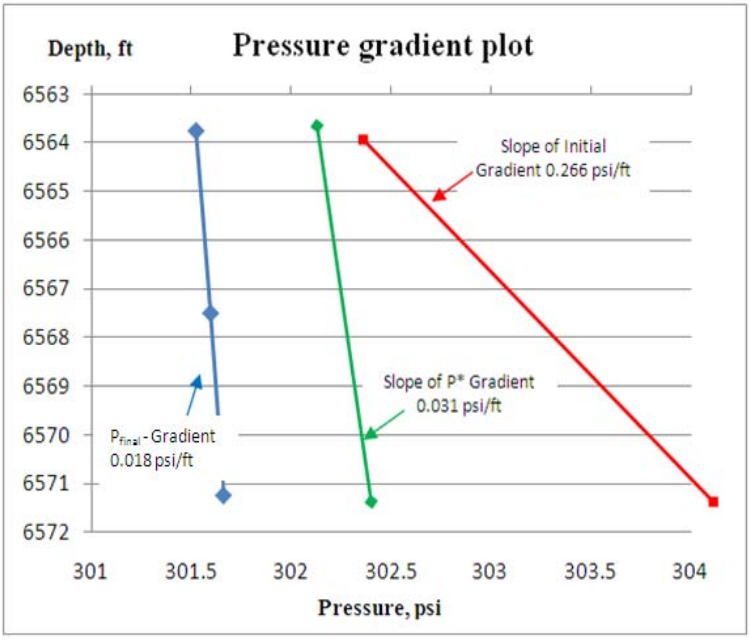

Figure 5.14: Pressure gradient plot from final reading pressure, extrapolation pressure and initial pressure for the restricted zone 10^{-6} mD

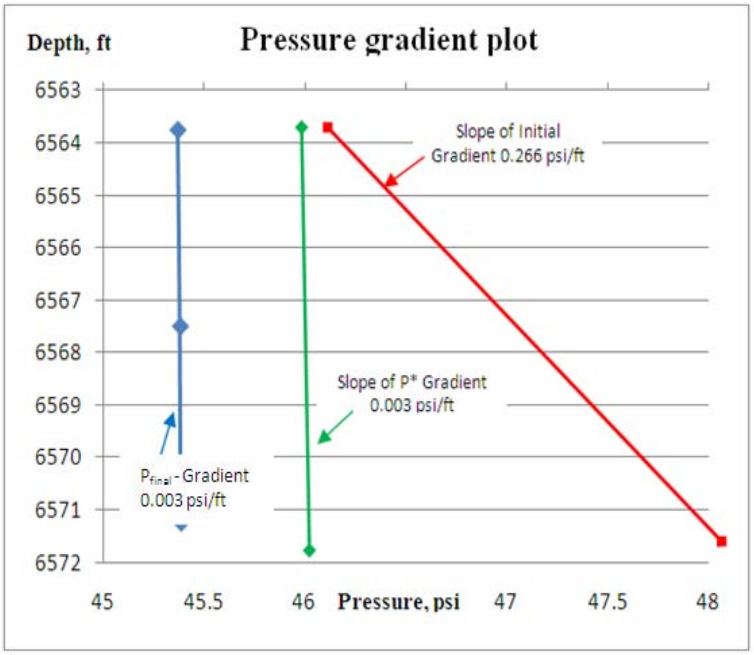

Figure 5.15: Pressure gradient plot from final reading pressure, extrapolation pressure and initial pressure for the restricted zone 10^{-7} m

Table 5.3: Final reading pressure in 30-minute

Depth	P_i	10^{-4} mD		10^{-5} mD		10^{-6} mD		10^{-7} mD	
ft	psi	P_{final} psi	Error %	P_{final} psi	Error %	P_{final} psi	Error %	P_{final} psi	Error %
6,571.25	2,852.98	2,852.82	-0.01	1,715.62	-39.87	301.66	-89.43	45.39	-98.41
6,567.50	2,851.99	2,851.83	-0.01	1,715.13	-39.86	301.60	-89.43	45.38	-98.41
6,563.75	2,850.99	2,850.82	-0.01	1,714.69	-39.86	301.52	-89.42	45.37	-98.41

Table 5.4: Extrapolation pressure in 30-minute

Depth	P_i	10^{-4} mD		10^{-5} mD		10^{-6} mD		10^{-7} mD	
ft	psi	P_{final} psi	Error %	P_{final} psi	Error %	P_{final} psi	Error %	P_{final} psi	Error %
6,571.25	2,852.98	2,911.40	+2.05	2,475.10	-13.25	495.6	-82.63	67.12	-97.65
6,567.50	2,851.99	2,910.40	+2.05	2,474.30	-13.25	495.49	-82.63	67.11	-97.65
6,563.75	2,850.99	2,909.40	+2.05	2,473.60	-13.25	495.37	-82.63	67.09	-97.65

Table 5.5: Summary of fluid gradient interpretation from the final reading pressure and extrapolated pressure in 30-minute

k_c mD	Initial P gradient, psi/ft	Final reading Pressure			Extrapolate Pressure		
		gradient, psi/ft	Error %	Interpreted Gradient	gradient, psi/ft	Error %	Interpreted Gradient
10^{-4}	0.266	0.267	+0.26	Oil	0.267	+0.26	Oil
10^{-5}	0.266	0.125	-53.00	N/A	0.200	-24.80	N/A
10^{-6}	0.266	0.018	-93.23	N/A	0.031	-88.52	N/A
10^{-7}	0.266	0.003	-98.87	N/A	0.003	-98.70	N/A

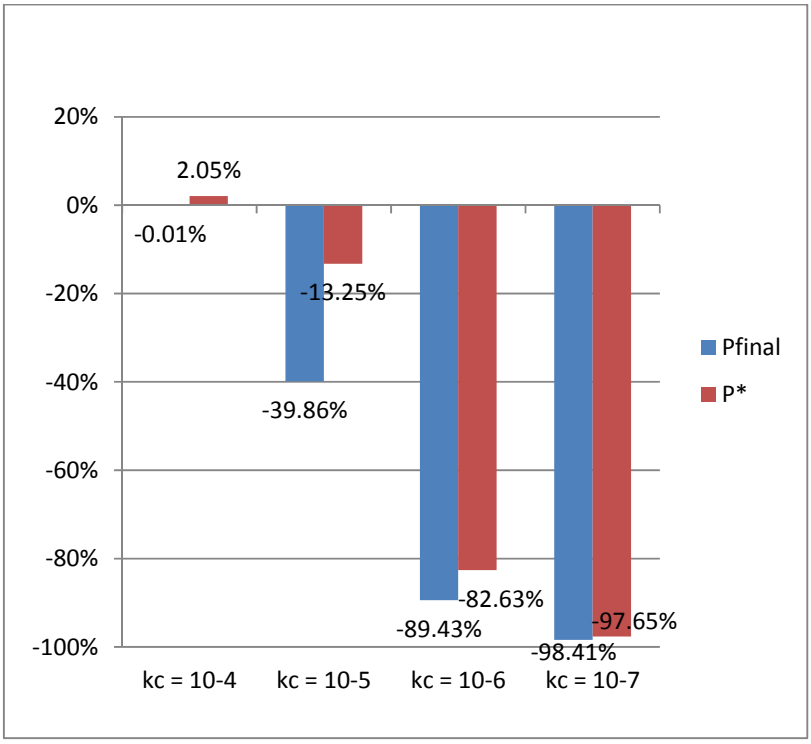

Figure 5.16: Final pressure error from final reading pressure and extrapolation pressure in 30-minute

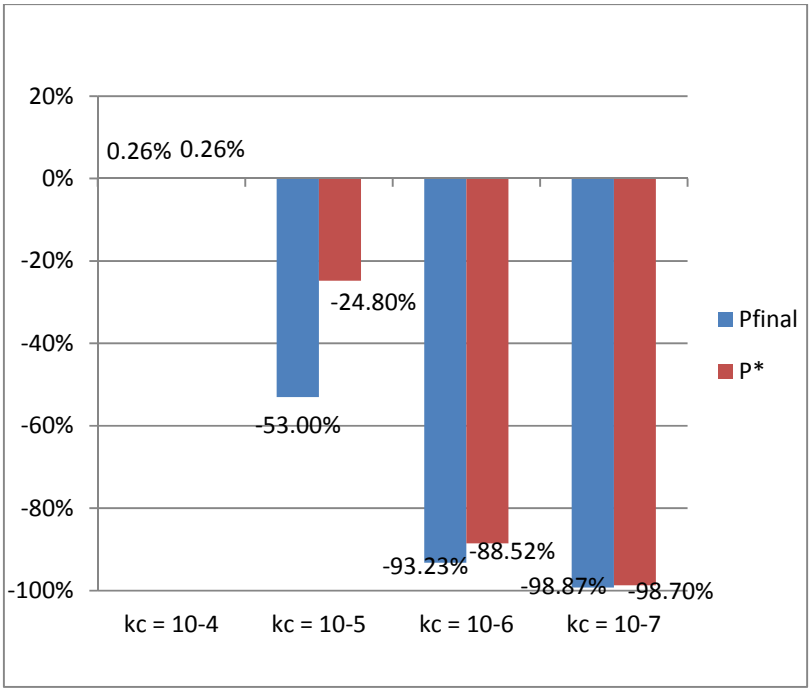

Figure 5.17: Fluid gradient error for final reading pressure and extrapolation pressure in 30-minute

As the result shown in Figure 5.16 and 5.17, the pressure response from 10^{-4} mD to 10^{-7} mD is mainly from the wellbore storage and transition period. Using pressure in this period will lead to wrong results because spherical flow interpretation method is based on the single rate drawdown and neglects the wellbore storage effect in the pretest sampling system. Figure 5.16 show that the final reading pressure, the maximum error is up to 98.41% (underestimate) and 97.65% (underestimate) from extrapolation pressure. The error from fluid gradient interpretation in this regime in Figure 5.17 shows the same trend and maximum error is as high as 99% (underestimate). The result confirms that both techniques cannot be used to indicate oil gradient in the reservoir.

However, if the probe is inserted into a shale region or restricted zone, more time is needed for the chamber pressure to reach the initial reservoir pressure. The more severe the restricted zone, the longer the time for chamber pressure to reach the initial reservoir pressure. The result during the early time period the dominant flow period is the wellbore or chamber storage period. This is confirmed by the unit slope lines. The lower the permeability value of the restricted zone is, the longer the wellbore/chamber storage

period. Table 5.5 shows that using RFT pressure readings at the 30-minute time to evaluate initial reservoir pressure or pressure gradient for the restricted zone cases will lead to wrong estimates, except for the case of the restricted zone permeability of 10^{-4} mD. Therefore, one should not use RFT pressure to estimate the initial reservoir pressure or pressure gradient as long as the pressure readings are still in the wellbore/chamber storage period.

5.3 Curve Fitting for Oil Reservoir

The final reading pressure and the conventional technique were invalid for the restricted zone permeability lower than 10^{-4} mD with the 30-minute buildup time. Because the tool storage effect still dominate in the 30-minute. To determine the end of tool storage and transition regime, the mathematical concept is brought to determine the buildup time to reach stabilize condition. To verify the validation of exponential model the actual field data is used and the result is shown in Appendix B.

Table 5.6: Summary data of input value and coefficient of different restricted zone permeability for oil reservoir

k_c, mD	P_{est} ,psi	P_{dd}, psi	C_1	C_2
1	2,850.00	2,159.86	690.14	0.03148
10^{-1}	2,850.00	1,088.23	1,761.77	0.18245
10^{-2}	2,850.00	153.73	2,696.27	2.1751
10^{-3}	2,850.00	30.22	2,819.78	19.9158
10^{-4}	2,850.00	16.40	2,833.60	191.4351
10^{-5}	2,850.00	14.87	2,835.13	1,892.7400
10^{-6}	2,850.00	14.72	2,835.28	18,977.0806
10^{-7}	2,850.00	14.70	2,835.30	190,427.7763

To observe the rate of pressure change versus time from the stabilized test, the base case study is brought to investigate the rate of change. From the result, the differentiation value is relatively constant at $1x10^{-8}$ range. Figure 5.18 shows the

differentiation value plot at the stabilized pressure. Solving the differential equation the differential value is set to $1x10^{-8}$. The buildup time result from the differential equation and total testing time is show in Table 5.7.

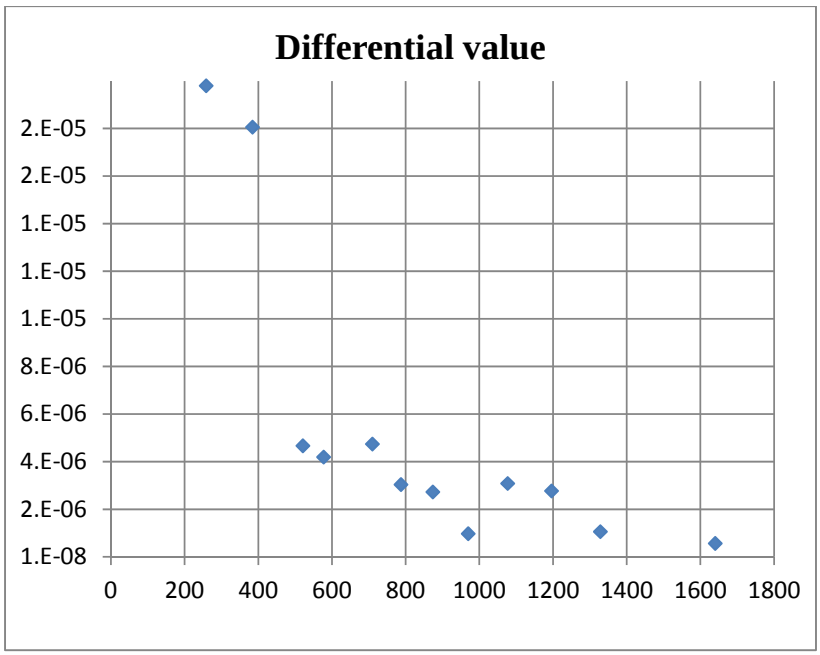

Figure 5.18: The differentiation value plot for a base case

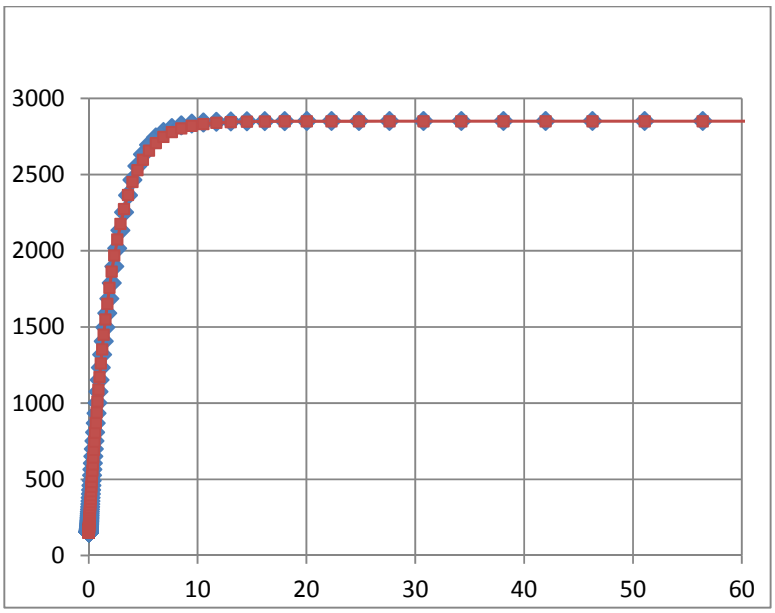

Figure 5.19: Pressure buildup profile from reservoir simulation and exponential model for the restricted zone permeability 10^{-2} mD

Table 5.7: The buildup time result for each restricted zone permeability

k_c, mD	$t_{buildup}$ (Δt_{est}), sec	t_{Total}, sec
1	0.89	10.89
10^{-1}	5.03	15.03
10^{-2}	55.56	65.56
10^{-3}	465.50	475.50
10^{-4}	4,042.23	4,052.23
10^{-5}	35,630.34	35,640.34
10^{-6}	313,493.61	313,503.61
10^{-7}	2,706,655.80	2,706,665.80

5.4 Effect of the Restricted Zone Severity in Low Permeability Oil Reservoir with Low Restricted Zone Permeability

This study investigates and analyzes pressure behavior of the restricted zone permeability ranging from 10^{-4} mD to 10^{-7} mD. After investigating pressure response, the method to analyze fluid gradient is determined. The restricted zone permeability is set in the range of 10^{-4}mD to 10^{-7}mD. The reservoir permeability is set to 1 mD and the schematic of reservoir model is shown in Figure 5.20. Three sampling point are set at depth of 6,571.25ft, 6567.5 ft, and 6,563.75 ft. The pretest chamber is fixed to 10 cc and a drawdown rate is 1cc/sec, Figure 5.21 shows schematic reservoir description for testing point for the restricted zone permeability of 10^{-4} mD to 10^{-7} mD in oil reservoir.

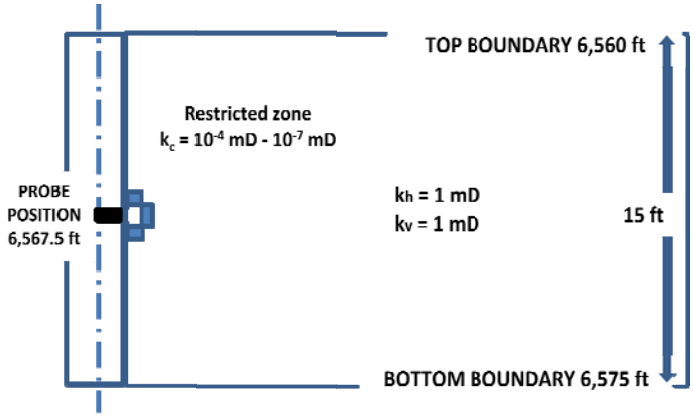

Figure 5.20: Schematic reservoir description for the restricted zone permeability of 10^{-4} mD to 10^{-7} mD for oil reservoir.

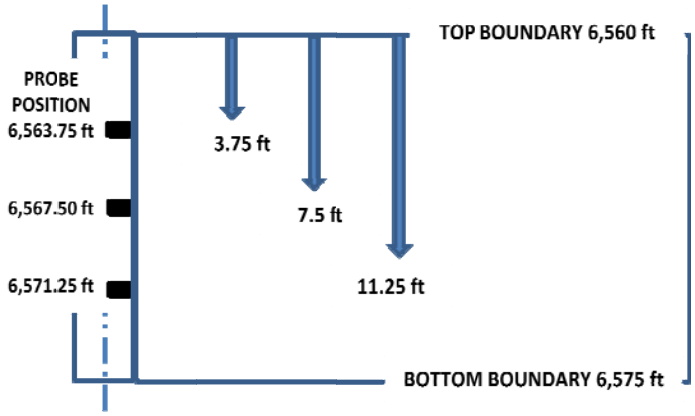

Figure 5.21: Schematic reservoir description for testing point for the restricted zone permeability of 10^{-4} mD to 10^{-7} mD for oil reservoir.

The curve fitting technique is used to estimate the total time to reach initial reservoir pressure for each restricted zone effect, (Table 5.8).

Table 5.8: Estimate total time to reach initial reservoir pressure for restricted zone effect

k_c, mD	t_{Total}
10^{-4}	67.54 min
10^{-5}	9.90 hrs
10^{-6}	3.63 days
10^{-7}	31.33 days

From Table 5.8, the extension time for each restricted zone permeability is used in

the reservoir simulation runs and the results are shown and scaled up (insert figure) in Figures 5.22 to 5.25. Figures 5.26 to 5.29 show the log-log plot, it is plotted to verify the wellbore storage, transition period in. The first reading pressure after transition period, P_{first}, is used to plot pressure gradient. Spherical buildup plot is used to determine extrapolation pressure starting from first reading pressure until estimate time in Table 5.6 and the extrapolation pressure, P*, is used to plot pressure gradient. Table 5.9 shows the summary of time readings from log-log plot.

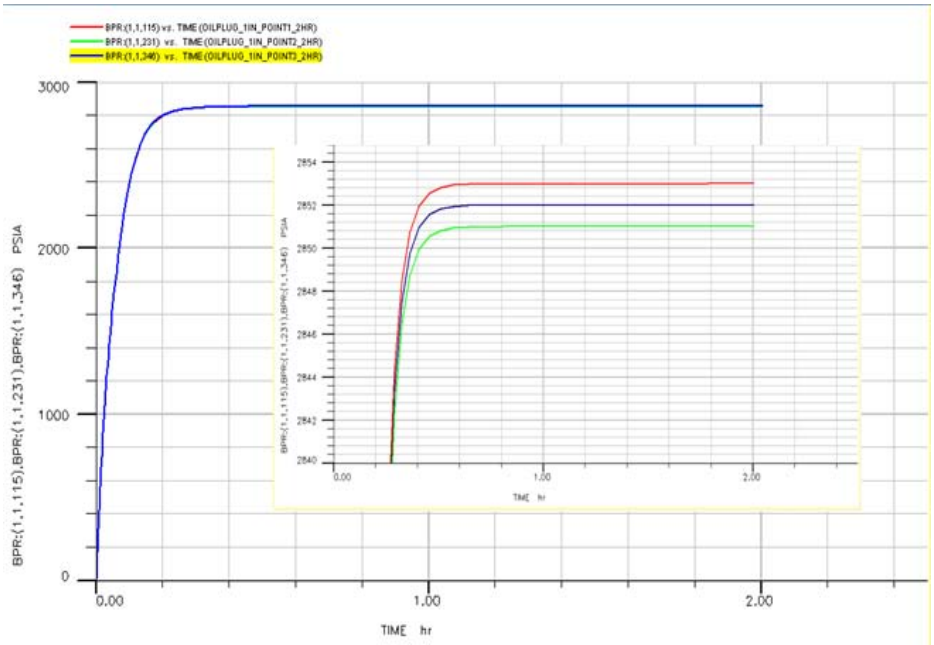

Figure 5.22: Pressure response for the restricted zone permeability 10^{-4} mD with 120 minutes

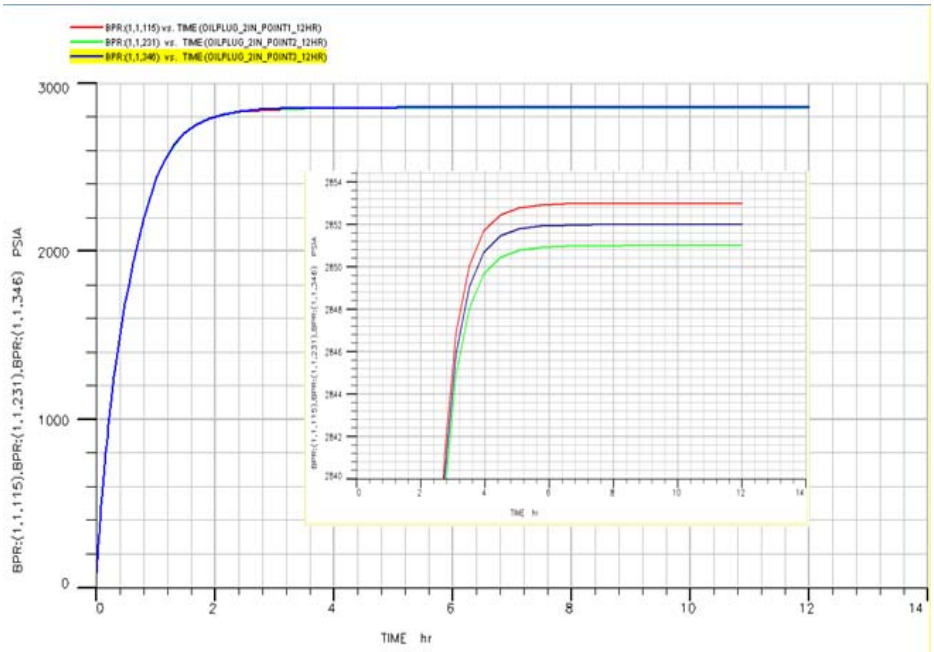

Figure 5.23: Pressure response for the restricted zone permeability 10^{-5} mD with 12 hours

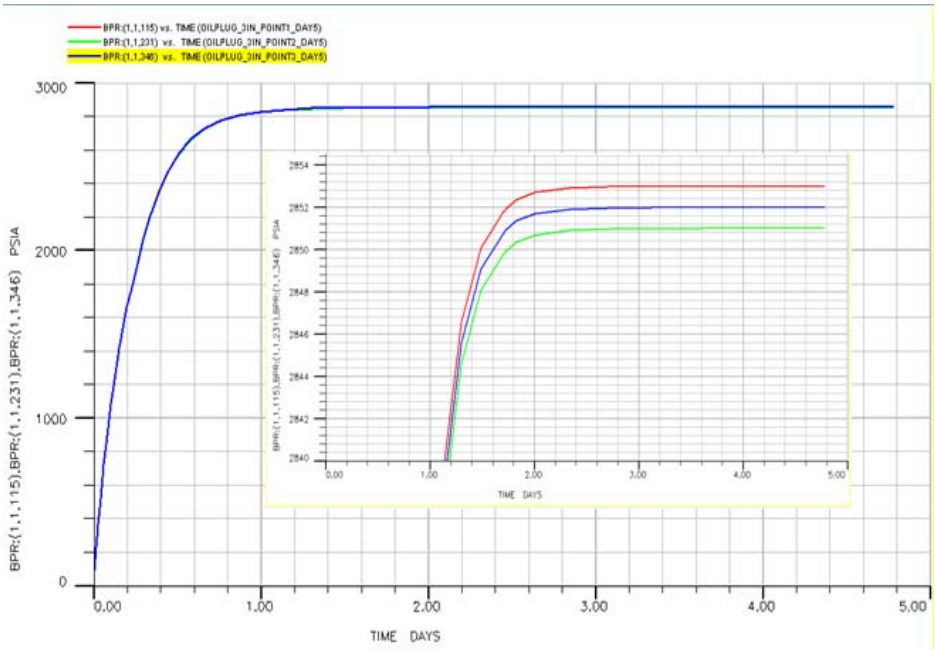

Figure 5.24: Pressure response for the restricted zone permeability 10^{-6} mD with 5 days

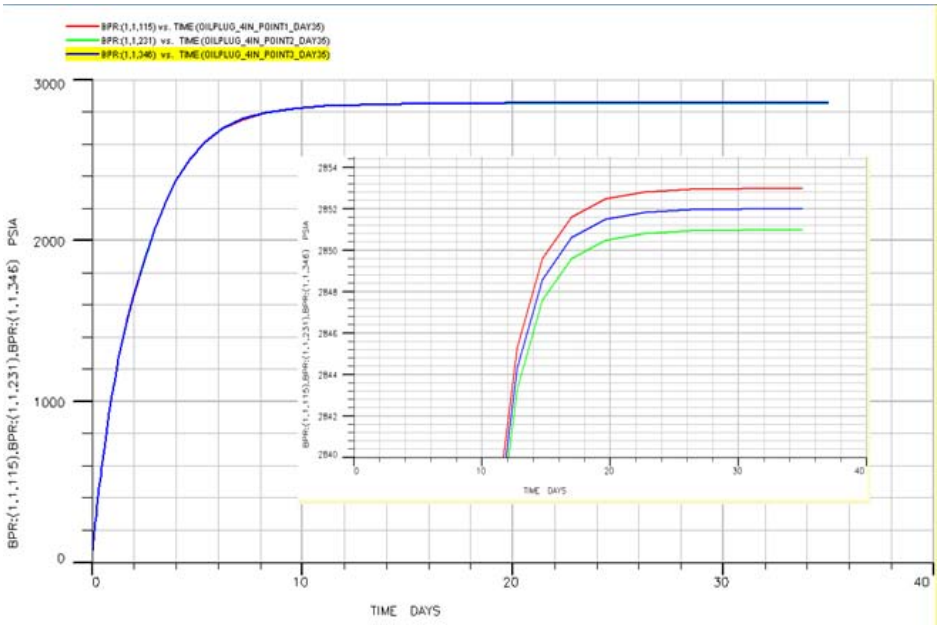

Figure 5.25: Pressure response for the restricted zone permeability 10^{-7} mD with 35 days

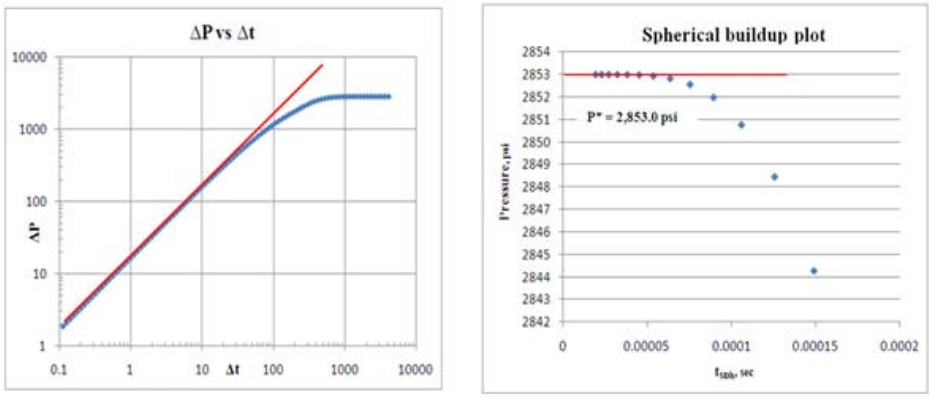

a)

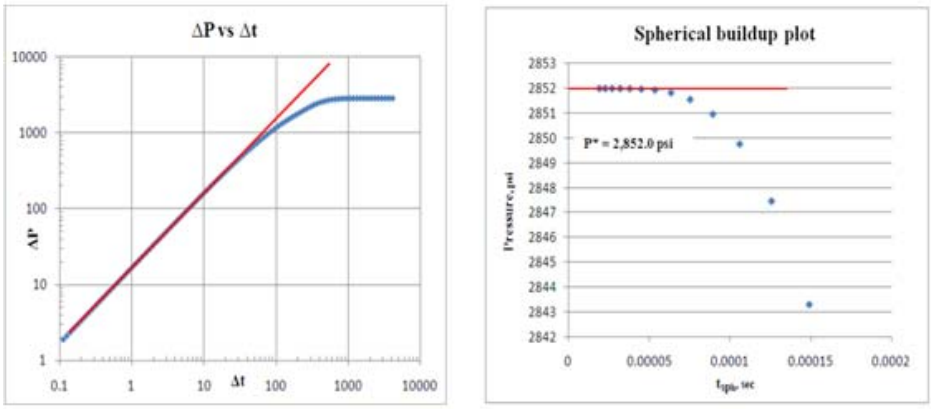

b)

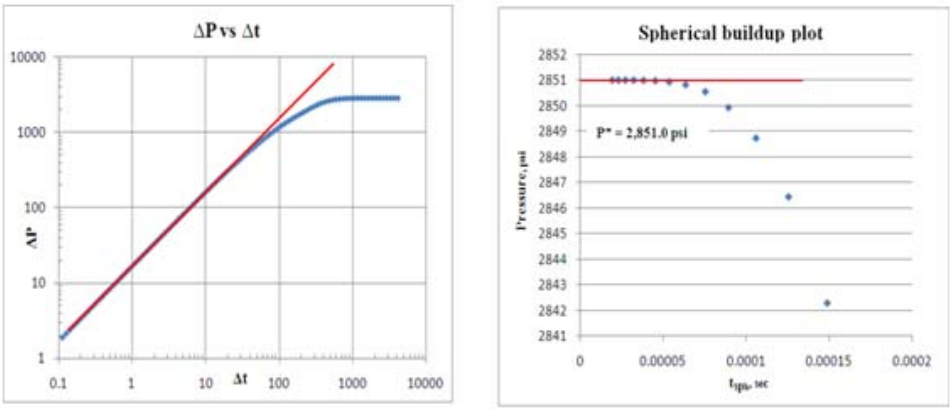

c)

Figure 5.26: Log-log plot of dP vs dt , unit slope line and spherical pressure buildup plot for the restricted zone 10^{-4} mD with 120 minutes a) depth 6,571.25ft b) depth 6,567.50 ft c) 6,563.75 ft

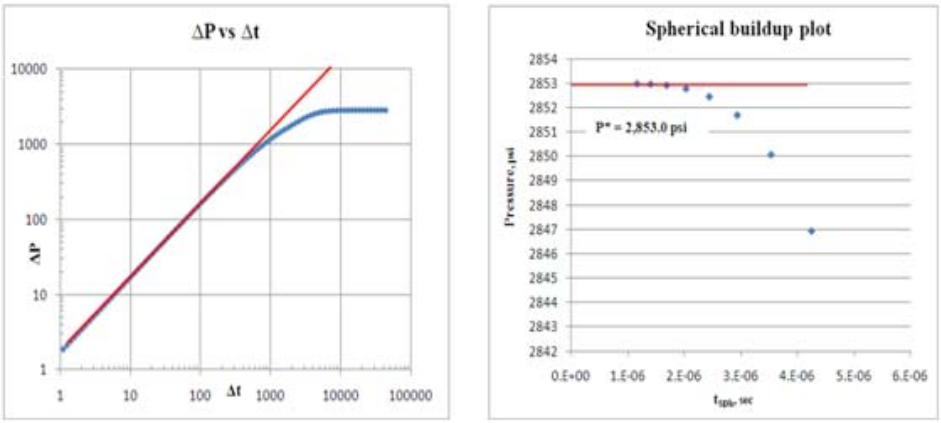

a)

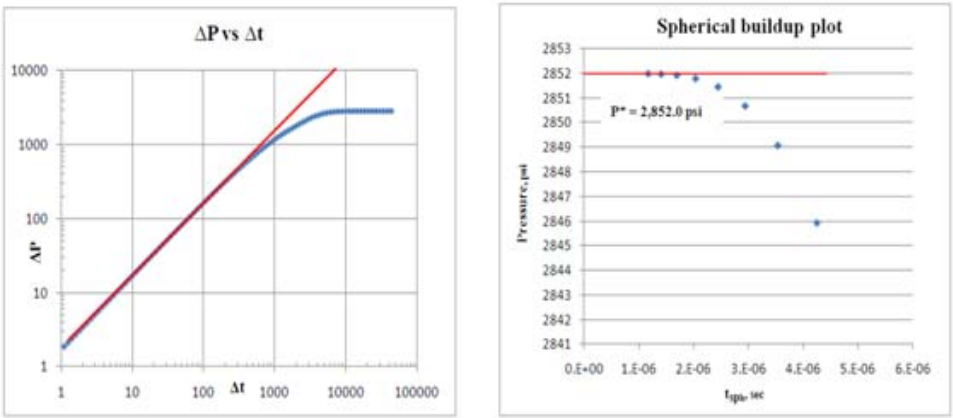

b)

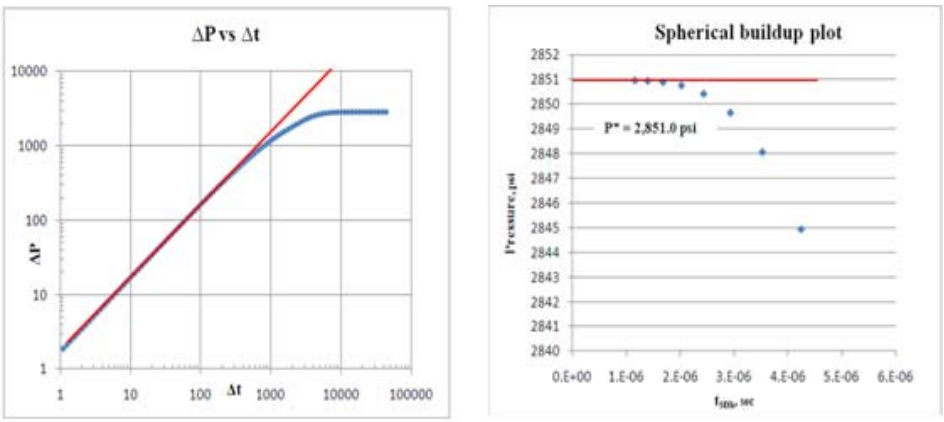

c)

Figure 5.27: Log-log plot of dP vs dt , unit slope line and spherical pressure buildup plot for the restricted zone 10^{-5} mD with 12 hours a) depth 6,571.25ft b) depth 6,567.50 ft c) 6,563.75 ft

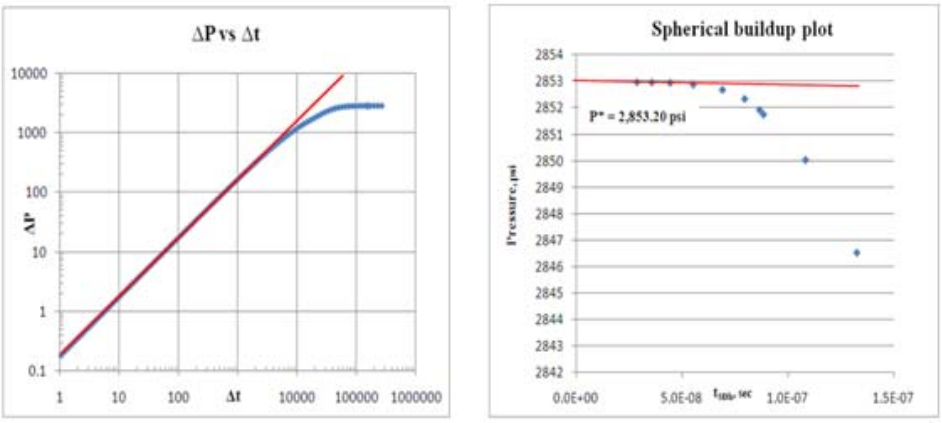

a)

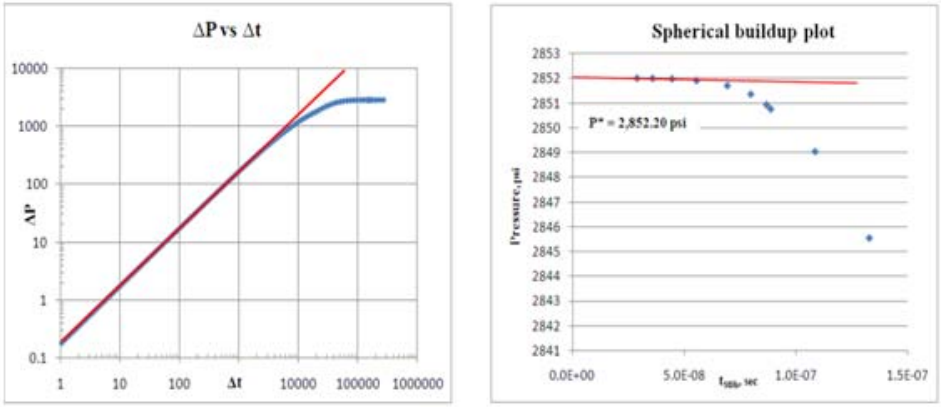

b)

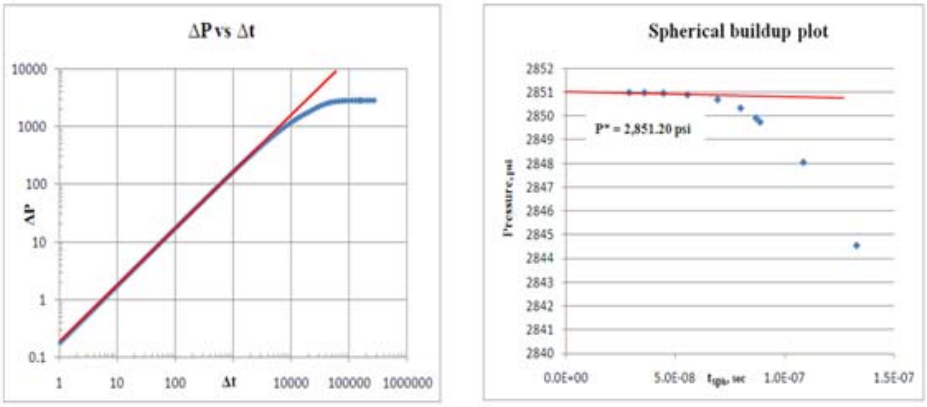

c)

Figure 5.28: Log-log plot of dP vs dt , unit slope line and spherical pressure buildup plot for the restricted zone 10^{-6} mD with 5 days a) depth 6,571.25ft b) depth 6,567.50 ft c) 6,563.75 ft

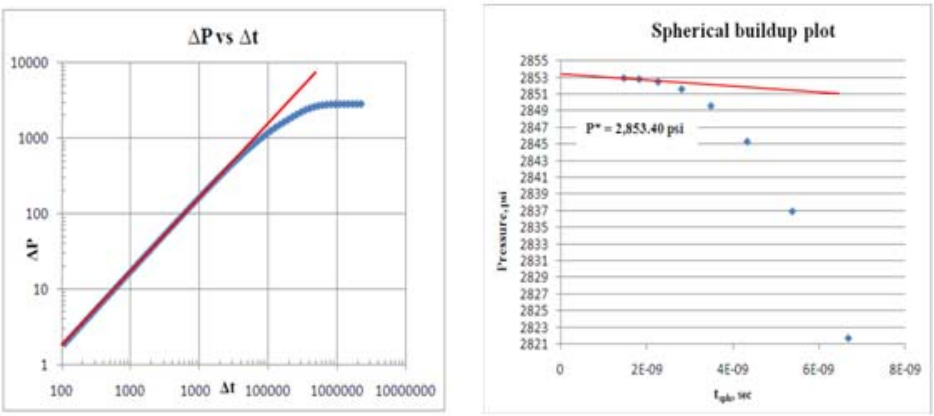

a)

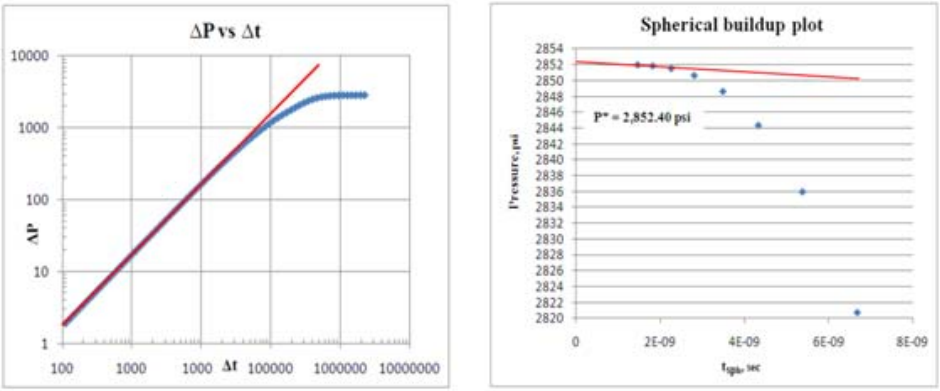

b)

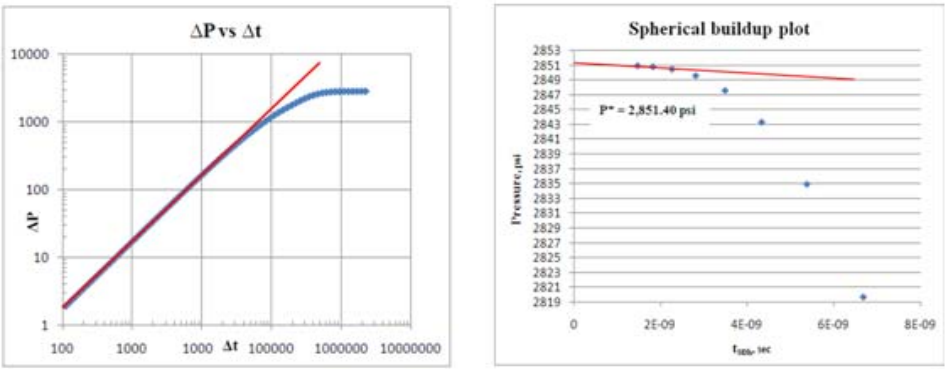

c)

Figure 5.29: Log-log plot of dP vs dt , unit slope line and spherical pressure buildup plot for the restricted zone 10^{-7} mD with 35 days a) depth 6,571.25ft b) depth 6,567.50 ft c) 6,563.75 ft

Table 5.9: Summary of time readings from log-log plot

k_c, mD	Total testing time, sec	WBS time, sec	Start of IFAS time sec
10^{-4}	4,052.23	45	3,300
10^{-5}	35,640.34	450	23,000
10^{-6}	313,503.61	4,000	200,000
10^{-7}	2,706,665.80	45,000	2,000,000

Figures 5.30 to 5.33 show the results of pressure gradient plot for the adjusted testing time, the red line represents slope of initial fluid gradient (plot on scale), the green line represents slope of extrapolation pressure gradient (plot on scale) and blue line represents final reading pressure (plot on scale). Tables 5.10 and 5.11 show the final reading pressure, extrapolated pressure after extended testing time, the error value of pressure is compared to its initial pressure on each point. Table 5.12 shows summary of fluid gradient interpretation from the first reading pressure and extrapolated pressure after extended testing time, the error value of fluid gradient interpretation is compared to its initial fluid gradient.

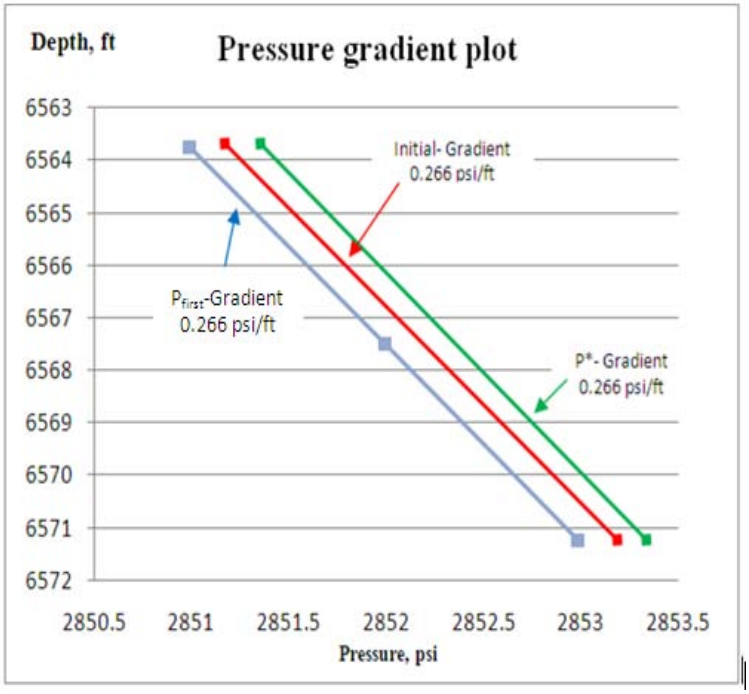

Figure 5.30: Pressure gradient result from the first reading pressure, extrapolation pressure and initial pressure for the restricted zone 10^{-4} mD

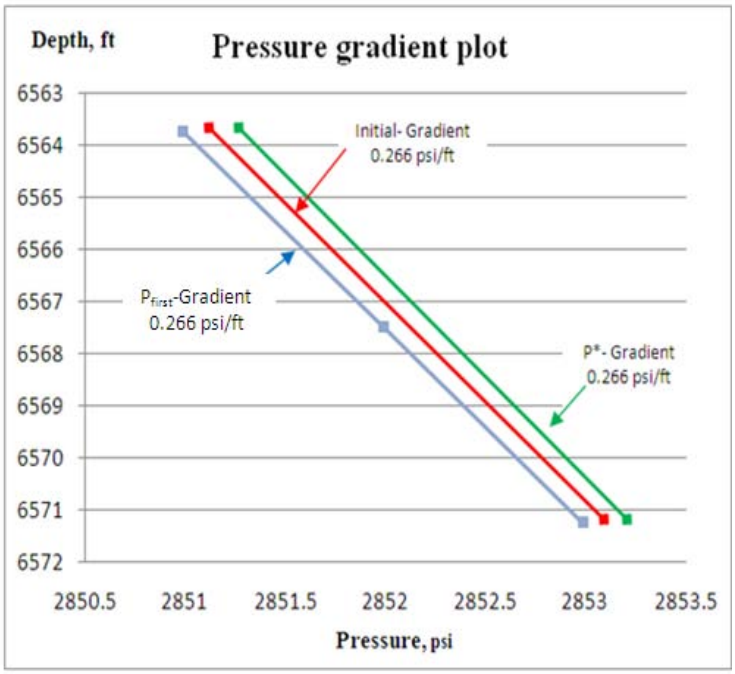

Figure 5.31: Pressure gradient result from the first reading pressure, extrapolation pressure and initial pressure for the restricted zone 10^{-5} mD

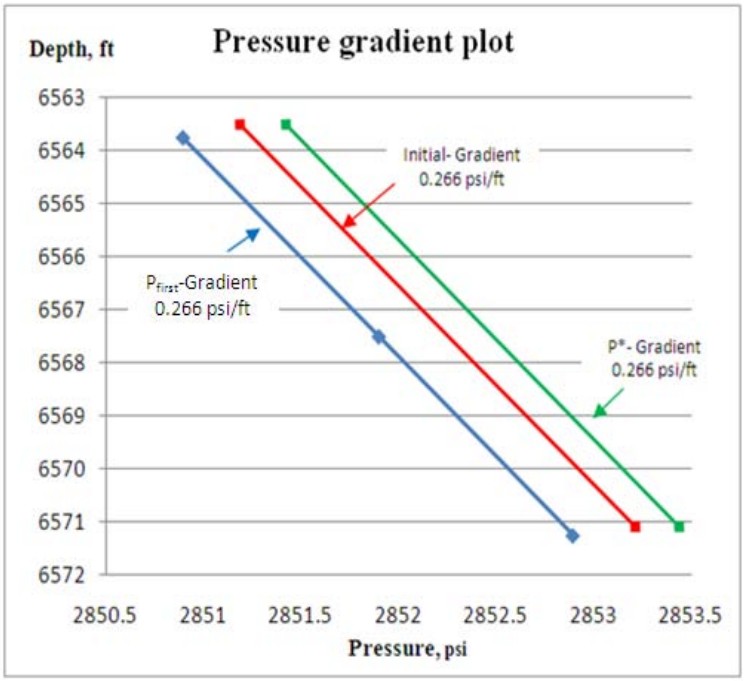

Figure 5.32: Pressure gradient result from the first reading pressure, extrapolation pressure and initial pressure for the restricted zone 10^{-6} mD

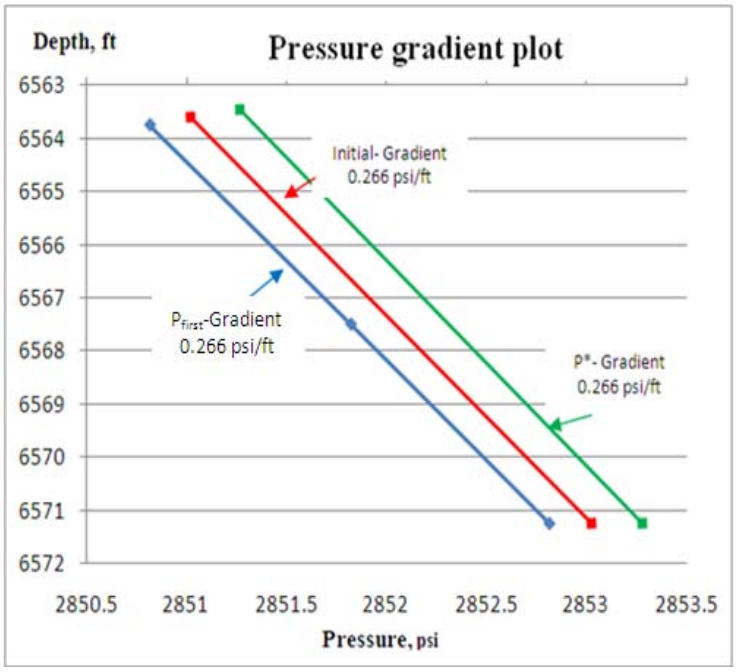

Figure 5.33: Pressure gradient result from the first reading pressure, extrapolation pressure and initial pressure for the restricted zone 10^{-7} mD

Table 5.10: First reading pressure after passing transition period.

Depth	P_i	10^{-4} mD		10^{-5} mD		10^{-6} mD		10^{-7} mD	
ft	psi	P_{first} psi	Error %	P_{first} psi	Error %	P_{first} ft	Error psi	P_{first} psi	Error %
6,571.25	2,852.98	2,852.98	0	2,852.96	-0.001	2,852.89	-0.003	2,852.82	-0.006
6,567.50	2,851.99	2,851.99	0	2,851.97	-0.001	2,851.90	-0.003	2,851.82	-0.006
6,563.75	2,850.99	2,850.99	0	2,850.96	-0.001	2,850.89	-0.003	2,850.82	-0.006

Table 5.11: Extrapolation pressure after extended time.

Depth	P_i	10^{-4} mD		10^{-5} mD		10^{-6} mD		10^{-7} mD	
ft	psi	P_{first} psi	Error %	P_{first} psi	Error %	P_{first} ft	Error psi	P_{first} psi	Error %
6,571.25	2,852.98	2,853.00	+0.0007	2,853.00	+0.0004	2,853.20	+0.0008	2,853.40	+0.015
6,567.50	2,851.99	2,852.00	+0.0004	2,852.00	+0.0004	2,852.20	+0.0007	2,852.40	+0.014
6,563.75	2,850.99	2,851.00	+0.0004	2,851.00	+0.0004	2,851.20	+0.0007	2,851.40	+0.014

Table 5.12:Summary of fluid gradient interpretation from the first reading pressure and extrapolated pressure after extended testing time.

kc mD	Initial P gradient, psi/ft	First reading Pressure			Extrapolate Pressure		
		gradient, psi/ft	Error %	Interpreted Gradient	gradient, psi/ft	Error %	Interpreted Gradient
10^{-4}	0.266	0.265	0	Oil	0.267	+0.53	Oil
10^{-5}	0.266	0.267	+0.53	Oil	0.267	+0.53	Oil
10^{-6}	0.266	0.267	+0.53	Oil	0.267	+0.53	Oil
10^{-7}	0.266	0.267	+0.53	Oil	0.267	+0.53	Oil

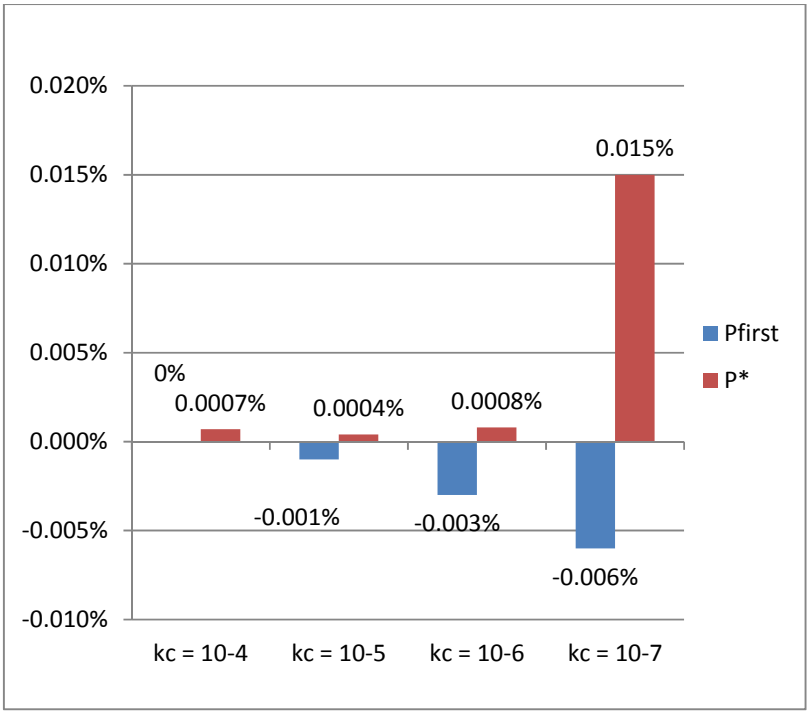

Figure 5.34: Final pressure error for the first reading pressure and extrapolation pressure after extended time

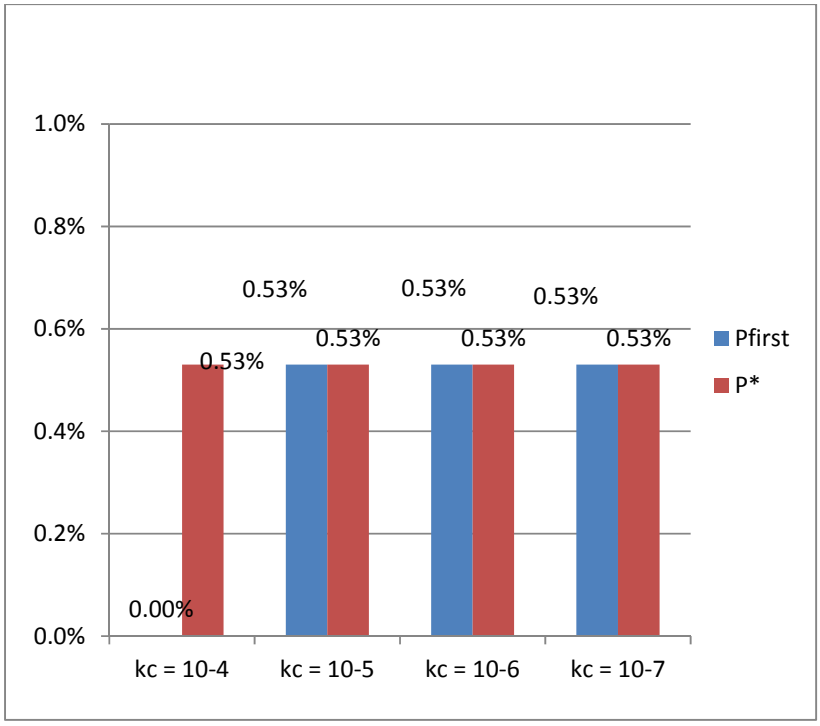

Figure 5.35: Fluid gradient error for the first reading pressure and extrapolation pressure after extended time

From the results, the curve fitting technique is used to extend testing time and the result is satisfied for pressure response. The pressure response is almost reached to initial pressure. The log-log plot confirms that pressure response has passed the wellbore storage and transition periods and reached the infinite acting (fully reservoir response) period. After end of wellbore storage and transition periods, the first reading pressure can be used directly as a pressure point to plot the pressure gradient (P_{first}). Figure 5.34 shows the maximum error of 0.006% (underestimate) and 0.015% (overestimate) for the extrapolation pressure (P*). The error from fluid gradient interpretation in this regime shown in Figure 5.35 is also low with maximum error will be 0.53% (overestimate). The result confirms that both techniques can be used to indicate oil gradient in the reservoir. The next study represents the pressure response in low permeability gas reservoir.

5.5 Pressure Response in Low Permeability Gas Reservoir

In this study, the same testing procedure is applied but only the fluid withdraw rate is fixed to 60cc/sec. From simulation result, the base case pressure response during producing and buildup time is shown in Figure 5.36. Figure 5.37 and Table 5.13 shows the other result from the simulation such as initial pressure, final drawdown pressure, fluid volume in pretest chamber and time to reach initial pressure (stabilized time) by different reservoir permeability value.

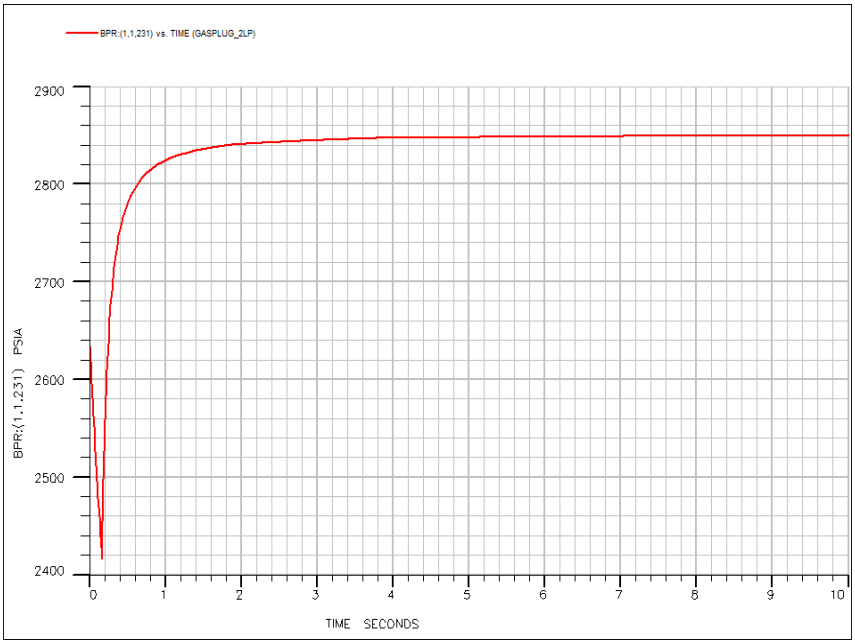

Figure 5.36: Pressure response for a base case gas reservoir

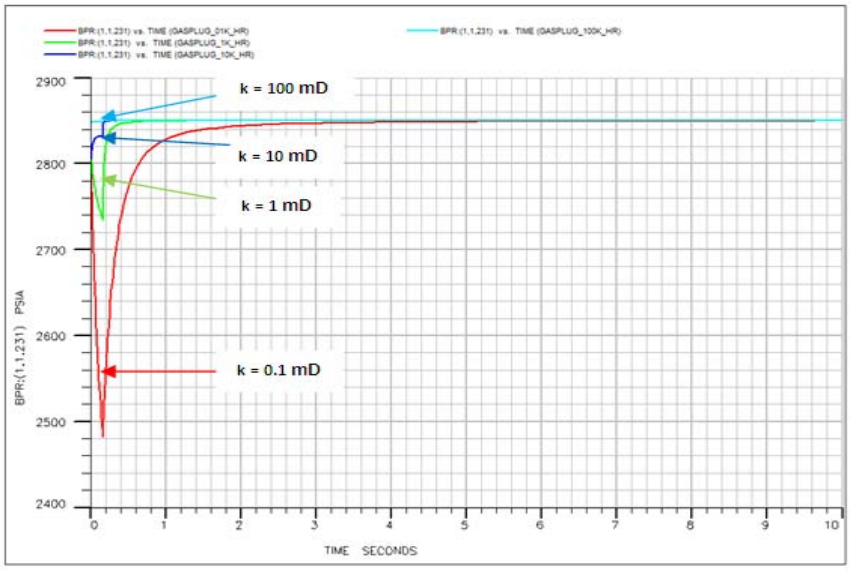

Figure 5.37: Pressure response with the different reservoir permeability in gas reservoir

Table 5.13: Summary data with the different reservoir permeability

k, mD	Initial Pressure, psi	Final Drawdown Pressure, psi	Final Buildup Pressure, psi	Fluid Volume, cc	Stabilized time, s
0.1	2,850.343	2,481.924	2,850.344	10.00	224.542
1	2,850.343	2,734.099	2,850.344	10.00	46.443
10	2,850.343	2,831.908	2,850.344	10.00	10.704
100	2,850.343	2,842.492	2,850.344	10.00	0.815

5.6 Effect of the Restricted Zone Severity in Gas Reservoir

From the simulation result, the similar behavior is happened in the gas reservoir. The total testing time is less than 5-minute for all the permeability value. Therefore, the restricted zone assumption is also included to gas reservoir. Based on the probe restricted flow assumption same as oil reservoir, some modification model and assumption are used instead of the base case model.

1. Probe restricted flow occurs in probe grid block. So, the permeability value is modified by reducing from original permeability value.

2. The permeability of probe block is reduced from original reservoir permeability by multiplying 0.1 in all direction. So, the probe block permeability varies from 10^{-1}mD to 10^{-7} mD.

3. This assumption neglects the supercharge effect and the restricted zone permeability in this study is called k_c

To study the effect of probe restricted flow on pressure response and buildup time, the reservoir simulation runs are conducted. The modification model is used with the reservoir permeability value 0.1 mD in all directions. The same procedure is applied to gas reservoir but a withdraw rate is 60cc/sec. The pressure response is shown in Figure 5.38a and 5.38b and Table 5.14 summarizes data with the different probe block permeability in 30-minute testing time.

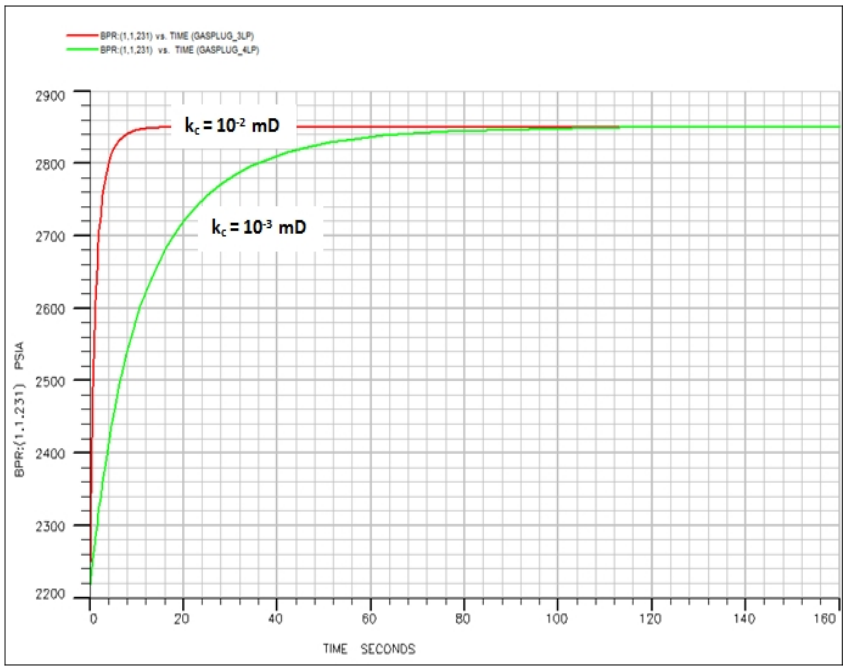

Figure 5.38a: Pressure response for the restricted zone permeability 10^{-2} mD to 10^{-3} mD at depth 6,567.5 ft

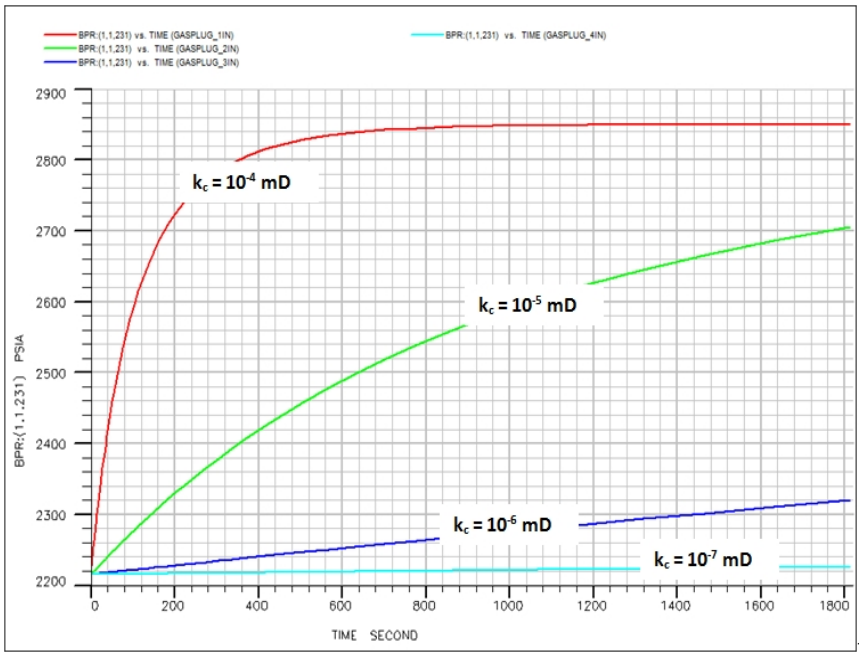

Figure 5.38b: Pressure response for the restricted zone permeability 10^{-4} mD to 10^{-7} mD at depth 6,567.5 ft

Table 5.14: Summary of data with the different restricted zone permeability in 30 minute testing time.

k_c, mD	Initial Pressure, psi	Final Drawdown Pressure, psi	Final Buildup Pressure, psi	Gas volume,	Stabilized time, s
Base case	2,850.344	2,416.242	2,850.344	10.00	124.331
0.01	2,850.344	2,237.690	2,850.344	10.00	124.331
0.001	2,850.344	2,217.764	2,850.344	10.00	203.074
0.0001	2,850.344	2,215.565	2,850.288	10.00	> 30 min
0.00001	2,850.344	2,215.344	2,704.994	10.00	> 30 min
0.000001	2,850.344	2,215.322	2,319.993	10.00	> 30 min
0.0000001	2,850.344	2,215.320	2,226.919	10.00	> 30 min

From the reservoir simulation result, the probe restricted flow is less effect on fluid withdrawal from the reservoir to probe due to the compressibility of gas. From the reservoir simulation result in Table 5.14, the restricted flow has a direct effect on the buildup pressure response and time for pressure build up to initial pressure in gas reservoir as same as the oil reservoir. Pressure response cannot reach to initial pressure in

30-minute from restricted zone permeability ranging from 10^{-4} mD to 10^{-7} mD same as the oil reservoir. It can be discussed at this point that with the probe permeability less than the 10^{-4} mD, the reservoir pressure cannot be reliably estimated from RFT data. To analyze pressure response, the conventional interpretation technique, the log-log plot is used to determine the flow regime. Then, extrapolation pressure technique is used to determine the reservoir pressure. Figures 5.39 to 5.42 show the log-log plot, extrapolation pressure and pressure gradient plot for 30-minute testing time.

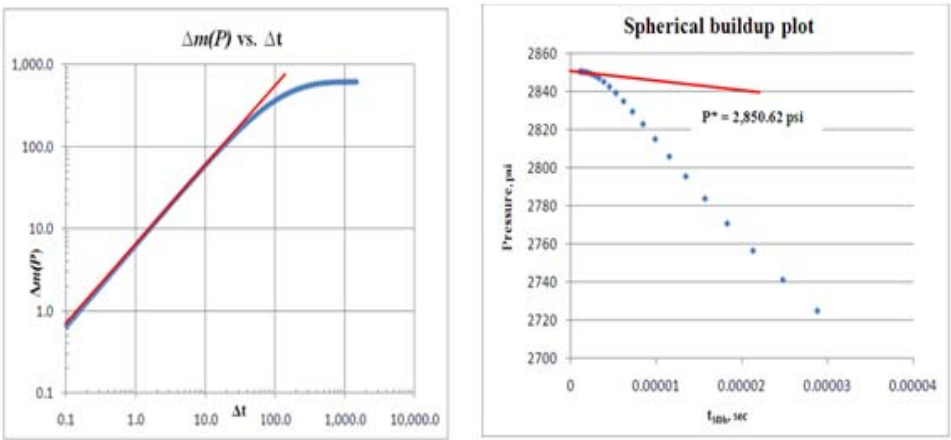

Figure 5.39: Log-log plot of d*m(P)* vs dt ,unit slope line and spherical pressure buildup plot for the restricted zone 10^{-4} mD at depth 6,567.5 ft with 30-minute testing time

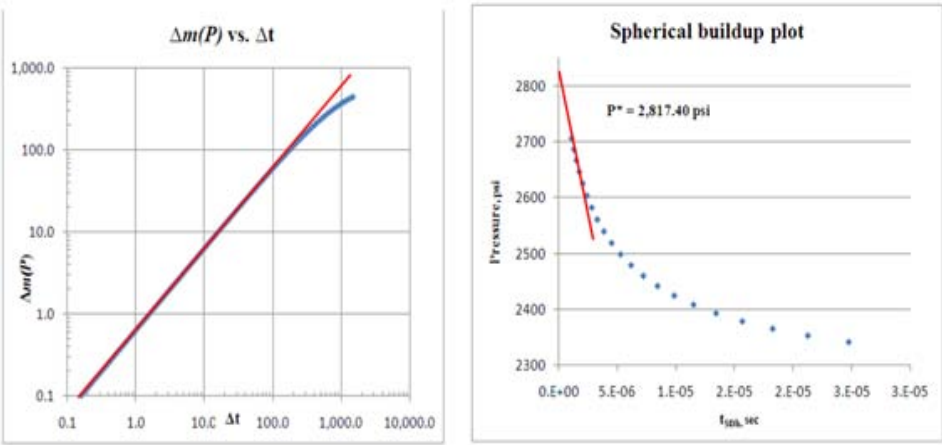

Figure 5.40: Log-log plot of d*m(P)* vs dt ,unit slope line and spherical pressure buildup plot for the restricted zone 10^{-5} mD at depth 6,567.5 ft with 30-minute testing time

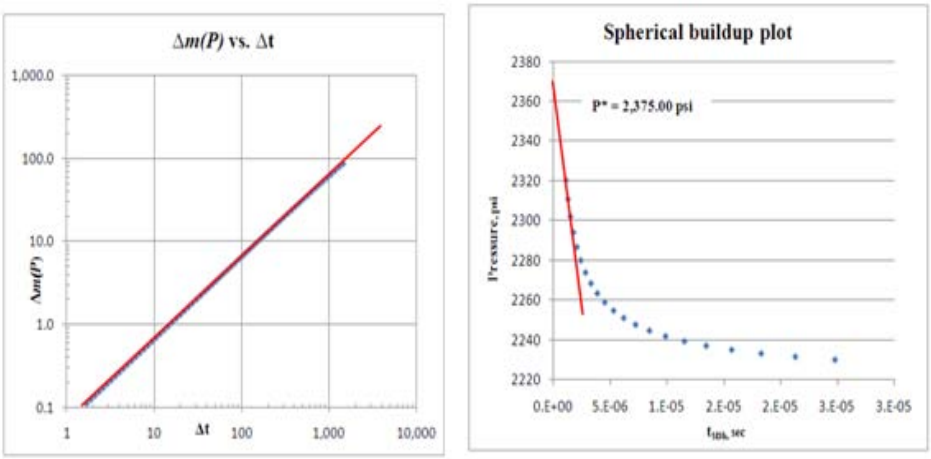

Figure 5.41: Log-log plot of d*m(P)* vs dt ,unit slope line and spherical pressure buildup plot for the restricted zone 10^{-6} mD at depth 6,567.5 ft with 30-minute testing time

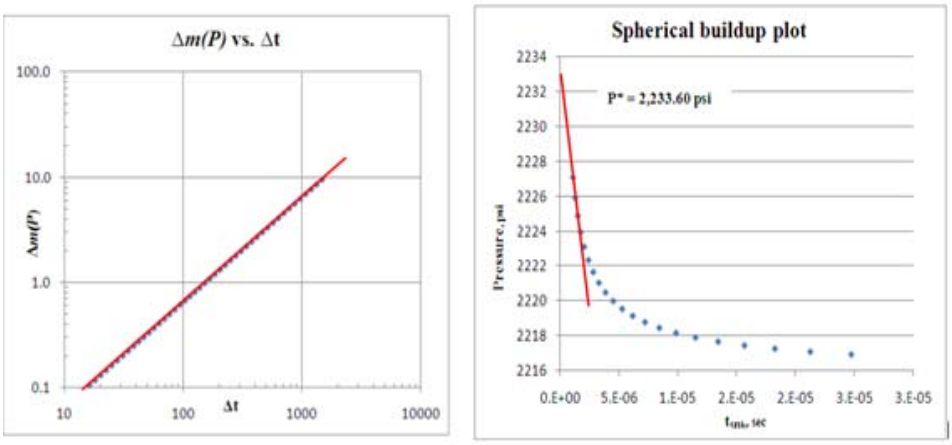

Figure 5.42: Log-log plot of d*m(P)* vs dt ,unit slope line and spherical pressure buildup plot for the restricted zone 10^{-7} mD at depth 6,567.5 ft with 30-minute testing time

Figures 5.43 to 5.46 show the result of pressure gradient plot for 30-minute testing time, the red line represents slope of initial fluid gradient (not on scale), the green line represents slope of extrapolation pressure gradient (not on scale) and blue line represents final reading pressure (plot on scale). Tables 5.15 and 5.16 show the final reading pressure, extrapolated pressure for 30-minute testing time, the error value of pressure is compared to its initial pressure on each point. Table 5.17 shows summary of fluid gradient interpretation from the final reading pressure and extrapolated pressure in 30-minute, the error value of fluid gradient interpretation is compared to its initial fluid gradient.

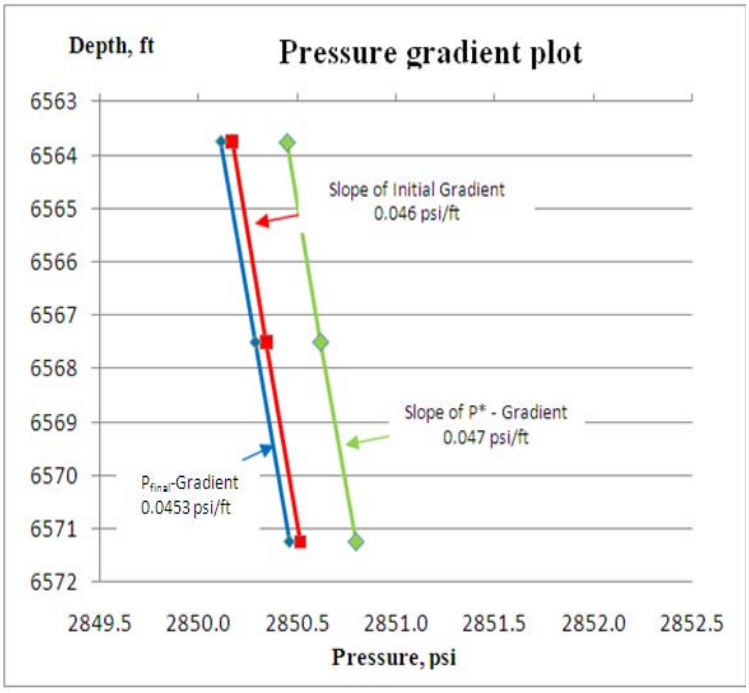

Figure 5.43: Pressure gradient plot from final reading pressure, extrapolation pressure and initial pressure for the restricted zone 10^{-4} mD

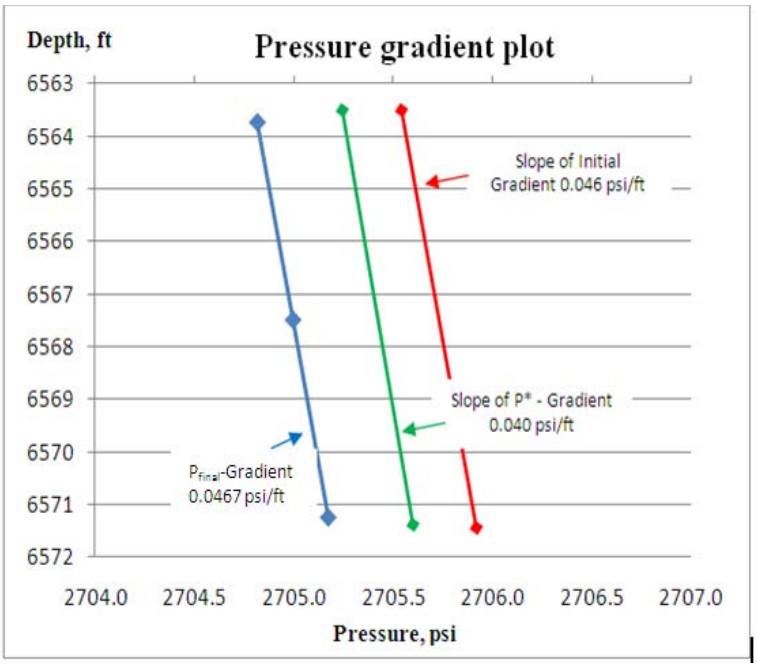

Figure 5.44: Pressure gradient plot from final reading pressure, extrapolation pressure and initial pressure for the restricted zone 10^{-5} mD

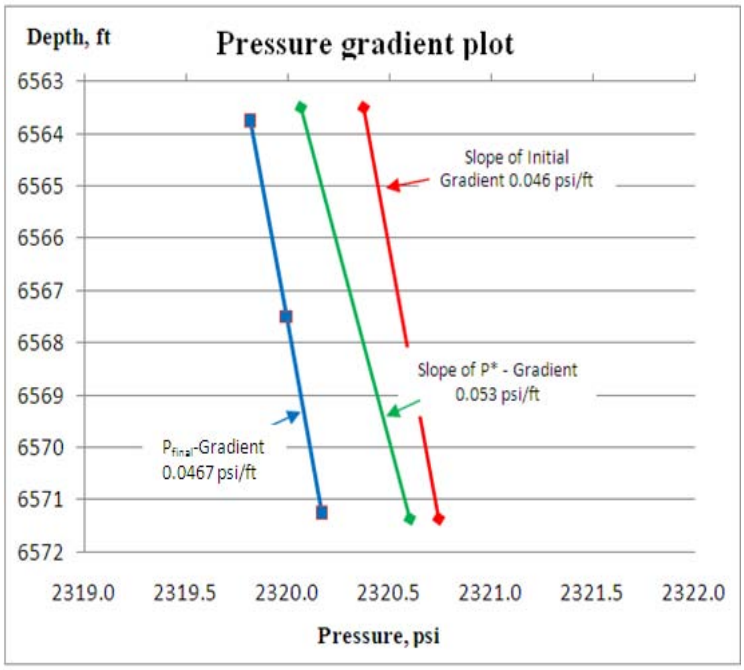

Figure 5.45: Pressure gradient plot from final reading pressure, extrapolation pressure and initial pressure for the restricted zone 10^{-6} mD

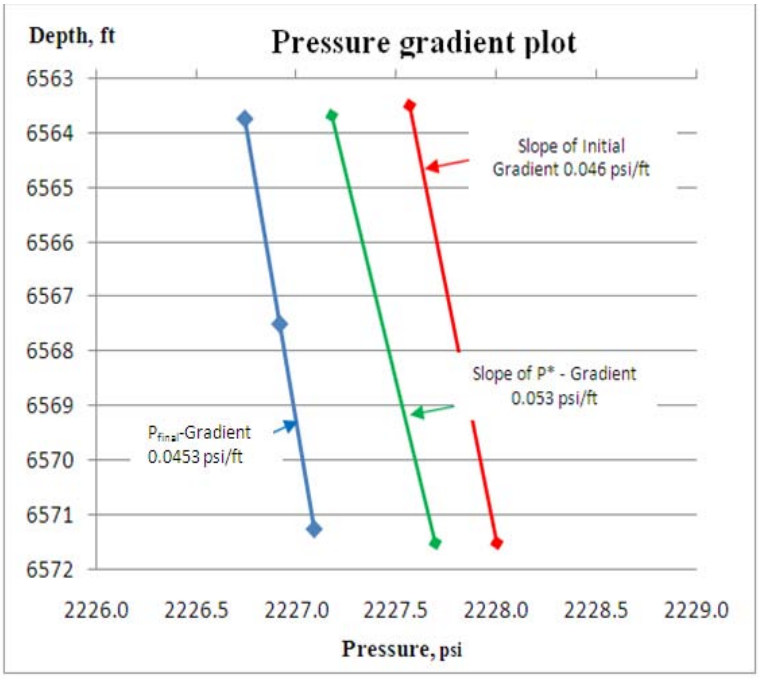

Figure 5.46: Pressure gradient plot from final reading pressure, extrapolation pressure and initial pressure for the restricted zone 10^{-7} mD

Table 5.15: Final reading pressure in 30-minute

Depth	P_i	10^{-4} mD		10^{-5} mD		10^{-6} mD		10^{-7} mD	
ft	psi	P_{final} psi	Error %	P_{final} psi	Error %	P_{final} psi	Error %	P_{final} psi	Error %
6,571.25	2,850.52	2,850.46	-0.0020	2,705.17	-5.10	2,320.17	-18.61	2,227.09	-21.87
6,567.50	2,850.34	2,850.29	-0.0020	2,704.99	-5.10	2,319.99	-18.61	2,226.92	-21.87
6,563.75	2,850.17	2,850.12	-0.0020	2,704.82	-5.10	2,319.82	-18.61	2,226.75	-21.87

Table 5.16: Extrapolation pressure in 30-minute

Depth	P_i	10^{-4} mD		10^{-5} mD		10^{-6} mD		10^{-7} mD	
ft	psi	P_{final} psi	Error %	P_{final} psi	Error %	P_{final} psi	Error %	P_{final} psi	Error %
6,571.25	2,850.52	2,850.80	+0.01	2,817.50	-1.16	2,375.20	-16.67	2,233.80	-21.64
6,567.50	2,850.34	2,850.62	+0.01	2,817.40	-1.16	2,375.00	-16.67	2,233.60	-21.64
6,563.75	2,850.17	2,850.45	+0.01	2,817.20	-1.16	2,374.80	-16.67	2,233.40	-21.64

Table 5.17: Summary of fluid gradient interpretation from the final reading pressure and extrapolated pressure in 30-minute

kc mD	Initial P gradient, psi/ft	Final reading Pressure			Extrapolated Pressure		
		gradient, psi/ft	Error %	Interpreted Gradient	gradient, psi/ft	Error %	Interpreted Gradient
10^{-4}	0.046	0.0453	-2.93	Gas	0.0467	0	Gas
10^{-5}	0.046	0.0467	0	Gas	0.0400	-14.35	N/A
10^{-6}	0.046	0.0467	0	Gas	0.0530	+15.94	N/A
10^{-7}	0.046	0.0453	-2.93	Gas	0.0530	+15.94	N/A

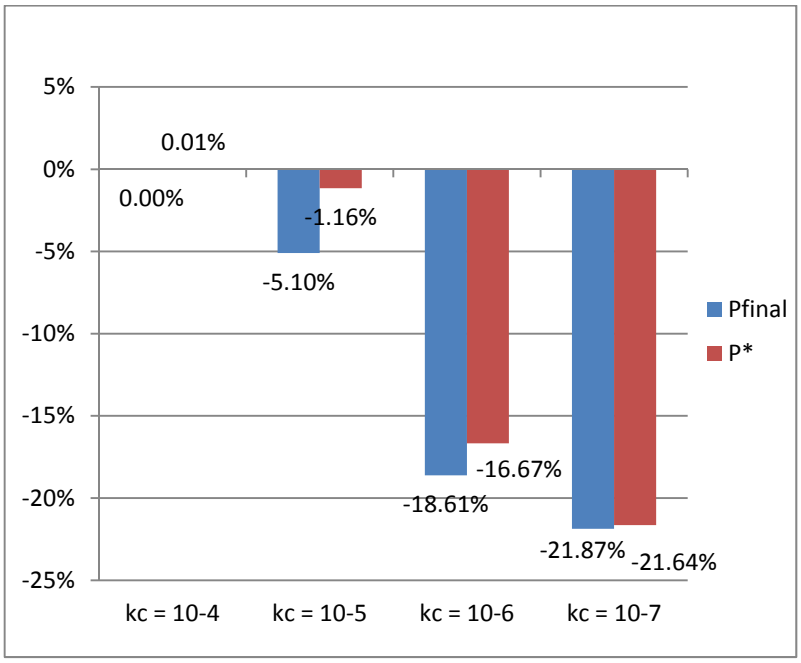

Figure 5.47: Pressure error from final reading pressure and extrapolation pressure in 30-minute

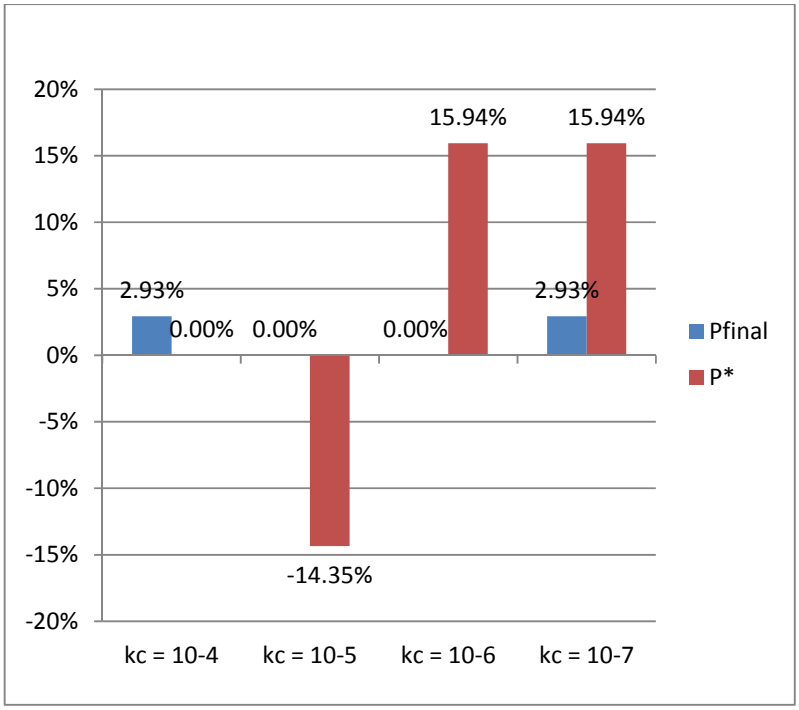

Figure 5.48: Fluid gradient error for final reading pressure and extrapolation pressure in 30-minute

As the result shown in Figure 5.47 and 5.48, the pressure response from 10^{-4} mD to 10^{-7} mD is mainly from the wellbore storage and transition period. The final reading pressure, both are underestimated and the maximum error is up to 21.87% and 21.64% from extrapolation pressure. The error trend is similar to oil reservoir but less severity because of gas has a higher compressibility value than oil. Therefore, the gas pressure can be expanded and compressed better than oil. So, pressure response in gas reservoir was not dropped rapidly like oil. The error from fluid gradient interpretation in this regime in Figure 5.48 shows the fluctuation in fluid gradient, the maximum error is up to 3% (underestimate) for final reading pressure and maximum error is up to 15.94% (overestimate) for extrapolation pressure. The error trend is not similar to oil reservoir due to the gas compressibility effect and result confirms that both interpretation techniques cannot use to indicate gas gradient in the reservoir.

Once the probe is inserted into a shale region or restricted zone, same as oil reservoir, more time is needed for the chamber pressure to reach the initial reservoir pressure. The more severe the restricted zone, the longer the time for chamber pressure to

reach the initial reservoir pressure. The lower the permeability value of the restricted zone is, the longer the wellbore/chamber storage period same as oil reservoir. Therefore, one should not used RFT pressure to estimate the initial reservoir pressure or pressure gradient as long as the pressure readings are still in the wellbore/chamber storage period.

5.7 Curve Fitting for Gas Reservoir

The final reading pressure and the conventional technique are invalid for gas reservoir that the restricted zone permeability lower than 10^{-4} mD with the 30-minute buildup time. Curve fitting is the concept of fitting equations to data similar to oil reservoir application.

Table 5.18: Summary data of input value and coefficient of different restricted zone permeability for gas reservoir

k_c, mD	P_{est} ,psi	P_{dd}, psi	C_1	C_2
10^{-1}	2,850.00	2,416.246	433.754	0.128447886
10^{-2}	2,850.00	2,237.690	612.310	1.1851
10^{-3}	2,850.00	2,217.765	632.235	11.3875
10^{-4}	2,850.00	2,215.565	634.435	113.4495
10^{-5}	2,850.00	2,215.344	634.656	1,138.4068
10^{-6}	2,850.00	2,215.322	634.678	11,287.1816
10^{-7}	2,850.00	2,215.320	634.680	113,664.4551

To observe the rate of pressure change versus time from the stabilized test, the base case study is brought to observe the rate of change. From the result, the differentiation value is relatively constant at $1x10^{-9}$ range. Figure 5.49 shows the differentiation value plot at the stabilized pressure. Solving the differential equation the differential value is set to $1x10^{-8}$. The buildup time result from the differential equation and total testing time is show in Table 5.19.

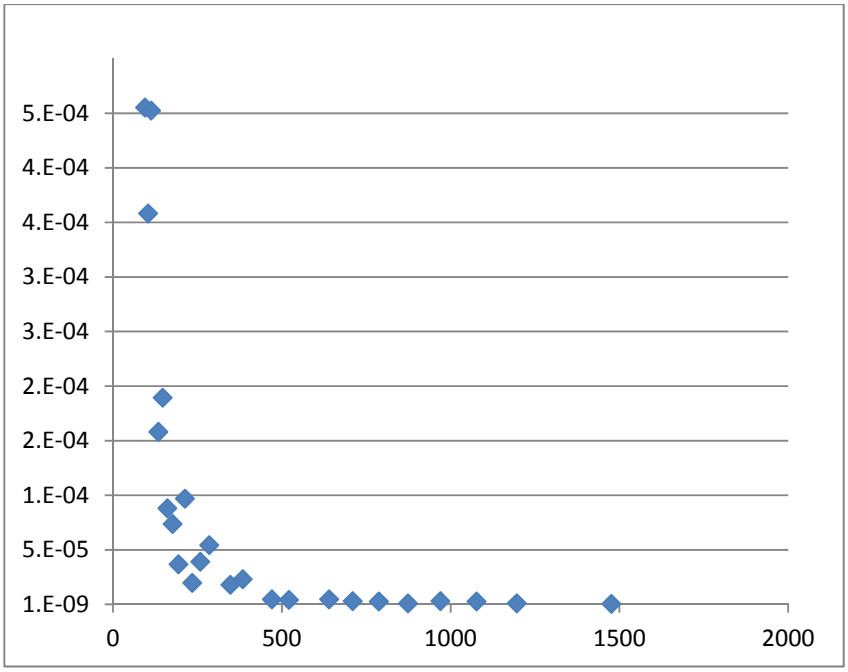

Figure 5.49: the differentiation value plot for a base case

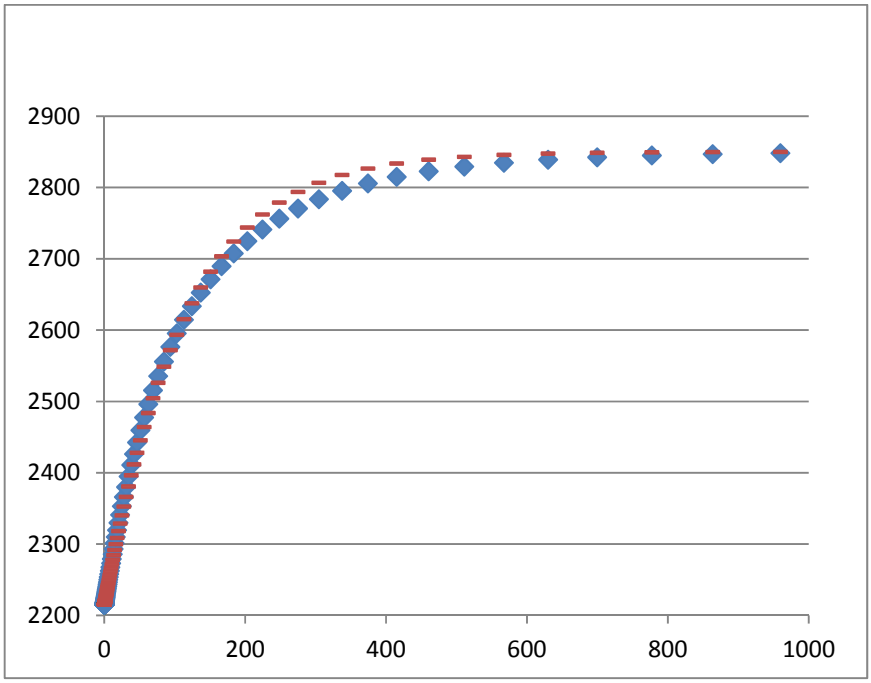

Figure 5.50: Pressure buildup profile from reservoir simulation and exponential model for the restricted zone permeability 10^{-4} mD

Table 5.19 The buildup time result for each restricted zone permeability

k_c, mD	$t_{buildup}$ (Δt_{est}), sec	t_{Total}, sec
10^{-1}	3.70	3.87
10^{-2}	31.96	32.13
10^{-3}	281.73	281.89
10^{-4}	2,546.33	2,546.50
10^{-5}	22,926.33	22,926.50
10^{-6}	201,419.32	201,419.48
10^{-7}	1,765,820.66	1,765,820.83

5.8 Effect of the Restricted Zone Severity in Gas Reservoir with Low Restricted Zone Permeability.

This study investigates and analyzes pressure behavior of the restricted zone permeability ranging from 10^{-4} mD to 10^{-7} mD. After investigating pressure response, the method to analyze fluid gradient is determined. The same testing procedure is applied except the testing time is adjusted. Then curve fitting technique is used to estimate the total time to reach initial reservoir pressure for each restricted zone effect as same as oil reservoir. The result from curve fitting technique is shown in Table 5.20.

Table 5.20: Estimate total time to reach initial reservoir pressure for restricted zone effect

k_c, mD	t_{Total}
10^{-4}	42.44 min
10^{-5}	6.37 hrs
10^{-6}	2.33 days
10^{-7}	20.44 days

From Table 5.20, the extension time for each restricted zone permeability is used in the reservoir simulation runs and the results are shown and scaled up (insert figure) in Figures 5.51 to 5.54. Figures 5.55 to 5.58 show the log-log plot. The plots are used to verify the wellbore storage, transition period and infinite acting solution. The first reading

pressure after transition period, P_{first}, is used to plot pressure gradient. Spherical buildup plot is used to determine extrapolation pressure starting from first reading pressure until estimate time in Table 5.20 and the extrapolation pressure, P*, is used to plot pressure gradient. Table 5.21 shows the summary of time readings from log-log plots.

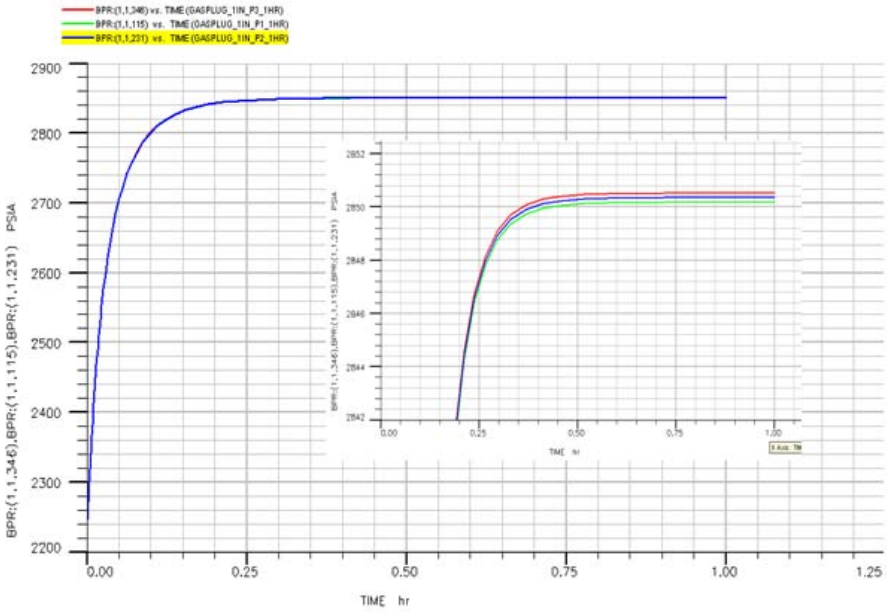

Figure 5.51: Pressure response for the restricted zone permeability 10^{-4} mD with 60 minutes

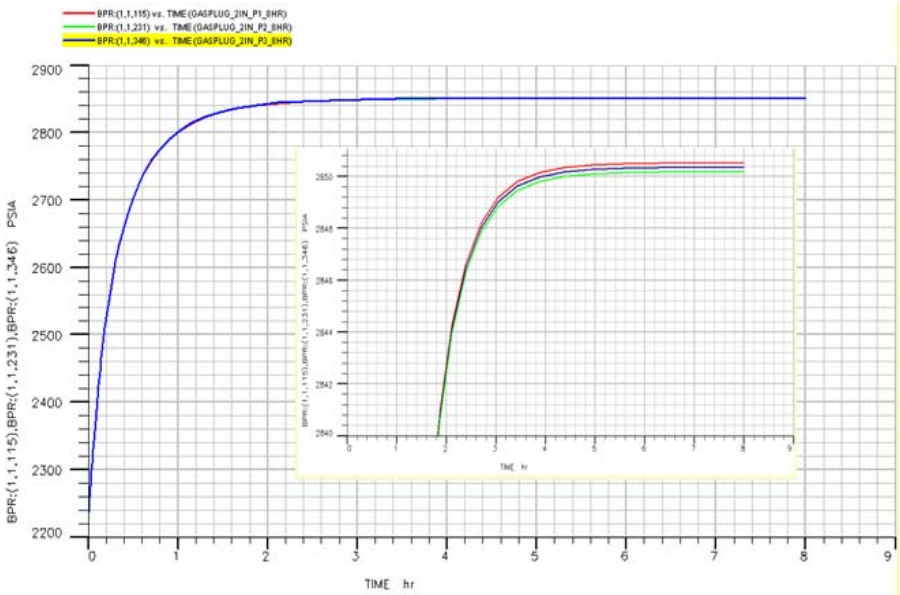

Figure 5.52: Pressure response for the restricted zone permeability 10^{-5} mD with 8 hours

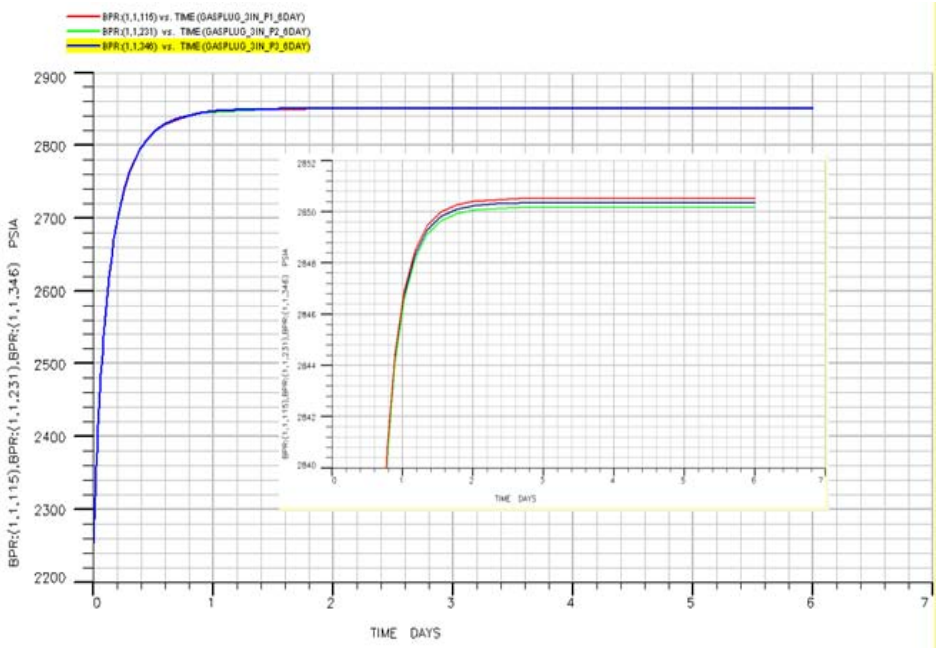

Figure 5.53: Pressure response for the restricted zone permeability 10^{-6} mD with 5 days

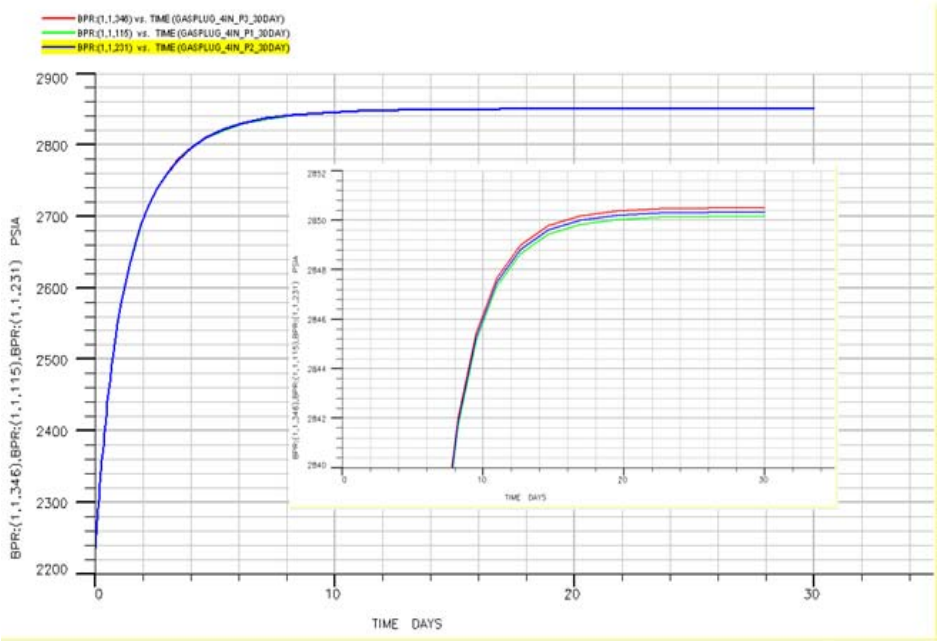

Figure 5.54: Pressure response for the restricted zone permeability 10^{-7} mD with 30 days

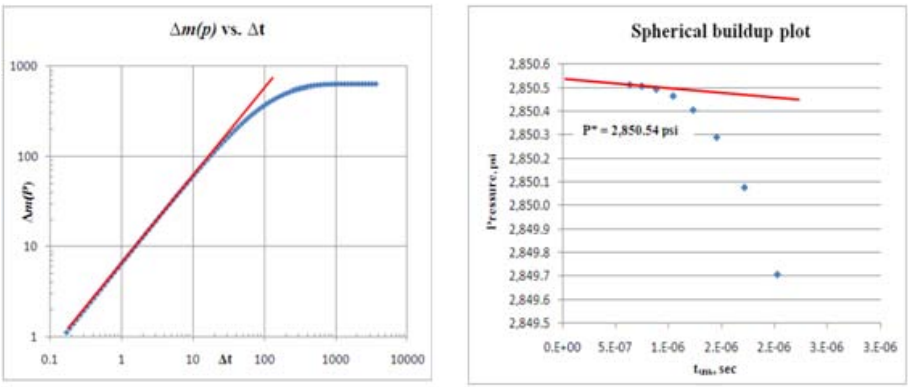

a)

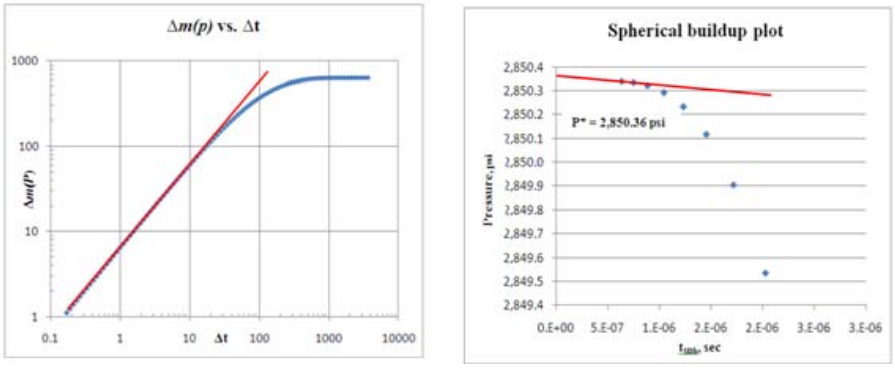

b)

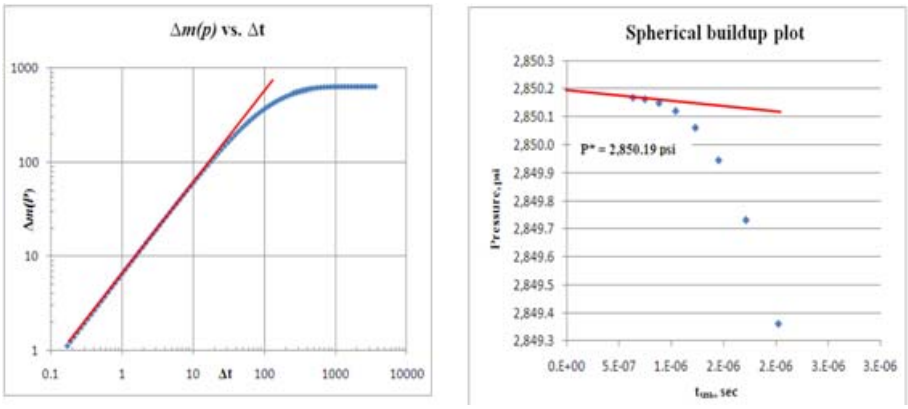

c)

Figure 5.55: Log-log plot of d*m(P)* vs dt , unit slope line and spherical pressure buildup plot for the restricted zone permeability 10^{-4} mD with 60 minutes a) depth 6,571.25ft b) depth 6,567.50 ft c) 6,563.75 ft

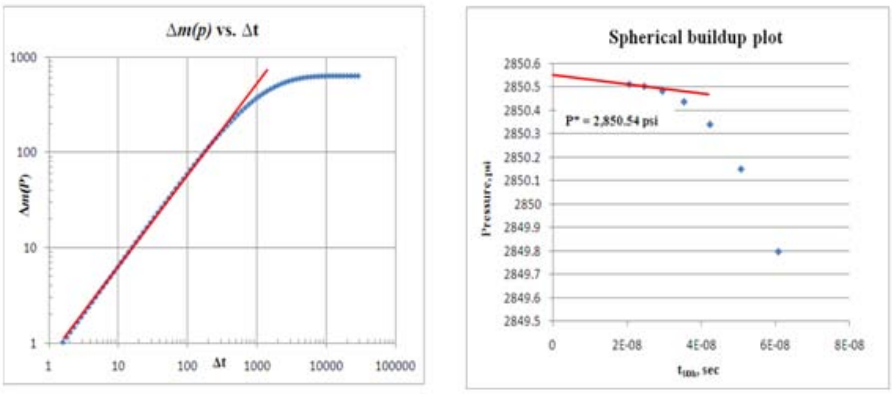

a)

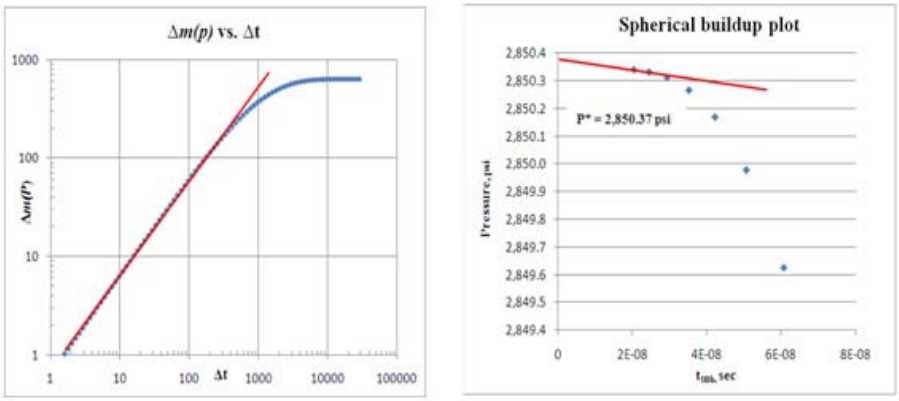

b)

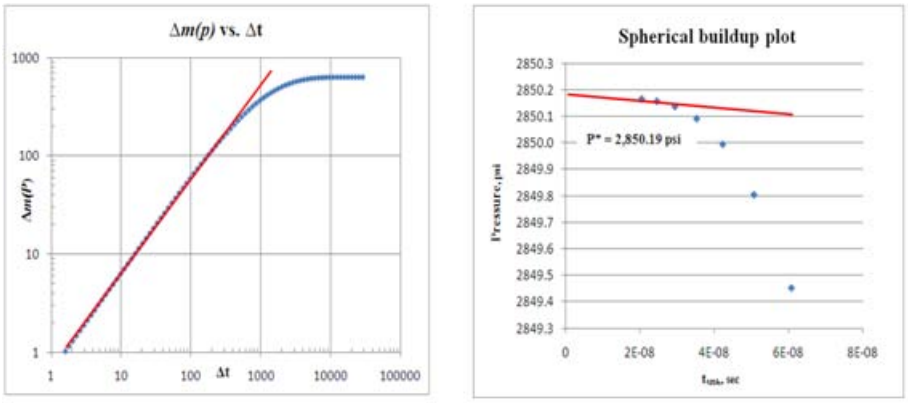

c)

Figure 5.56: Log-log plot of d*m(P)* vs dt , unit slope line and spherical pressure buildup plot for the restricted zone permeability 10^{-5} mD with 8 hours a) depth 6,571.25ft b) depth 6,567.50 ft c) 6,563.75 ft

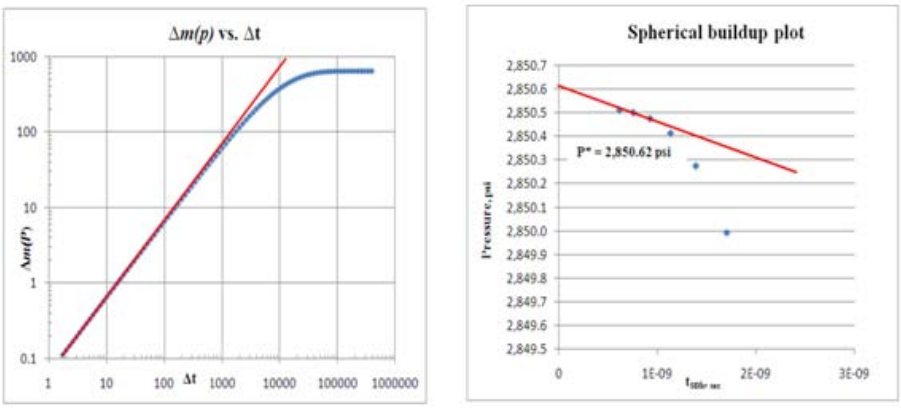

a)

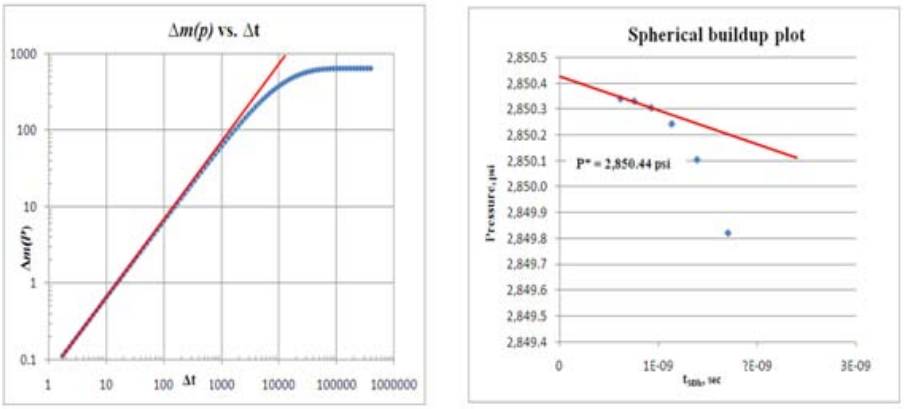

b)

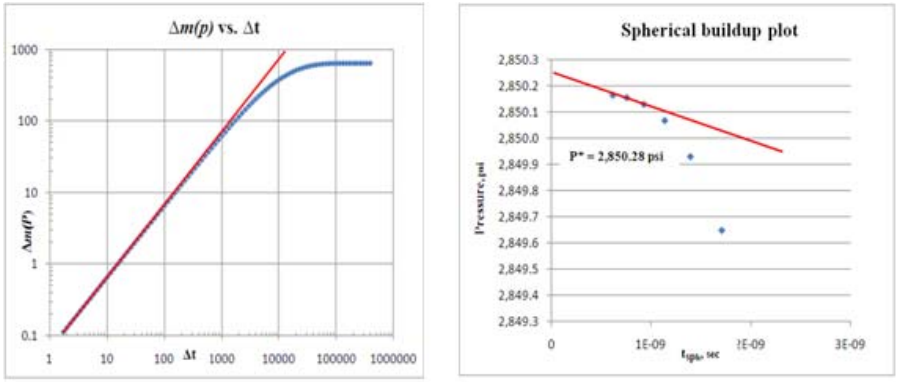

c)

Figure 5.57: Log-log plot of d*m(P)* vs dt , unit slope line and spherical pressure buildup plot for the restricted zone permeability 10^{-6} mD with 5 days a) depth 6,571.25ft b) depth 6,567.50 ft c) 6,563.75 ft

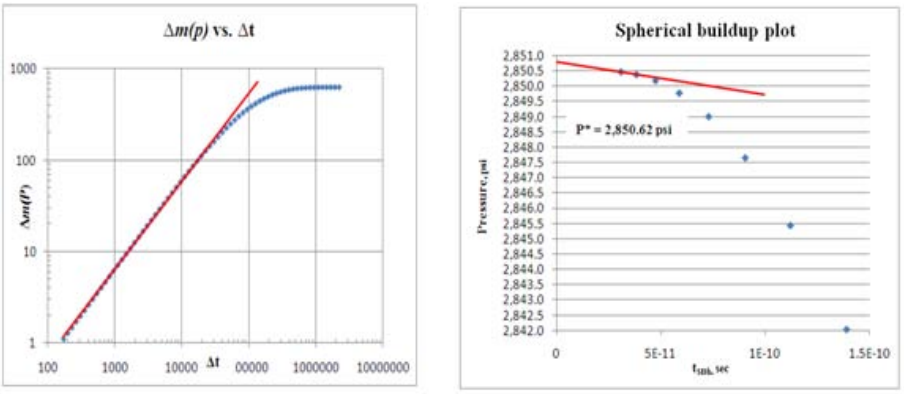

a)

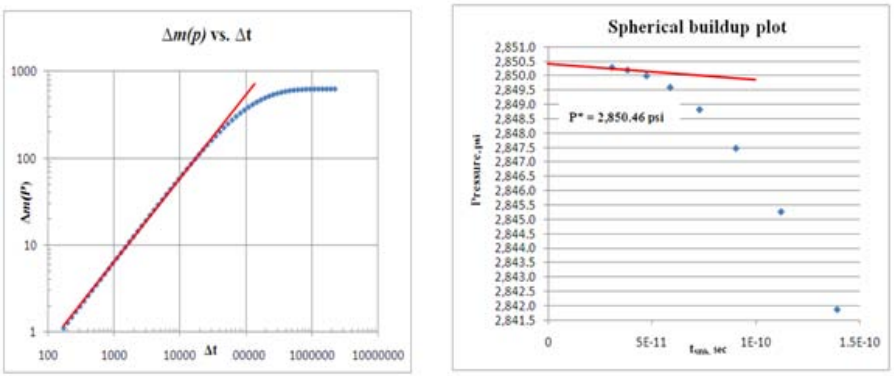

b)

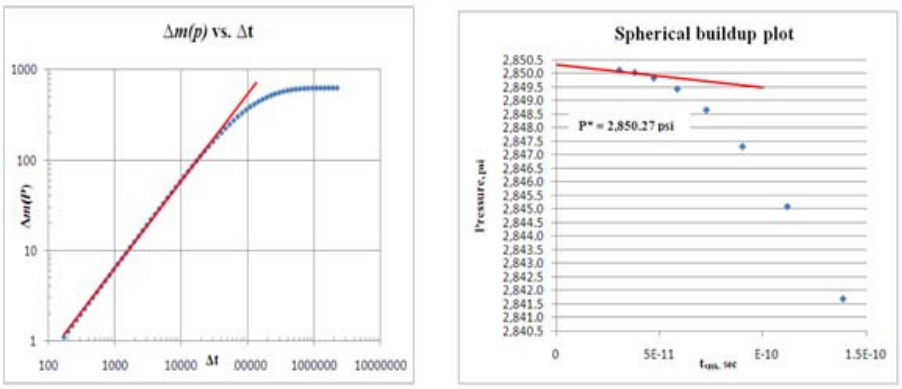

c)

Figure 5.58: Log-log plot of dm(P) vs dt , unit slope line and spherical pressure buildup plot for the restricted zone permeability 10-7 mD with 30 days a) depth 6,571.25ft b) depth 6,567.50 ft c) 6,563.75 ft

Table 5.21: Summary of time readings from log-log plot

k_c, mD	Total testing time, sec	WBS time, sec	Start of IFAS time sec
10^{-4}	2,546.50	30.00	2,000.00
10^{-5}	22,926.50	300.00	10,000.00
10^{-6}	201,419.48	3,500.00	100,000.00
10^{-7}	1,765,820.83	20,000.00	1,000,000.00

Figures 5.59 to 5.62 show the result of pressure gradient plot for the adjusted testing time, the red line represents slope of initial fluid gradient (plot on scale), the green line represents slope of extrapolation pressure gradient (plot on scale) and blue line represents final reading pressure (plot on scale). Tables 5.22 and 5.23 show the first reading pressure, extrapolated pressure after extended testing time, the error value of pressure is compared to its initial pressure on each point. Table 5.24 shows summary of fluid gradient interpretation from the final reading pressure and extrapolated pressure after extended testing time

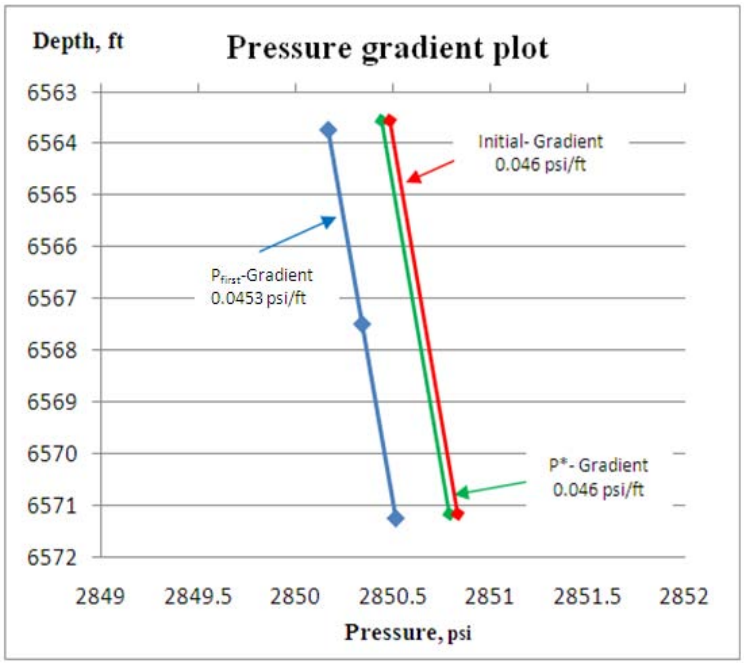

Figure 5.59: Pressure gradient result from the first reading pressure, extrapolation pressure and initial pressure for the restricted zone 10^{-4} mD

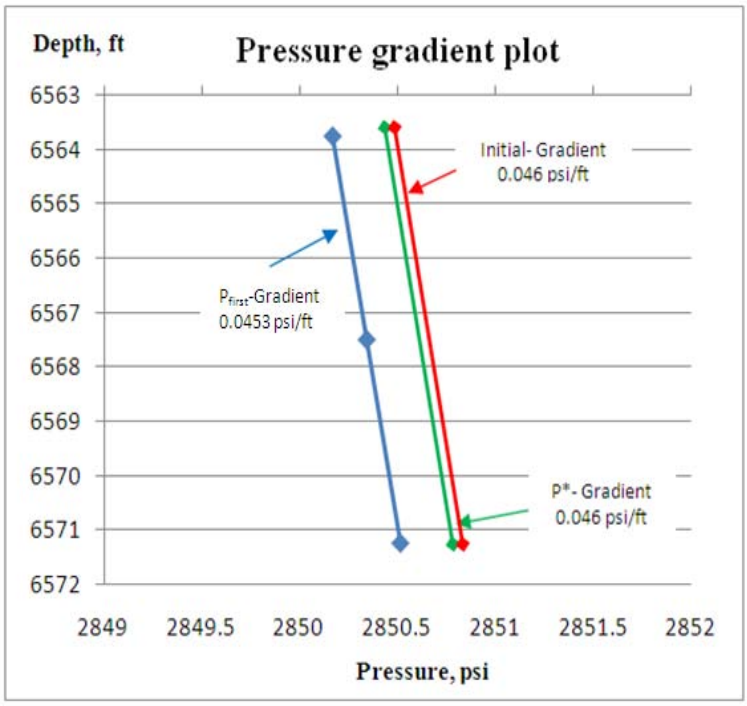

Figure 5.60: Pressure gradient result from the first reading pressure, extrapolation pressure and initial pressure for the restricted zone 10^{-5} mD

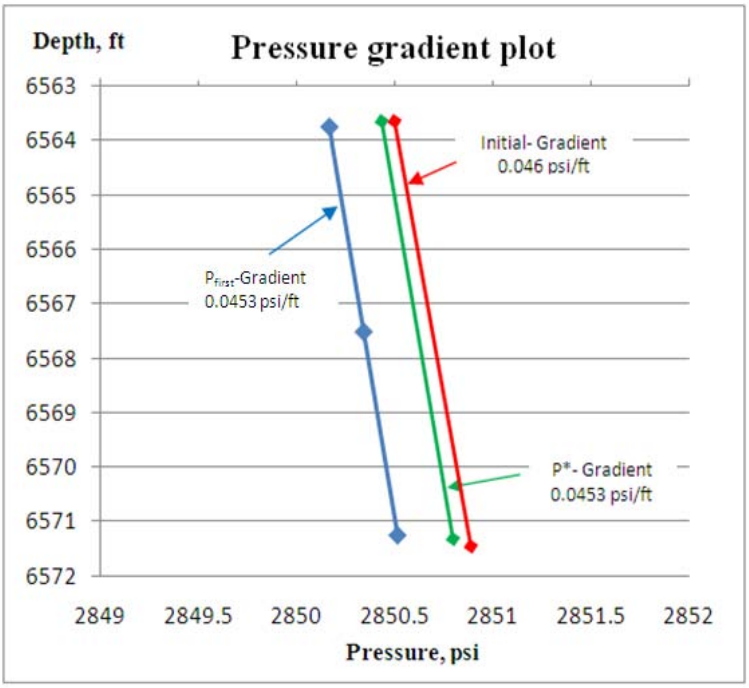

Figure 5.61: Pressure gradient result from the first reading pressure, extrapolation pressure and initial pressure for the restricted zone 10-6 mD

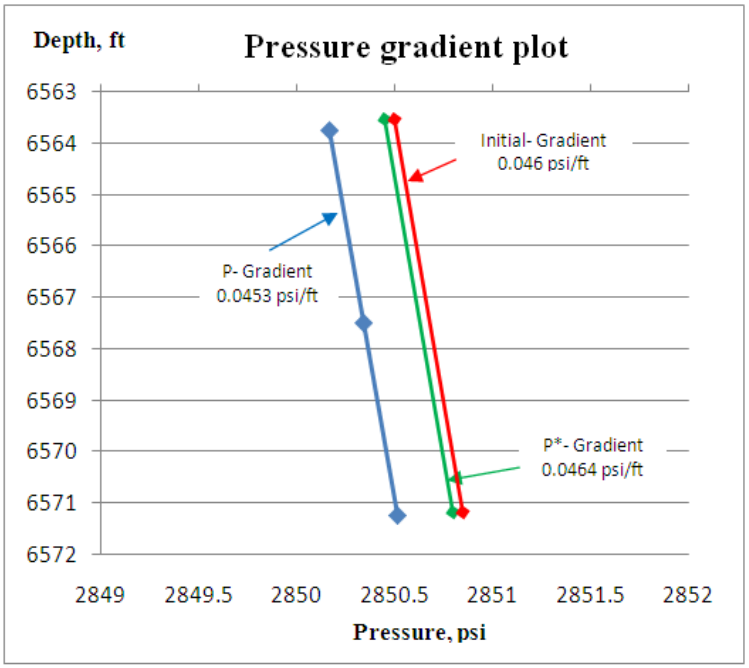

Figure 5.62: Pressure gradient result from the first reading pressure, extrapolation pressure and initial pressure for the restricted zone 10-7 mD

Table 5.22: First reading pressure after passing transition period.

Depth	P_i	10^{-4} mD		10^{-5} mD		10^{-6} mD		10^{-7} mD	
		P_{final}	Error	P_{final}	Error	P_{final}	Error	P_{final}	Error
ft	psi	psi	%	psi	%	psi	%	psi	%
6,571.25	2,850.52	2,850.49	-0.001	2,849.18	-0.047	2,848.50	-0.071	2,848.99	-0.054
6,567.50	2,850.34	2,850.32	-0.001	2,849.01	-0.047	2,848.33	-0.071	2,848.83	-0.053
6,563.75	2,850.17	2,850.15	-0.001	2,848.84	-0.047	2,848.16	-0.071	2,848.65	-0.053

Table 5.23:Extrapolation pressure after extended time.

Depth	P_i	10^{-4} mD		10^{-5} mD		10^{-6} mD		10^{-7} mD	
		P_{final}	Error	P_{final}	Error	P_{final}	Error	P_{final}	Error
ft	psi	psi	%	psi	%	psi	%	psi	%
6,571.25	2,850.52	2,850.54	+0.001	2,850.54	+0.001	2,850.62	+0.004	2,850.62	+0.004
6,567.50	2,850.34	2,850.36	+0.001	2,850.37	+0.001	2,850.44	+0.004	2,850.46	+0.004
6,563.75	2,850.17	2,850.19	+0.001	2,850.19	+0.001	2,850.28	+0.004	2,850.27	+0.004

Table 5.24: Summary of fluid gradient interpretation from the final reading pressure and extrapolated pressure after extended time

k_c mD	Initial P gradient, psi/ft	First reading Pressure			Extrapolate Pressure		
		gradient, psi/ft	Error %	Interpreted Gradient	gradient, psi/ft	Error %	Interpreted Gradient
10^{-4}	0.046	0.0453	-2.93	Gas	0.0467	0	Gas
10^{-5}	0.046	0.0453	-2.93	Gas	0.0467	0	Gas
10^{-6}	0.046	0.0453	-2.93	Gas	0.0453	-2.93	Gas
10^{-7}	0.046	0.0453	-2.93	Gas	0.0464	+0.64	Gas

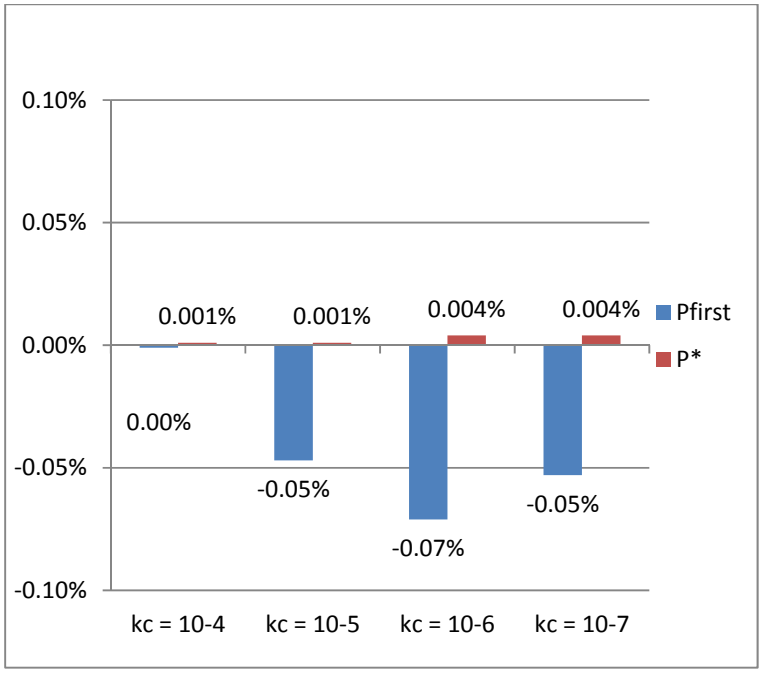

Figure 5.63: Final pressure error for the first reading pressure and extrapolation pressure after extended time

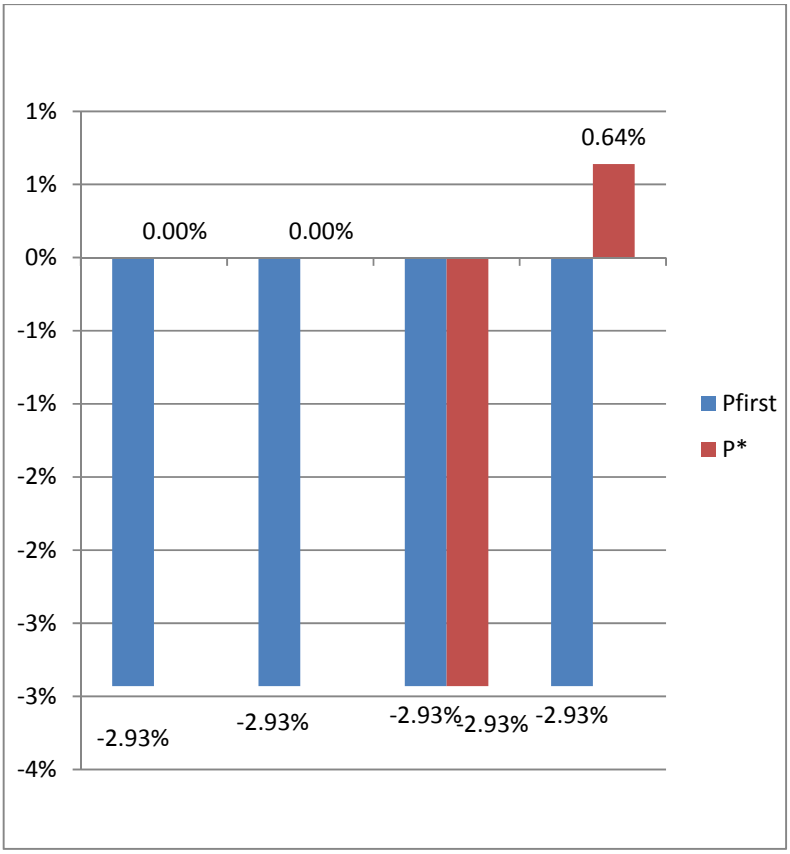

Figure 5.64: Fluid gradient error for the first reading pressure and extrapolation pressure after extended time

From the results, the curve fitting technique is used to extend testing time and the result is satisfied for pressure response. The pressure response almost reached to initial pressure. The log-log plot confirms that pressure response has passed the wellbore storage and transition periods and reached the infinite acting (fully reservoir response) period. After end of wellbore storage and transition periods, the first reading pressure can be used directly as a pressure point to plot the pressure gradient (P_{first}). Figure 5.63 shows the maximum error of 0.007% (underestimate) and 0.004% (overestimate) for the extrapolation pressure (P*). The error from fluid gradient interpretation in this regime shown in Figure 5.64 is also low with maximum error is 2.93% (underestimate). The result confirms that both techniques can be used to indicate gas gradient in the reservoir.

From the previous results, it can be concluded that as long as the restricted reservoir permeability value is not less than 0.0001 mD, we should be confident to use

RFT data for estimation of initial reservoir pressure and fluid type because pretest time should not be more than 5 min. After applying the restricted zone permeability effect, the 30-minute testing time is not enough to reach stabilized condition. The final reading pressure and the spherical interpretation cannot be applied because the pressure response is mainly in the wellbore storage and transition regime as can be seen in the log-log plot. The reason behind this is that the low permeability values of restricted zone act as a choke to the flow from reservoir to probe and then the chamber, compared to flow in porous medium or majority of the reservoir. The lower the permeability value, the slower the flow. This leads to slower increase in pressure in the chamber and results in slower increase in pressure in the chamber. After adjusted testing time, the RFT pressure can be used to estimate the initial reservoir pressure and the pressure gradient. It was found out that whenever the flow regime is infinite acting period, i.e. the flow is fully under influence of the reservoir flow, not wellbore/chamber storage alone or transition period, the appropriated RFT pressure data can be used to estimate the initial reservoir pressure and pressure gradient or fluid type. In other words, as long as the pressure response is in the infinite acting flow regime, appropriated pressure values can be used to estimate fluid gradient for both oil and gas reservoir.

CHAPTER VI

CONCLUSION AND RECOMMENDATION

This chapter concludes the restricted zone effect on pressure response in the low permeability reservoir, method to determine the fluid gradient and discusses about limitation from the study and the recommendations for future works.

In this study, reservoir simulator is used as a tool to simulate pressure response when Repeat Formation Tester is run in the low permeability reservoir. The study described in this report focuses on a single layered reservoir with different restricted zone/near probe damage to determine fluid gradient. By varying the severity of restricted zone/ near probe damage, the pressure response is simulated and interpreted by the conventional technique.

First, a single layered homogeneous reservoir is simulated with the 30-minute observation time. The isochronal concept (pressure point) and conventional interpretation are applied to determine fluid gradient.

Second, curve fitting technique is applied to estimate the total testing time for each scenario. After determining the estimated time, both techniques are applied to determine fluid gradient.

Finally, the fluid gradient is interpreted from both techniques.

6.1 Conclusions

From the results of this study, it can be concluded as follows:

1. From the simulation result on low permeability reservoir, the total testing time is less than 5-minute for all the permeability value. The reservoir permeability, itself, is not only one factor that affects the pressure response.
2. The situation that RFT probe is inserted into the shale region can be simulated by

using the concept of the restricted zone. The restricted zone reduces the flow from the reservoir into the probe and the chamber. The more severe the restricted zone is, the less fluid can flow from the reservoir to the probe and the chamber. With reduction of flow from the reservoir to the probe, flow regime can be under influence of wellbore/chamber storage. Regardless of fluid types. Correct estimation of the initial reservoir pressure and the pressure gradient can be obtained only when appropriate RFT pressure in the infinite acting regime is used for estimation.

3. As long as the restricted reservoir permeability is not less than 0.0001 mD, RFT pressure will reach the initial reservoir pressure within 5 minutes and it can be used to estimate the initial reservoir pressure, the pressure gradient, and fluid type.
4. The curve fitting method can be used to estimate total testing time. By using the curve fitting procedure, it can be used as a tool to help whether to continue testing or not. However, one should be noted that these methods do not take into account the reservoir properties, only the pressure response is considered.

6.2 Recommendations

The following points are recommendations for future study:

1. In this study, a single layered reservoir is considered. This model considers the vertical grid in equality linear grid block, Shale or restricted zone model is igloo shape and considered to be near wellbore effect.
2. The curve fitting method can be used to estimate the total testing time. To get the input value, and coefficient value, the iteration method is used but it is time consuming process.

REFERENCES

[1] Moran, J. H., and Finklea, E. E.. "Theoretical Analysis of Pressure Phenomena Associated with the Wireline Formation Tester," paper SPE 177. This paper was presented at 36th Annual Fall Meeting of SPE in Dallas, USA. : October 8-11, 1962.

[2] Culham, W. E.. "Pressure Buildup Equations for Spherical Flow Regime" Paper SPE 4053. This paper was presented at the SPE-AIME 47th Annual Fall Meeting held in San Antonio, Tex., Oct. 8-11, 1974.

[3] Smolen, J. J., and Litsey, L. R.. "Formation evaluation using Wire line formation tester pressure data" paper SPE 6822. This paper was presented at SPE-AIME 52nd Annual Fall technical Conference and Exhibition, held in Denver, Oct. 9-12, 1977.

[4] Pelissier-Combescure, J., Pollock, D., and Wittmann, M.. "Application of Repeat Formation Tester Pressure Measurements in the Middle East," paper SPE 7775. Thias paper was presented at the Middle East Oil Technical Conference of the Society of Petroleum Engineers, Manama, Bahrain, 25-29 March 1979.

[5] Stewart, G., and Wittmann, M.. "Interpretation of the Pressure Response of the Repeat Formation Tester," paper SPE8362. This paper was presented at the 54th Annual Fall Technical Conference and Exhibition of the Society of Petroleum Engineers of AIME, Nevada, 23-26 September 1979.

[6] Stewart, G., and Ayestaran, L.. “The interpretation of vertical pressure gradient measured at observation wells in developed reservoirs” paper SPE 11132. This paper was presented at 72th Annual Fall Technical Conference and Exhibition of Society of Petroleum Engineer of AIME, held in New Orleans LA, Sept. 26-19, 1982.

[7] Kasap, E., Huang, K., Shwe, T., and Georgi, D.. “Robust and Simple Graphical Solution For Wireline Formation Tests: Combined Drawdown and Buildup Analyses” paper SPE 36525. This paper was presented for presentation at the 1996 SPE Annual Technical Conference and Exhibition held in Denver, Colorado, USA, Oct. 6-9, 1996.

[8] Lee, J., and Michaels, J.. “Enhanced Wireline Formation Tests in Low-Permeability Formations: Quality Control Through Formation Rate Analysis” paper SPE 60293. This paper was prepared for presentation at the 2000 SPE Rocky Mountain Regional/Low Permeability Reservoirs Symposium and Exhibition held in Denver, Colorado, 12–15 March 2000.

[9] Yildiz, T., and Bassiouni, Z.. “Interpretation of Wireline Formation Tester Data in Tight gas Sands” paper 92-20 Annual Technical Meeting, Jun 7 - 10, 1992 , Calgary, Alberta. This paper was prepared and published on journal of Canadian Petroleum Technology: December 1997.

[10] Soliman, M.Y.. “Analysis of Buildup Tests with Short Producing Time” paper SPE 11083. This paper was presented at the 1982 SPE Annual Technical Conference and Exhibition held in New Orleans, September 26-29, 1982.

[11] Crook, P. Y.. “Reservoir analysis by wire line formation tester: Pressures, Permabilities, Gradients, and Net pay” paper 1984-vXXVn6a3. This paper was presented at the Indonesian Petroleum Association Convention in May 1984 p. 38-46.”

[12] Jeffrey, A. J., and Leonard, F. K.. “Unsteady-State Spherical Flow with Storage and Skin” paper SPE 12950. This paper was received in the society of Petroleum Engineers office Feb 28, 1984. Paper was accepted for publication Jan 9, 1985.

[13] Jawaid, S.. “Interpretation and use of vertically distributed pressures from Repeat Formation Tester measurement” paper PETSOC 86-37-36. This paper was presented at the annual technical meeting of petroleum society of CIM held in Calgary June 8-11 1986.

[14] Waid, M.C., Proett, Ma., Chen C.C., and Ford W.T.. “Improved Models for Interpreting the Pressure response of Formation Testers” paper SPE 22754. This paper was presented at 66 Annual Technical Conference and Exhibition of Society of Petroleum Engineer, held in Dallas TX, Oct. 6-9,1991.

[15] Yildiz, T., and Langlinals, J.. “A reservoir model for Wireline formation testing” paper SPE 18952. This paper was presented at the 1989 SPE Rocky Mountain Refional/Low Permeability Reservoirs Symposium and Exhibition held in Denver, March 6-8.

[16] Dussan, V., and Sharma, Y.. “Analysis of the pressure response of a single-probe formation tester” paper SPE 16801. This paper was presented at 1987 SPE Annual Technical Conference and Exhibition, Dallas, Sept. 27-30.

[17] Daungkaew, S., Prosser, D. J., Manescu, A., and Morales, M.. “An Illustration of the information that can be obtained from Pressure Transient Analysis of Wireline Formation Test Data” paper SPE 88650. This paper was prepared for presentation at the SPE Asia Pacific Oil and Gas Conference and Exhibition held in Perth, Australia, 18-20 October 2004.

[18] Kumar, V., Dunlap, J., and Klimentos, T., Zuber, K., and Foarooqui, M.Y.. "The Use of Wireline Formation Tester for Optimization of Conventional Well Test Design and Interpretation" paper SPE 129031. This paper was prepared for presentation at the SPE Oil and Gas India Conference and Exhibition held in Mumbai, India 20-22 January 2010.

[19] Joseph, J. A., and Koederitz, F.. "Unsteady-State Spherical Flow with Storage and Skin" paper SPE 12950. This paper was accepted for publication on Society of Petroleum engineer journal. Jan 9, 1985.

[20] Ahmed, U., Kuchuk, F., and Ayestaran, L.. "Short-Term Transient-Rate and Pressure-Buildup Analysis of Low-Permeability Reservoirs" paper SPE 13870. This paper was presented at the SPE/DOE Low permeability gas reservoir symposium held in Denver, May 19-22 ,1987.

[21] Jahanbani, A., and Aguilera, R. "Well Testing of Tight Gas Reservoirs" paper SPE 130066. This paper was presented at the 9th Canadian International Petroleum Conference (the 59th Annual Technical Meeting of the Petroleum Society), June 17–19, 2008, in Calgary, Alberta. Journal of Canadian Petroleum Technology 8 Sept 2009

[22] Lee, W.J. "Pressure-Transient Test Design in Tight Gas Formations" paper SPE 17088. This paper used to inform the general readership of recent advances in various areas of petroleum engineering, SPE Distinguished Author Series, Dec. 1981-Dec 1983.

[23] Soliman, M.Y., Azari. M., SPE, and Ansah, J., and Kabir, C.S. "Review and Application of Short-Term Pressure Transient Testing of Wells" paper SPE 93560. This paper was prepared for presentation at the 14 SPE Middle East Oil & Gas Show and Conference held in Bahrain International Exhibition Centre. Bahrain, 12-15 March 2005.

[25] Branagan. P., and Cotner, G. “A Competent and Practical Approach to Well Testing and Analysis in Tight Gas Reservoirs” paper SPE/DOE 10843. This paper was presented at the SPE/DOE Unconventional Gas Recovery Symposium of the Society of Petroleum Engineers held in Pittsburgh, PA, MAY 16-18, 1982.

[26] Garcia, J.P., Pooladi-Darvish., M., Santo. M., and Mattar, L. “Well Testing of Tight Gas Reservoirs” paper SPE 100576. This paper was prepared for presentation at the 2006 SPE Gas Technology Symposium held in Calgary, Alberta, Canada, 15-17 May 2006.

[27] Holditch, S.A. “Tight Gas Sands” paper SPE 103356. This paper used to inform the general readership of recent advances in various areas of petroleum engineering, SPE Distinguished Author Series, JPT June 2006.

[28] Raghavan, R., Reynolds Jr. A.C., Meng, H., “Analysis of Pressure Buildup Data Following a Short Flow Period” paper SPE 9290. This paper was presented at the SPE 55th Annual Technical Conference and Exhibition held in Dallas September. 21-23, 1980.

[29] Basic petroleum geology. Peter K. Link. OGCI publications : 2001.

[30] RFT Essentials of Pressure Test Interpretation. Schlumberger : 1996.

[31] Guidelines for HSFT pressure testing and pressure response analysis for the Gulf of Thailand. Halliburton : 2005.

[32] Well Test Interpretation. Schlumberger : 2002.

[33] Wireline Formation Testing and Sampling. Schlumberger Wireline & Testing. Schlumberger: 1996.

[34] MDT Modular Formation Dynamics Tester. Schlumberger : 2005

APPENDICES

APPENDIX A: Sample ECLIPSE data file:

```
RUNSPEC
 TITLE
title
 START
 1 'JAN' 1983 /
 FIELD
 RADIAL
OIL
WATER
DIMENS
 50 20 462 /
ENDSCALE
/
TABDIMS
 1 1 20 57 1 20 20 1 /
 WELLDIMS
 2 2 2 2 /
 GRID
 INIT
GRIDFILE
 0 1 /
 GRIDUNIT
 'FEET'  /
MAPAXES

        0        0        0        0        0        0 /
COORDSYS

        1       462 'COMP' 'JOIN' /
 DRV
0.04589112 0.05414993 0.06389503 0.07539391 0.08896219 0.10497229 0.12386365
0.1461548 0.17245757 0.20349393 0.24011576 0.28332824 0.33431746 0.39448296
0.46547616 0.54924567 0.64809077 0.76472455 0.90234836 1.06473965 1.25635573
1.48245603 1.74924651 2.06405 2.43550715 2.87381367 3.3910001 4.00126208
4.72134998 5.57102864 6.57361989 7.75664265 9.15256834 10.79971207 12.74328433
```

```
15.03663195 17.74270232 20.93577116 24.70348124 29.149248 34.39509804
40.58501848 47.88890915 56.5072459 66.6765833 78.67604745 92.83499749
109.54206569 129.25582464 152.51737402
/

DTHETAV
7.29644 9.29115 10.9063 12.80223 15.02774 17.64012 20.70664 24.30624 28.53158
33.49145 33.49145 28.53158 24.30624 20.70664 17.64012 15.02774 12.80223 10.9063
9.29115 7.29644
/
DZ
462000*0.0325
/
BOX
        1        50        1        20        1        1 /
TOPS
1000*6560
/
ENDBOX
INRAD
 0.255208333333333 /
 EQUALS
PORO 0.12 /
/
EQUALS
PERMR 1 /
/
 EQUALS
PERMTHT 1 /
/
EQUALS
PERMZ 1 /
/
PROPS
 ECHO
PVTW
2850 0.6787892 3.8077076211661e-006 0.20072356664432 8.81955432471481e-006
```

```
/
 PVDO
2131.5789        1.2968817        0.27617129
2210.5263        1.2950637        0.27874498
2289.4737        1.2933733        0.28140753
2368.4211        1.2917976        0.28415688
2447.3684        1.2903253        0.28699112
2526.3158        1.2889466        0.28990844
2605.2632        1.2876528        0.29290717
2684.2105        1.2864362        0.29598571
2763.1579        1.2852902        0.29914259
2850             1.2841041        0.30270392
2921.0526        1.2831868        0.3056857
3000             1.2822193        0.3090693
/
 DENSITY
   49.1635008003666 62.4280113471297 0.0436995816077201
/
 ROCK
       2850 5.40925837847278e-006
/
SWOF
0.2      0.000    0.500    0
0.25     0.016    0.479    0
0.3      0.044    0.449    0
0.35     0.081    0.388    0
0.4      0.125    0.378    0
0.5      0.230    0.259    0
0.6      0.354    0.015    0
0.65     0.422    0.007    0
0.7      0.494    0.000    0
/
SOLUTION
EQUIL
   6560   2850   6575    1*    6560    1*    1*    1*    1*    1*   1*
/
RPTSOL
```

```
RESTART=2  /
 --RPTRST
   --BASIC=2  PRESSURE SOIL /
 SUMMARY
BPR
1 1 346  /
 /
BPR
1 1 231  /
 /
BPR
1 1 115  /
 /
SCHEDULE
  WELSPECS
'W1' '1' 1 1 6567.5 'OIL' 1* 'STD' 'SHUT' 'YES' 1* 'SEG' 3* 'STD' /
 /
 COMPDAT
'W1' 2* 231 231 'OPEN' 2* 0.510416666666667 3* 'Z' 1* /
 /
 WCONPROD
'W1' 'OPEN' 'BHP' 5* 14.7 3* /
 /
 TSTEP
1.15741e-011 /
….
TSTEP
1.739e-005 /
 WCONPROD
'W1' 'SHUT' 10* /
 /
TSTEP
1.15741e-011 /
 ….
TSTEP
2.1157e-003 /
 END
```

APPENDIX B: Sample curve fitting data:

Δt	P sim_1	P mod_1	error
0	14.69953	14.69953	0.0000
2E-06	14.69953	14.69953	0.0000
1.2E-05	14.69954	14.69953	0.0000
2.2E-05	14.69954	14.69953	0.0000
5.8E-05	14.69954	14.69953	0.0000
6.4E-05	14.69954	14.69953	0.0000
8E-05	14.69954	14.69954	0.0000
8.9E-05	14.69954	14.69954	0.0000
1E-04	14.69954	14.69954	0.0000
0.000111	14.69954	14.69954	0.0000
0.000123	14.69954	14.69954	0.0000
0.000137	14.69954	14.69954	0.0000
0.000153	14.69954	14.69954	0.0000
0.000269	14.69954	14.69954	0.0000
0.001596	14.69956	14.69956	0.0000
0.001983	14.69957	14.69956	0.0000
0.002209	14.69957	14.69957	0.0000
0.002742	14.69958	14.69957	0.0000
0.008957	14.69969	14.69967	0.0000
0.009972	14.69971	14.69968	0.0000
0.012359	14.69975	14.69972	0.0000
0.015317	14.6998	14.69976	0.0000
0.017051	14.69983	14.69979	0.0000
0.023789	14.69994	14.69989	0.0000
0.033718	14.70011	14.70004	0.0000
0.037801	14.70018	14.7001	0.0000
0.042347	14.70026	14.70016	0.0000
0.059306	14.70055	14.70042	0.0000
0.066282	14.70067	14.70052	0.0000
0.09231	14.70111	14.70091	0.0000
0.114933	14.70149	14.70125	0.0000
0.159394	14.70225	14.70191	0.0000
0.177684	14.70257	14.70218	0.0000
0.2207	14.7033	14.70282	0.0000
0.305233	14.70474	14.70408	0.0000
0.421794	14.70673	14.70581	0.0000

0.582518	14.70947	14.70821	0.0000
0.648636	14.7106	14.70919	0.0000
0.996783	14.71653	14.71438	0.0000
1.109725	14.71846	14.71606	0.0000
2.351111	14.73963	14.73454	0.0000
2.913247	14.74921	14.74291	0.0000
3.242819	14.75484	14.74782	0.0000
4.01794	14.76805	14.75936	0.0001
5.541172	14.79403	14.78204	0.0001
6.167797	14.80471	14.79137	0.0002
8.505538	14.84458	14.82617	0.0003
9.467257	14.86098	14.84049	0.0004
11.72904	14.89954	14.87416	0.0006
13.0551	14.92216	14.89391	0.0008
16.17389	14.97533	14.94034	0.0012
22.30275	15.07983	15.03158	0.0023
24.82399	15.12282	15.06912	0.0029
30.75371	15.22392	15.15739	0.0044
34.23027	15.28319	15.20915	0.0055
38.09979	15.34916	15.26675	0.0068
41.96929	15.41512	15.32435	0.0082
46.27616	15.48854	15.38846	0.0100
51.06989	15.57026	15.45982	0.0122
56.40553	15.66121	15.53924	0.0149
62.34423	15.76243	15.62763	0.0182
68.95426	15.87509	15.72602	0.0222
76.3114	16.00048	15.83552	0.0272
84.50022	16.14003	15.95739	0.0334
93.61456	16.29534	16.09303	0.0409
102.7289	16.45064	16.22866	0.0493
112.8731	16.62348	16.37962	0.0595
124.1647	16.81584	16.54763	0.0719
136.7325	17.02993	16.73463	0.0872
150.7206	17.26818	16.94274	0.1059
166.2899	17.53334	17.17436	0.1289
183.6192	17.82842	17.43214	0.1570
202.9071	18.1568	17.71903	0.1916
248.2705	18.92893	18.39365	0.2865
274.8662	19.38147	18.7891	0.3509
304.4686	19.88505	19.22918	0.4302

374.0897	21.06892	20.26393	0.6480
414.9076	21.76268	20.87042	0.7961
460.3393	22.53458	21.5453	0.9787
510.9067	23.39339	22.29629	1.2036
567.1902	24.34885	23.13193	1.4809
699.562	26.59418	25.09628	2.2437
777.1698	27.90943	26.24732	2.7626
863.55	29.37233	27.52792	3.4019
959.6959	30.99937	28.95261	4.1892
1066.711	32.80879	30.53751	5.1587
1185.822	34.82081	32.30051	6.3519
1318.394	37.05785	34.26146	7.8198
1465.948	39.54476	36.4424	9.6246
1630.186	42.30923	38.86796	11.8423
1812.982	45.38159	41.56514	14.5653

The exponential model in this buildup study has the following equation

$$P_{(t)} = P_{dd} + (C_1) * \left(1 - e^{-\frac{\Delta t}{C_2}}\right)$$

Where

$P_{(t)}$ = pressure response at time t, psi

P_{dd} = final pressure drawdown, psi

P_{est} = estimate pressure, (0.433 * TVD), psi

Δt = buildup time, sec

C_1 = constant for pressure, P_{est} - P_{dd}

C_2 = constant for each restricted zone/near probe permeability

P_{est}	2850
P_{dd}	14.700
C_1	2835.300
C_2	190,427.776

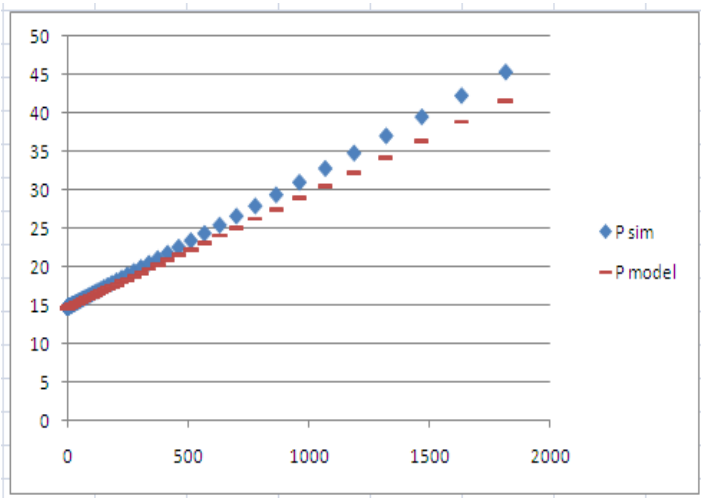

Figure B-1: Pressure buildup from simulation and exponential model plot versus buildup time

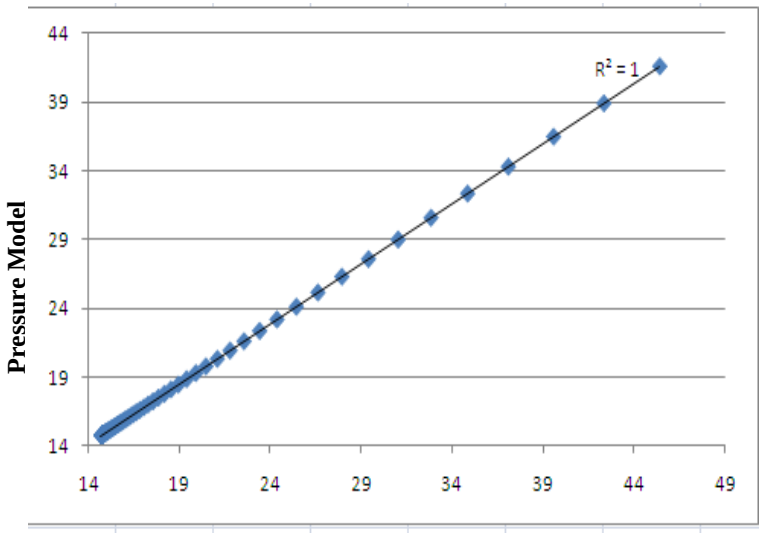

Figure B-2: R2 value from simulation and exponential model

To verify the exponential model, the real data was brought to this study. The same concept is applied to find out the result. Table B-1 summarizes the input value and coefficient value. The rate of change is increased as high as $1x10^{-20}$. Figure B-2 show the differentiation value plot for the real data. Figure B-4 to B-6 show the result from curve fitting.

Table B-1: summary data of input value and coefficient of tight reservoir

Mobility, mD/cp	P est	P dd	C_1	C_2
2.19	3710	2,964.89	745.11	25.62
1.22	2150	314.79	1,835.21	12.05
3.76	3000	2,069.47	930.53	6.40
0.53	3500	83.29	3,416.71	26.13
2.24	3400	2,923.31	476.69	6.38
0.91	3400	2,608.70	791.30	10.93
0.41	3400	1,350.71	2,049.29	16.14
0.49	5100	397.33	4,702.67	14.56
2.41	5050	3,426.07	1,623.93	2.95
2.61	2400	422.37	1,977.63	2.95
1.31	2850	72.69	2,777.31	9.89
1.22	2850	77.33	2,772.68	8.07

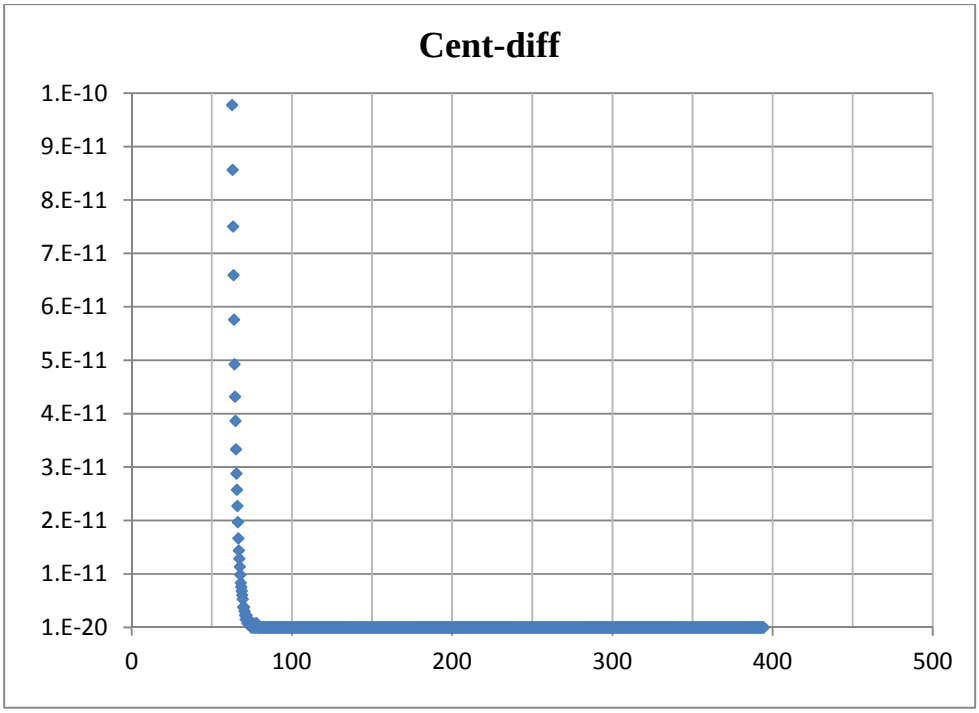

Figure B-3: the differentiation value plot for tight reservoir

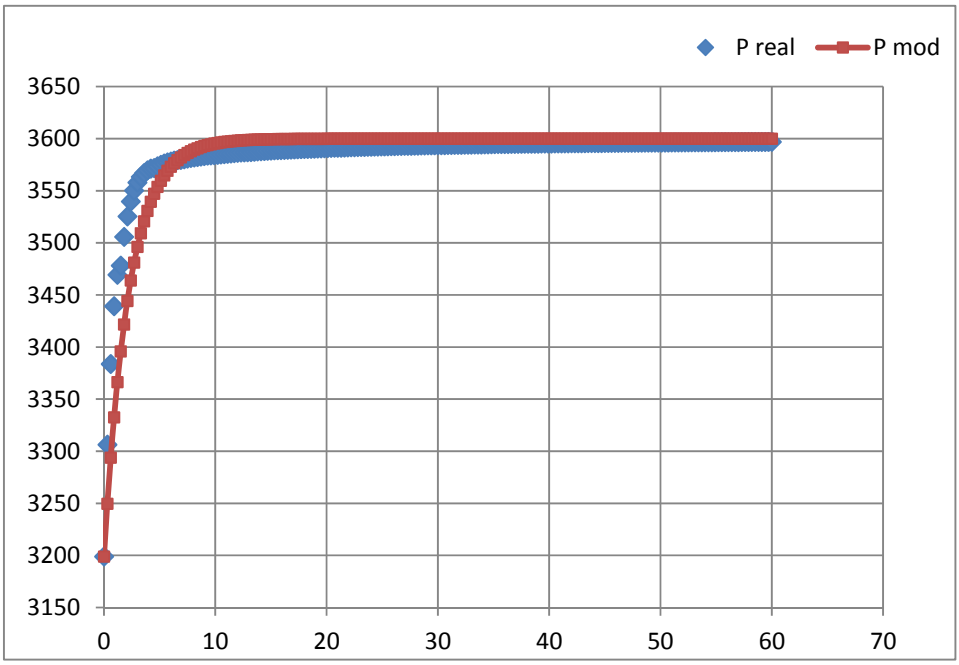

Figure B-4: Pressure buildup profile from real data and exponential model for the mobility 1.83 mD/cp

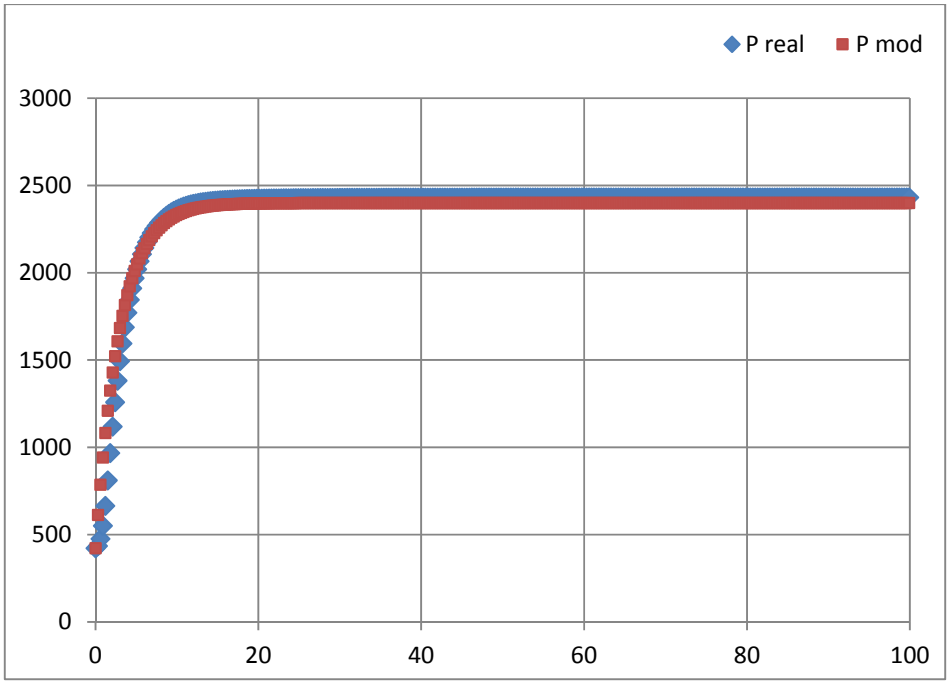

Figure B-5: Pressure buildup profile from real data and exponential model for the mobility 2.61 mD/cp

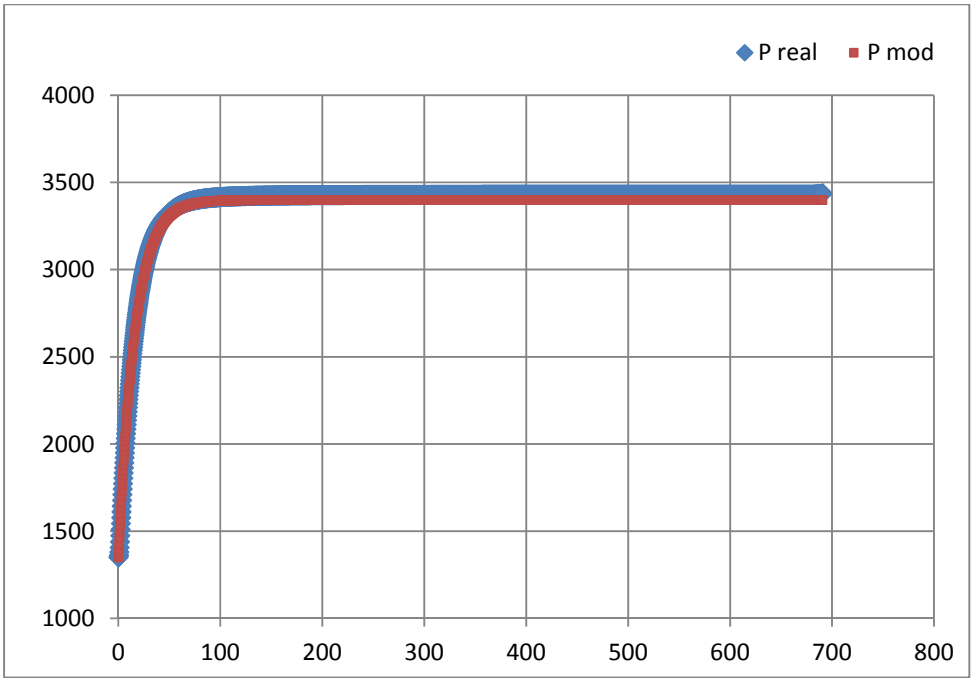

Figure B-6: Pressure buildup profile from real data and exponential model for the mobility 0.41 mD/cp

Table B-2: summary data from Exponential model and real data

Mobility, mD/cp	T_{est} sec	T_{real} sec
2.19	1,266.4	643.2
1.22	615.3	353.7
3.76	326.3	195.6
0.53	1,330.6	802.2
2.24	321.4	209.1
0.91	550.2	312.9
0.41	821.3	662.7
0.49	754.5	117.6
2.41	154.5	22.8
2.61	155.1	128.7
1.31	510.9	468.3
1.22	418.5	336.9

VITAE

Attawit Choodesh was born on May 23, 1979 in Bangkok, Thailand. He received his B.Eng. in Production Engineering from the Faculty of Engineering, King Mongkut's Institute of Technology North Bangkok in 2002. After graduating, He worked for the Unocal Thailand exploration and production contractor for 3 years as well service representative. Then Unocal was merged with Chevron in year 2005, he transferred to Chevron contractor as well site manager. In 2008, he resigns from Chevron for study in the Master of Petroleum Engineering program at the Department of Mining and Petroleum Engineering, Faculty of Engineering, Chulalongkorn University. Now, he works for PTT Exploration and Production Company Limited as a Well engineer, Well engineering department.